

T CELL PLASTICITY AND CO-INFECTIONS IN MYCOBACTERIAL DISEASES

by

Leticia Monin Aldama

BSc in Biochemistry, Universidad de la República, Uruguay, 2009

MSc in Biological Sciences, Universidad de la República, Uruguay, 2011

Submitted to the Graduate Faculty of
University of Pittsburgh in partial fulfillment
of the requirements for the degree of
Doctor of Philosophy

University of Pittsburgh

2015

UNIVERSITY OF PITTSBURGH

SCHOOL OF MEDICINE

This thesis was presented

by

Leticia Monin Aldama

It was defended on

June 29th, 2015

and approved by

Anuradha Ray, PhD, Professor of Medicine and Immunology

Jennifer Bomberger, PhD, Assistant Professor of Microbiology and Molecular Genetics

Tim D. Oury, MD, PhD, Professor of Pathology

Dissertation Advisors: Shabaana A. Khader, PhD, Associate Professor of Molecular

Microbiology, Washington University School of Medicine in St. Louis

Jay Kolls, MD, Professor of Pediatrics and Immunology

T CELL PLASTICITY AND CO-INFECTIONS IN MYCOBACTERIAL DISEASES

Leticia Monin Aldama, PhD

University of Pittsburgh, 2015

Copyright © by Leticia Monin Aldama

2015

Copyright permission was granted for the use of parts from:

Mucosal Immunology, **Monin, L.**, Griffiths, K.L., Slight, S., Lin, Y., Rangel-Moreno, J. & Khader, S.A., Immune requirements for protective Th17 recall responses to *Mycobacterium tuberculosis* challenge. (2015)

Seminars in Immunology, 26(6):552-8, **Monin, L.** & Khader, S.A., Chemokines in tuberculosis: the good, the bad and the ugly, Copyright (2014) , with permission from Elsevier.

Letters are on file with Leticia Monin.

The genus *Mycobacterium* comprises a variety of organisms, of which only a few are pathogenic, causing diseases of varying nature and severity. Despite this diversity, it is well established that CD4⁺ T helper type 1 (Th1) cells are instrumental in generating effective anti-mycobacterial immune responses. In addition, Th17 cells are required for mucosal vaccine recall responses. In this work, we studied T cell plasticity and how cytokine defects or co-infections that skew the immune response to a predominantly Th2 or Th17 type, can affect the outcome of primary and recall responses to mycobacterial infections. We explored the plasticity of *Mycobacterium tuberculosis* (*Mtb*)-specific Th responses, showing that *Mtb*-specific Th1 and Th17 cells can acquire the cytokine secretion patterns of other Th subsets. In a vaccination setting, where *Mtb*-specific Th17 cells are required for protection, we studied the requirements for *Mtb* control following Th17 transfer. Firstly, we found that upon re-exposure to *Mtb* antigen, Th17 cells were plastic and required external signaling via IL-23 and CXCR5 expression for protection. Surprisingly, IFN- γ -deficient Th17 cells conferred enhanced protection against *Mtb*. Together, our data suggest that optimizing vaccine strategies to boost CXCR5 and IL-23 expression, while limiting IFN- γ production, may enhance vaccine efficacy. In countries with poorly developed infrastructure, *Mtb* is often co-endemic with helminth infections. Thus, using a model helminth organism (*Schistosoma mansoni*), we assessed whether helminth co-infection or antigens impact T cell plasticity during *Mtb* infection. Our data show that helminth infection enhances arginase expression in macrophages within the lung, reduces Th1 responses and diminishes *Mtb* control. Importantly, antihelminthic treatment of co-infected mice was sufficient for restoring T cell responses and reducing inflammation, suggesting that T cell modulation is reversible. In addition, we determined the effect of *Aspergillus fumigatus* co-infection on *Mycobacterium abscessus* (*Mabs*), which is an emerging pathogen in cystic fibrosis.

Interestingly, we found that *A.fumigatus* alleviated *Mabs*-induced lung pathology in a mouse model. Future studies will establish if modulation of Th1 and Th17 commitment toward a regulatory phenotype underlies the decreased inflammation. Together, our results provide novel information on the dynamic interplay between host genetics, competing host responses to parasitic and fungal antigens and *Mtb* co-infection.

TABLE OF CONTENTS

TABLE OF CONTENTS	VI
LIST OF TABLES	IX
LIST OF FIGURES	X
ACKNOWLEDGEMENTS	XIII
ABBREVIATIONS	XVI
1.0 INTRODUCTION-THE IMPACT OF MYCOBACTERIAL DISEASE.....	1
2.0 TUBERCULOSIS	3
2.1.1 Disease manifestations	3
2.1.2 Disease burden and challenges to its control.....	4
2.1.3 Animal models.....	6
2.1.4 Immune mechanisms involved in control of mycobacteria.....	9
2.1.5 Vaccination strategies against TB	14
2.1.6 T cell plasticity.....	16
3.0 REQUIREMENTS FOR TH17-INDUCED RECALL PROTECTION IN TUBERCULOSIS	18
3.1 SUMMARY	18
3.2 METHODS.....	19
3.3 RESULTS	24

3.4	DISCUSSION.....	40
3.5	ACKNOWLEDGEMENTS	44
4.0	CO-INFECTIONS SHAPE DISEASE OUTCOME DURING TB	46
4.1.1	Co-endemicity of diseases with TB.....	46
4.1.2	Helminth modulation of host immune responses.....	48
4.1.3	Tuberculosis and helminth co-infections	50
4.1.4	<i>Schistosoma mansoni</i>	51
5.0	THE EFFECT OF SCHISTOSOMA MANSONI CO-INFECTION AND ANTIGENS ON TUBERCULOSIS	55
5.1	SUMMARY	55
5.2	METHODS.....	56
5.3	RESULTS	65
5.4	DISCUSSION.....	94
5.5	ACKNOWLEDGEMENTS	101
6.0	NTM DISEASE, AN EMERGING OPPORTUNISTIC INFECTION.....	103
6.1.1	Non-tuberculous mycobacteria.....	103
6.1.2	Host responses to NTM infection.....	104
6.1.3	Co-infections during NTM infections in CF.....	106
7.0	THE EFFECT OF TH17-SKEWING INFECTIONS ON IMMUNITY TO NON-TUBERCULOUS MYCOBACTERIA	108
7.1	SUMMARY	108
7.2	METHODS.....	109
7.3	RESULTS.....	114

7.4	DISCUSSION.....	127
7.5	ACKNOWLEDGEMENTS	134
8.0	CONCLUSIONS, SIGNIFICANCE AND FUTURE DIRECTIONS	135
9.0	RELEVANT PUBLICATIONS	139
	BIBLIOGRAPHY	141

LIST OF TABLES

Table 1. Induction of genes associated with Th1 cell function in CD4 ⁺ T cells during <i>Mtb</i> infection.	81
Table 2. Top down- and upregulated genes in CD4 ⁺ T cells from <i>Mtb</i> -infected mice following ex vivo treatment with SEA.....	83
Table 3. Top 15 genes upregulated in lungs of DO mice with severe inflammation (SI) compared to mice with enhanced mycobacterial control (EC).....	90

LIST OF FIGURES

Figure 1. Mechanisms that mediate lung <i>Mtb</i> containment.....	13
Figure 2. In vitro-differentiated Th17 cells produce high levels of Th17 cognate cytokines, but not IFN- γ	25
Figure 3. Th17 recall responses mediate <i>Mtb</i> control through an IL-12 and IL-21-independent but IL-23-dependent mechanism.	27
Figure 4. <i>Mtb</i> -specific T cell subsets exhibit variable plasticity in an in vitro setting.	30
Figure 5. In vivo primed, <i>Mtb</i> -specific T cell populations are plastic.....	33
Figure 6. IFN- γ production in Th17 cells decreases the potency of recall protection against <i>Mtb</i> challenge.	35
Figure 7. IFN- γ -deficient adoptively transferred Th17 cells induce long-lasting protection against <i>Mtb</i> challenge.....	37
Figure 8. CXCR5 expression on Th17 cells is critical to mediate protective recall responses following <i>Mtb</i> challenge.	39
Figure 9. <i>Schistosoma mansoni</i> life cycle.....	53
Figure 10. <i>S. mansoni</i> induces arginase-1-expressing type 2 granulomas and exacerbates inflammation during co-infection with <i>Mtb</i>	66
Figure 11. <i>S. mansoni</i> co-infection leads to increased lung pathology during TB.	68

Figure 12. <i>S. mansoni</i> co-infection leads to increased lung pathology, impaired Th1 responses and increased susceptibility to <i>Mtb</i> infection.....	70
Figure 13. Praziquantel treatment of <i>S.mansoni</i> infection reverses the increased inflammation seen in <i>Mtb-S. mansoni</i> co-infected mice.	73
Figure 14. Praziquantel treatment of <i>Mtb-S.mansoni</i> co-infected mice reduces <i>Schistosoma</i> egg burden and leads to decreased lung pathology upon <i>Mtb</i> infection.....	75
Figure 15. <i>Tie2^{Cre} Arg1^{fllox/fllox}</i> BMC co-infected mice have reduced lung pathology.	77
Figure 16. SEA immunization increases susceptibility to <i>Mtb</i> infection.....	79
Figure 17. PPD and BSA immunization of <i>Mtb</i> -infected mice does not exacerbate lung inflammation and <i>Mtb</i> control.	80
Figure 18. SEA treatment impairs <i>Mtb</i> -driven Th1 responses and increases susceptibility to <i>Mtb</i> infection.	86
Figure 19. Impairment of Th1 responses in SEA treated Th cells is reversible.	88
Figure 20. SEA treatment increases TB reactivation in mice.....	89
Figure 21. Arginase-1 expression during <i>Mtb</i> infection in genetically diverse mice and in humans correlates with increased inflammation and lung damage.....	92
Figure 22. <i>M. abscessus</i> infection is rapidly controlled by C57BL/6 mice and induces potent Th17 responses.....	115
Figure 23. Adaptive immunity, and IFN- γ , but not IL-17R signaling, are required for <i>M.abscessus</i> control.....	117
Figure 24. <i>A. fumigatus</i> infection enhances <i>M.abscessus</i> control via a mucus-independent mechanism.	119

Figure 25. *A. fumigatus*-induced *M. abscessus* control is STAT-1 independent but IL-17RA, Tbx21 and Rorc-dependent..... 121

Figure 26. *A.fumigatus* infection reduces *M.abscessus*-driven lung inflammation. 123

Figure 27. *A.fumigatus* reduced *M.abscessus*-driven lung inflammation is associated with increased IL-10 and Treg accumulation in infected lungs..... 125

Figure 28. CF patients co-infected with NTM and *A.fumigatus* exhibit increased sputum IL-17A, IL-6, IP-10 and RANTES levels..... 126

ACKNOWLEDGEMENTS

When I started my PhD almost four years ago, little could I have imagined what a challenging yet absolutely rewarding experience it would turn out to be. I was fortunate to have the guidance and support of many people along the way.

I would like to offer my sincere gratitude to Shabaana, my mentor, who shared her contagious energy, excitement and motivation for science during each of our talks. She is an exemplary researcher, an inspiring role model and is devoted to helping all of her mentees develop to their fullest potential. She has taught me volumes about identifying potential areas of research, the importance of collaboration, science communication, laboratory management and organization, and I will strive to apply everything I learnt with her to future ventures. Most of all, I have been able to learn that she is not only an excellent researcher, but a caring and considerate person, who offered her help and support when I needed it the most. For that, I am forever grateful, and I hope that we can maintain this relationship as we both progress in our careers.

I would also like to thank Jay, who welcomed me into his lab and offered his guidance during the last year of my PhD. His expertise in lung immunology and productive discussions and suggestions during lab meetings and conference calls have made the time in his lab an excellent learning experience.

During my PhD, I have had the honor of working and learning with a group of extremely talented people, without whom this work would not have been possible. In particular, I would like to thank Samantha Slight and Radha Gopal for their dedication to my initial phases of training in the Khader lab, and for their assistance in many experiments. They have been excellent colleagues and friends. Most of all, I would like to thank Kristin Kallapur, who has been an amazing friend and flatmate. She has greatly contributed to the work done in the *Schistosoma* project, starting and carrying out experiments in St. Louis in my absence. We have shared lovely experiences and have supported each other at difficult times. I would like to thank many other people in the Khader and Kolls labs who made all of this work possible, including Dan Mallon, Waleed Elsegeiny, Taylor Eddens, Hillary Cleveland, Derek Pociask, and William Horne. In addition, I would like to recognize Alison Logar for sitting with me for hours at the flow cytometer, for providing helpful experimental advice and for all of our talks. I find myself remembering her often.

During this work, we have received help from many collaborators, who have contributed so much to the advancement of our projects. I specifically want to thank Javier Rangel-Moreno, for his work and dedication. He has been responsible for generating so many of our beautiful histology and immunofluorescence images, has worked tirelessly during paper resubmissions, and has provided insightful suggestions throughout this work. None of this would have been possible without him.

In addition, I would like to thank my committee members, Anuradha Ray, Jennifer Bomberger, Tim Oury, Shabaana Khader and Jay Kolls for investing their time in fruitful discussions on how to improve our work.

Last but not least, I would like to thank my family, friends and Gerard for their love, support and care. I have shared joys and sorrows with friends from Uruguay and from Pittsburgh, and the latter have made me feel at home despite the distance. One in particular, gives meaning to the word home. T'estimo tant. My parents and grandparents, my sister and brother and the rest of our beautiful family have been an inspiration. They have taught me the importance of hard work, dedication and education, and have supported me and provided advice during every stage of my life. Despite the distance that currently separates us, they are always present. I cannot thank them enough.

ABBREVIATIONS

AIDS	Acquired Immunodeficiency Syndrome
<i>Af</i>	<i>Aspergillus fumigatus</i>
APC	Antigen Presenting Cell
ATB	Active Tuberculosis
B6	C57BL/6
BCG	Bacille Calmette-Guérin
Breg	B regulatory
CD	Cluster of Differentiation
CFU	Colony Forming Units
ESAT-6	6 kDa Early Secretory Antigenic Target
DC	Dendritic Cell
FFPE	Formalin Fixed, Paraffin Embedded
HIV	Human Immunodeficiency Virus
iBALT	inducible Bronchus Associated Lymphoid Tissues
Ig	Immunoglobulin
BMDC	Bone Marrow-derived Dendritic Cell
BMDM	Bone Marrow-Derived Macrophage
IFN	Interferon

IL	Interleukin
iNOS	inducible Nitric Oxide Synthase
i.v.	Intravenous
i.t.	Intratracheal
LTB	Latent Tuberculosis
MDR	Multi-Drug Resistant
<i>Mabs</i>	<i>Mycobacterium abscessus</i>
<i>Mtb</i>	<i>Mycobacterium tuberculosis</i>
NHP	Non-Human Primate
NK	Natural Killer
NTM	Non-tuberculous mycobacteria
PBMC	Peripheral Blood Mononuclear Cell
PPD	Purified Protein Derivative
SEA	<i>Schistosoma</i> egg antigen
SLO	Secondary Lymphoid Organ
<i>Sm</i>	<i>Schistosoma mansoni</i>
TB	Tuberculosis
TCR	T Cell Receptor
Tfh	T follicular helper
Th	T helper
TLR	Toll-Like Receptor
Tg	Transgenic
TGF	Tumor Growth Factor

TNF	Tumor Necrosis Factor
Treg	T regulatory
WHO	World Health Organization
XDR	Extensively Drug Resistant

1.0 INTRODUCTION-THE IMPACT OF MYCOBACTERIAL DISEASE

The genus *Mycobacterium* comprises a variety of mostly saprophytic organisms, of which only a few members are pathogenic, causing diseases of varying nature and severity. Several mycobacterial pathogens can establish infections that pose a serious challenge to global health. Infection by *Mycobacterium tuberculosis* (*Mtb*), the etiological agent of tuberculosis (TB), constitutes the second leading cause of death from an infectious disease in the world, with 9 million new TB cases and 1.5 million TB-related deaths per annum [1]. Furthermore, about one third of the world's population is latently infected with *Mtb*, and at risk of progressing to active disease. In fact, of the two billion infected individuals, 10%, that is, 200 million people, will likely progress to active disease throughout their lifetime [1]. Current efforts to control this disease are aimed at the development of novel, effective vaccines, the generation of new drug regimens and an improvement in diagnostic and prognostic markers [2-4].

In turn, non-tuberculous mycobacterial (NTM) infections are currently emerging as a serious health concern in patients with previous lung conditions and transplant patients, including cystic fibrosis (CF) patients [5]. Of particular relevance is *M. abscessus* infection, which constitutes the most drug-resistant NTM and is associated with poor treatment outcome. Indeed, sputum conversion occurs in 50-60% of treated patients, highlighting the low efficacy of treatment. Further, transition of *M. abscessus* from an environmentally-adapted form to the human-adapted morphotype has been associated with development of a highly invasive and

pathogenic disease [6]. Defining the mechanisms that potentiate bacterial persistence in patients at high risk of NTM infections will enable the development of novel therapeutic avenues for treatment of NTM disease.

In natural populations, mycobacterial infections rarely occur in isolation, and can be affected by a range of physiological and environmental factors, including socio-economical factors, nutritional status, and the presence of other co-colonizing or co-infecting organisms. While the full impact of co-infections on the severity of mycobacterial diseases and the development of immunity to mycobacteria remains an open question, there is a wealth of persuasive published evidence, supported by our data, to warrant investigation of co-infections as a relevant and important factor for the control of mycobacterial disease. An important secondary consideration is that it will be important to understand whether treatments for mycobacteria affect disease manifestations associated with co-infections. In this work, we have studied T cell plasticity during mycobacterial infections, specifically the effect of changes to the host microenvironment elicited by co-infections or alterations in the balance of cytokines on the outcome of mycobacterial infections and vaccine-induced protection against TB.

2.0 TUBERCULOSIS

2.1.1 Disease manifestations

Mtb can establish infection upon reaching the lower airways of the lung via inhalation of droplets containing the bacterium, generated during coughing or sneezing. Successful transmission can be detected in 20-50% of individuals exposed to *Mtb* by the presence of antigen-specific T cell responses [7], which are usually apparent within 42 days after exposure [8, 9]. In infected individuals, TB can manifest as a spectrum of disease, ranging from absence of clinical signs (latent TB-LTB) in the majority of infected individuals to primary active clinical TB disease in 5-10% of individuals, with symptoms typically including cough, sputum production, appetite loss, weight loss, fever, chest pain, fatigue and hemoptysis [10]. However, latently infected individuals constitute a reservoir for the bacterium, as 10% of them will progress to develop active TB (ATB) during their lifetime and become contagious, a process called reactivation [10]. Although the lung is the primary organ affected by the disease, extrapulmonary tuberculosis can occur in 10 to 42% of patients and affect different organs in the body, including the spleen, lymph node, kidneys, joints and central nervous system [11].

The hallmark feature of TB is the granuloma, an organized collection of immune and stromal cells with a macrophage-rich center and a leukocytic periphery, which can be detected by chest X-rays in individuals with LTB, primary ATB and TB reactivation [12]. Given their

structure, granulomas were classically thought to constitute a physical barrier to contain an infectious organism that could not be eradicated, forming a wall that prevents *Mtb* dissemination. However, over the past two decades, our understanding of the granuloma has shifted toward a more dynamic, complex structure, that may limit or favor bacterial persistence depending on host, pathogen and environmental factors [13].

2.1.2 Disease burden and challenges to its control

The World Health Organization (WHO) declared TB a global emergency in 1993. Since then, the 2015 Millenium Development Goal of halting and reversing TB incidence has been achieved globally, with TB incidence falling at a rate of 1.5% per year between 2000 and 2013 [1].

However, despite over half a century of anti-TB chemotherapy, one third of the world's population remains latently infected with *Mtb*, 10% of which is at risk for development of active TB [1]. This is further aggravated by the burden of the HIV epidemic, which constitutes the most important risk factor for progression to active TB, increasing the risk of latent TB reactivation 26 to 31-fold [14]. Of the 9 million people who developed active TB in 2013, 1.1 million (13%) were HIV-positive [1]. Despite the favorable drop in the number of TB HIV-related deaths over the past decade, TB remains the largest single cause of death in patients with AIDS, accounting for 26% of AIDS-related deaths [14].

The current recommended antibiotic regimen for drug-susceptible TB has a high efficacy, with cure rates of about 90% in HIV-negative patients [15]. It consists of an initial 2-month phase of isoniazid, a rifamycin, pyrazinamide and ethambutol, followed by a 4-month continuation phase of isoniazid and a rifamycin [15]. However, these treatments are lengthy and require patient compliance with the treatment regimen for the entire treatment period.

In recent years, emergence of drug-resistant *Mtb* strains is presenting new challenges in the management and control of this disease. It has been estimated that 3.5% of new and 20.5% of previously treated TB cases were caused by multidrug resistant TB (MDR-TB) in 2013, while 9% of patients with MDR-TB had extensively drug resistant TB (XDR-TB) [16]. Treatment of MDR-TB, which is resistant to isoniazid and rifampicin, takes at least 20 months of treatment, with lower cure rates and increased side effects [15]. XDR-TB, in turn, is resistant to isoniazid and rifampicin, fluoroquinolones and any second-line injectable drugs (amikacin, kanamycin or capreomycin) and is associated with very high mortality rates [15]. In addition, in HIV and *Mtb* co-infected patients, interactions between some of the anti-TB and antiretroviral drugs limit treatment options. Given that the last licensed TB antibiotic with a defined mechanism of action was rifampicin, which was discovered in 1963, and taking the aforementioned factors into consideration, drug development is therefore an area of strong investigation and 10 new or repurposed drugs are currently under Phase II or Phase III trials [15].

An alternative strategy to control the emergence of MDR-TB and XDR-TB is the development of an effective vaccine against TB. The current available vaccine, *Mycobacterium bovis* BCG (Bacille Calmette-Guérin), is effective at preventing disseminated cases of TB in children, particularly meningitis. However, it confers variable protection to adult pulmonary TB, ranging from 0 to 80%. A great deal of effort has been invested in the development of new vaccines, and currently, 15 vaccine candidates are in different stages in clinical trials, ranging from Phase I to Phase III. However, the failure of the MVA85A booster, an attenuated vaccinia virus vector expressing *Mtb* antigen Ag85A, to enhance protection against pulmonary TB despite its strong immunogenicity in animal models [17-20], highlights our incomplete understanding of the immunological pathways that should be harnessed to elicit improved, long-lasting protection

to TB. If we want to reach the deadline of elimination of TB as a public health problem by 2050, the development of safe and more effective vaccines against TB is urgent and an area of top priority.

2.1.3 Animal models

One of our current limitations to study and understand human TB is the inherent variability of human populations. In fact, environmental factors, genetic diversity, age, sex, differences in bacterial strains and infectious load, as well as the duration of infection, can confound conclusions drawn from *Mtb*-infected human subjects. In addition, human tissues for study normally derive from either deceased patients or lung resections, two scenarios representing terminal or serious disease [13]. When available, samples from latently infected individuals are normally peripheral cells, which may not represent events occurring at the primary site of infection. Furthermore, since patients diagnosed with TB are readily put on an antibiotic treatment regimen, samples from untreated individuals are extremely scarce [21]. TB is a disease that takes years to progress, and as such, obtaining a clear understanding of the mechanisms required for *Mtb* containment and the factors leading to reactivation throughout every step of the disease is paramount. Over the past decades, a number of animal models have been developed to address these issues.

Guinea pigs have been instrumental in TB studies, as the initial experiments performed by Koch that established *Mtb* as the etiological agent of TB were done in that model [22]. Importantly, guinea pigs can be infected with very low doses of *Mtb*, and possess granuloma features similar to those present in humans, including multinucleated giant cells and lung necrosis [23]. However, unlike humans, they are highly susceptible to TB disease, the majority

of infected animals developing features of active disease that eventually leads to their death [22]. Rabbits have also proven a useful model for TB, as they display a spectrum of disease that is similar to that seen in human TB [24]. Unlike guinea pigs, and similar to humans, rabbits are mostly resistant to TB, and lung pathological features seen in humans can be reproduced by infecting the animals with *M. bovis* [25]. However, tools to study immune responses in the guinea pig and the rabbit models are limited, which is an obstacle to the use of these models to establish the mechanistic basis of disease progression.

Mice have several advantages for modeling disease, including their relatively low cost, low generation time, the availability of numerous tools to study their immune system, and relative simplicity to alter their genotype. Numerous mouse models have been used to study TB, but arguably the low-dose aerosol model of TB is the one that best reproduces the natural route of infection in humans [26]. In this model, mice are exposed to droplet nuclei containing *Mtb* in a chamber where mice can move naturally [27]. Following a growth lag during the first 3 days after infection, *Mtb* grows exponentially in the lungs for about two weeks, a time where adaptive immune cells begin to infiltrate the lung [28]. Following this phase, the bacterial burden in the lung plateaus at a level dependent on the mouse genotype, typically 5-6 logs for C57BL/6 mice [29]. This is a chronic disseminated model of disease, where bacteria can be detected throughout the life of the animal at both pulmonary and extrapulmonary sites, such as the lymph nodes, spleen and liver. Much has been debated about the utility of the mouse model of TB, mainly due to the different granulomatous structures formed in this model and to the chronic nature of the disease [29]. Namely, mouse granulomas are more lymphocytic in nature, less structured than human granulomas and generally do not caseate. However, they serve as an extremely useful tool to study mechanistic immunological processes that are conserved between mice and humans

[22]. Although the infection in mice is chronic, several models of latency have been developed, including the modified Cornell mouse model, where mice are put on an antibiotic regimen consisting of isoniazid and rifampicin in the drinking water, until bacteria are no longer cultivable. Following that phase, antibiotics are suspended and mice will spontaneously “reactivate”, which is detected as new bacterial growth arising from persisting bacteria [30].

Although the mouse model has greatly contributed to our understanding of TB, non-human primates (NHP) are arguably the model that best reproduces the pathological features of human TB [31]. Not only do they develop the spectrum of granuloma formation and disease observed in humans [32], but they can also be infected with the simian immunodeficiency virus (SIV, the NHP variant of HIV) to model TB and HIV co-infection [29]. However, the elevated cost and infrastructure requirements of this model, the limited tools to study the immune response in NHPs and ethical considerations are some of the constraints to the widespread use of this model [31].

More recently, infection of zebrafish embryos [33, 34] or adult organisms with *Mycobacterium marinum*, a mycobacterial species related to *Mtb* [35], has provided a novel tool for the study of TB. Infection can be performed by intraperitoneal injection of the microorganism, and is associated with the formation of caseous granulomas [36], as is the case in humans. Despite the fact that these organisms form granulomas containing a larger proportion of innate cells [36], the variety of genetic tools to study zebrafish, the transparency of the embryos facilitating imaging experiments and the possibility of performing large scale drug screens together make this an interesting organism for TB research.

2.1.4 Immune mechanisms involved in control of mycobacteria

Although *Mtb* infects a substantial proportion of the human population worldwide, only a small percentage of individuals progress to active disease [1]. HIV infection [37], malnutrition [38] and anti-TNF- α therapy [39] all have been shown to increase the risk of TB reactivation, illustrating that specific immune mechanisms can restrict bacterial growth. Upon entry into the lung, mycobacteria are taken up by alveolar macrophages, where *Mtb* replicates while inhibiting macrophage killing mechanisms [40]. Despite this, ligation of pattern recognition receptors (PRRs) in infected cells initiates a response characterized by the secretion of proinflammatory cytokines, such as IL-12 and TNF- α , chemokines and the upregulation of adhesion receptors [41]. This activation of innate cells results in the recruitment and activation of several immune cell populations to the lung [40]. Indeed, in the mouse model of low dose aerosol infection, around day 12 post-infection there is an early influx of innate cells into the lungs, including $\gamma\delta$ T cells, NK cells, monocyte-derived macrophages, dendritic cells and neutrophils [42]. Despite the accumulation of these innate immune cells, *Mtb* continues to grow exponentially over the first 2-3 weeks following infection [42]. Thus, activation of adaptive immunity and recruitment of effector T cells into the lung is required for bacterial burden control [43]. The priming of T cells is initiated by dendritic cells (DCs), primary antigen presenting cells (APCs) that serve as a direct link between the innate branch of the immune response and the adaptive response [44].

Lung resident DCs can take up live *Mtb* within the lungs and transport them to the lung-draining mediastinal lymph nodes [45]. Migration of DCs from the lungs to the mediastinal lymph nodes is governed by chemokine-receptor interactions, and occurs around day 14 post-infection in the mouse model of TB [45]. Uptake of *Mtb* by DCs leads to the upregulation of CCR7 expression [46], which guides the cells to the mediastinal lymph node following a

gradient of the homeostatic chemokines CCL-19 and CCL-21 [45]. Recently, it has come to light that the myeloid cell populations that become infected and carry antigen to the lymph node, and those that directly prime the T cells, are distinct. Indeed, infected CCR2⁺ inflammatory monocytes are important for antigen delivery into the lung, where they release soluble antigen that can be taken up and presented by resident lymph node DCs [47, 48]. Subsequent recognition of *Mtb* antigens by naïve T cells bearing specific T cell receptors, in the presence of costimulatory signals and adequate cytokines in the microenvironment leads to the activation, proliferation and differentiation of naïve T cells into effector cells [49].

While *Mtb* actively replicates in the lung, induction of inflammatory chemokines ultimately results in the recruitment of newly activated effector T cells from the periphery. This onset of adaptive immunity correlates with arrest of bacterial growth in the mouse model of TB [50]. As the increased incidence of mycobacterial TB reactivation in HIV patients demonstrates, CD4⁺ T helper cells (Th) cells are key to infection containment [37, 51]. Th cell responses can be classified into different subsets according to their functional characteristics. These subsets include Th1 cells, which have classically been viewed as orchestrators of immune responses against intracellular bacteria and viruses, Th2 cells, which have been associated with anti-helminth responses, and, more recently, the Th17, Treg and T follicular helper (Tfh) subsets [52]. Multiple studies have shown that Th1 cells, which are generated in the presence of IL-12 and secrete IFN- γ , play a major role in the adaptive branch of the response against mycobacteria [53, 54]. Th1 cell activity, through IFN- γ secretion, is instrumental for macrophage activation, a process that leads to the potentiation of macrophage killing mechanisms, such as the production of reactive oxygen and nitrogen species [55]. Additional T cell subsets, namely, Tfh-like cells have also been shown to participate in primary containment of *Mtb* infection [56] and Th17 cells

have been involved in vaccine recall responses to *Mtb* challenge [57]. However, T cell plasticity in the context of mycobacterial infections is an understudied area of research.

T cells that exit the lymph node are able to enter the lung via the circulation through ligation of surface endothelial receptors that are upregulated in response to inflammation. Upon commitment to the Th1 subset, the main CD4⁺ T cell subset implicated in *Mtb* control, effector T cells upregulate the chemokine receptors CXCR3 and CCR5 [58, 59]. It is thought that this is directly related to their recruitment into the infected lung, as the ligands for these receptors, CXCL-9, CXCL-10 and CXCL-11 for CXCR3 and CCL-3, CCL-4, CCL-5 and CCL-8 for CCR5, are upregulated in *Mtb*-infected mouse [42] and NHP lungs [60].

Upon entry into the lung parenchyma, however, proper *Mtb* containment is dependent on the correct localization of effector T cells in apposition to *Mtb*-infected macrophages. In recent years, several reports have demonstrated the expression of homeostatic chemokines, which are commonly expressed in secondary lymphoid organs (SLOs), in *Mtb*-infected lungs [42, 61]. Such chemokines, including CCL-19, CCL-21, CXCL-12 and CXCL-13, drive the organization of lymphoid follicles in SLOs and in the periphery [61]. These organized lymphoid and stromal aggregates, known as ectopic lymphoid follicles, have been reported in conditions of chronic infection and inflammation [62]. Interestingly, during *Mtb* infection in mice, non-human primates and humans, CXCR5-expressing CD4⁺ T cells also accumulate in the lungs, within ectopic lymphoid follicles [56]. Importantly, these CXCR5⁺ CD4⁺ T cells produce high levels of proinflammatory cytokines and upon accumulation in the lung, respond to CXCL-13 likely produced by stromal cells early during infection, and localize near *Mtb*-infected macrophages to mediate *Mtb* control [56]. Accordingly, both CXCR5 and CXCL13-deficient mice lacked the formation of ectopic lymphoid follicles and exhibited decreased control of *Mtb*, thus projecting a

non-redundant role for the CXCR5-CXCL-13 axis in TB. CXCR5 deficiency resulted in localization of CD4⁺ T cells around blood vessels in the *Mtb*-infected lungs, forming perivascular cuffs indicative of their inability to localize in apposition to infected macrophages [56]. Therefore, not only is the timely induction of chemokine-mediated recruitment of T cells to the lung critical for *Mtb* control, but emerging evidence suggests that chemokines also play a critical role in the precise positioning of *Mtb*-specific T cells within the lung parenchyma for maximal *Mtb* control. Indeed, early vaccine-induced production of CXCL-9, CXCL-10 and associated recruitment of CXCR3-expressing T cells is beneficial in vaccine-induced protection against *Mtb* challenge [63]. In addition, vaccine strategies that induce early CXCL-13 production to enhance and improve early T cell localization near *Mtb*-infected macrophages can be harnessed for vaccine design against TB [64].

Together, there is accumulating evidence that the cytokines and chemokines induced in response to *Mtb* infection effectively mediate DC activation and trafficking to the LNs, priming and recruitment of activated T cells to the lung and correct localization of T cells within the lung parenchyma to mediate optimal *Mtb* control (Fig 1). However, although these processes mediate control of *Mtb* growth, they often do not completely eliminate the bacteria. Further understanding of the mechanisms that lead to *Mtb* containment will not only allow the better development of novel therapies against TB, but will be of particular relevance for vaccine and adjuvant design.

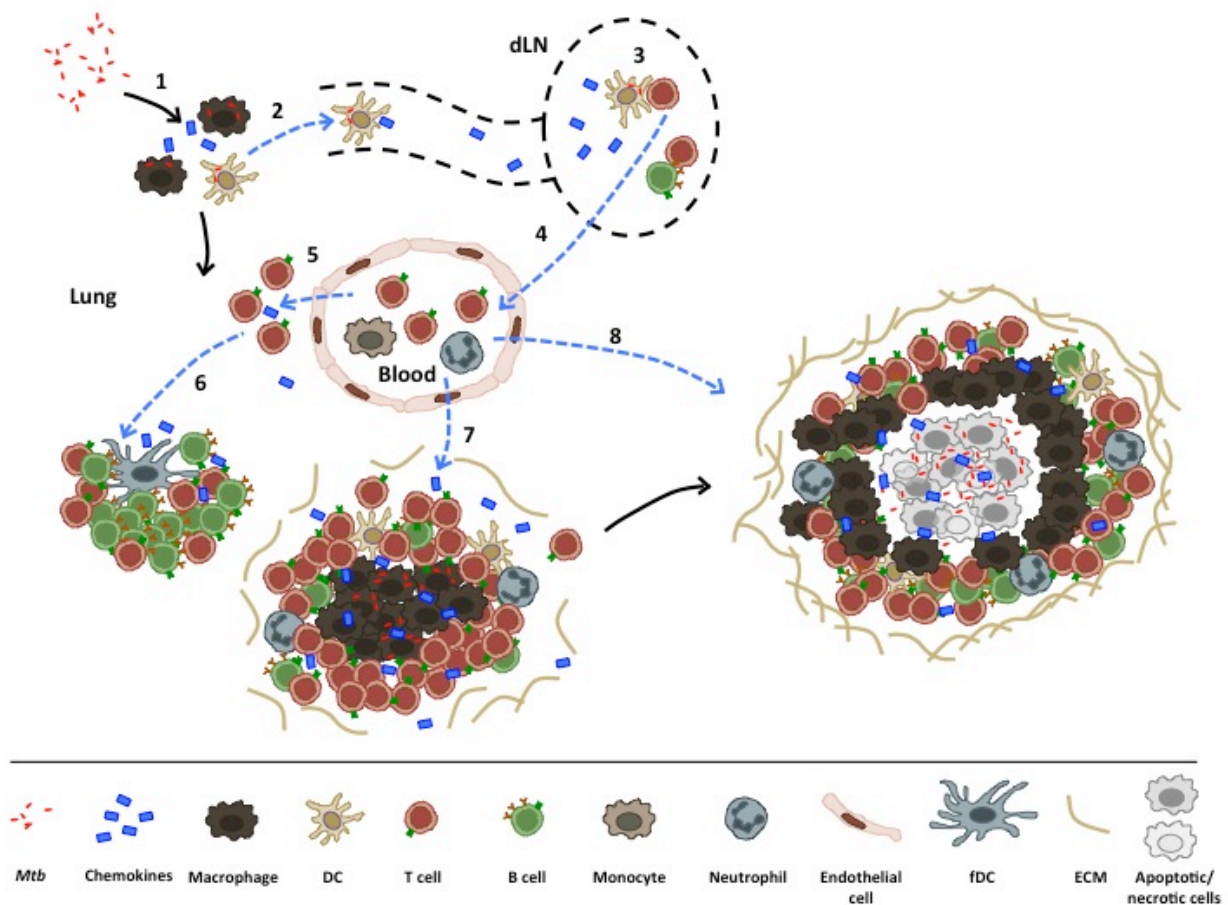


Figure 1. Mechanisms that mediate lung *Mtb* containment.

Upon *Mtb* entry into the lungs, alveolar macrophages become infected, leading to secretion of cytokines and chemokines, which drive additional innate cell recruitment (1). Infected DCs migrate into the lung draining lymph nodes (dLN) (2), carrying antigen that can be subsequently taken up by other APCs to activate naïve T cells (3). After activation, T cells (along with B cells) regulate their chemokine receptor expression, which guide their exit from the lymph node (4), homing to the infected lung (5), and subsequent migration. These responses are mediated by differential expression of chemokines, a process that enables ectopic lymphoid follicle formation (6). Additional innate cells, such as monocytes and neutrophils are also recruited into the lung (7). Together, interactions between innate and adaptive cells lead to granuloma formation and *Mtb* containment (8). Dashed blue lines represent chemokine-driven mechanisms.

2.1.5 Vaccination strategies against TB

The Bacille Calmette-Guérin (BCG) vaccine, remains the sole licensed vaccine against TB and constitutes the most widely used vaccine worldwide, with more than three billion doses administered [65]. It was developed by Albert Calmette and Camille Guérin in the early 1900s through attenuation of a virulent *M. bovis* isolate by 230 serial passages on bile potato medium [66]. BCG is effective in preventing disseminated forms of TB in children. However, the variable efficacy of the current TB vaccine *Mycobacterium bovis* BCG against adult pulmonary TB, along with the recent emergence of drug-resistant *Mtb* strains has prompted the search for novel vaccines for TB [67].

IFN- γ has been shown to promote macrophage activation, enhancing of antimicrobial mechanisms, and is required primary protection against TB. Hence, the paradigm for TB vaccine development in the past decade has been focused on targeting enhancement of IFN- γ secretion in T cells to mediate early macrophage activation and bacterial killing [68]. However, a number of studies have shown that IFN- γ is not a good correlate of vaccine-mediated protection [69, 70]. More recently, this has been highlighted by the failure of the recombinant TB vaccine MVA85A to enhance protection against *Mtb* infection in human clinical trials [71], despite induction of high levels of IFN- γ in humans [72] and animal models [17]. There are currently 11 TB vaccine candidates at different stages in clinical trials, including genetically modified strains of BCG, attenuated *Mtb*, subunit vaccines and viruses expressing *Mtb* proteins [73]. Exploring new and more effective pathways associated with vaccine protection will enable us to better assess current candidates whilst allowing rational design of novel vaccines against TB.

Th17 cells, which produce the cytokines IL-17A, IL-17F, IL-21, TNF- α and IL-22, differentiate in a multistep process that is initiated by antigen presentation in the presence of the cytokines IL-6 and TGF- β [74-76]. This induces strong IL-21 production by these differentiating cells, which is then thought to amplify differentiation through autocrine signaling [77]. Finally, signaling from IL-23 seems to be required for full differentiation and commitment to the Th17 subset [78, 79]. In recent years, Th17 cells have emerged as one of the primary effector cells that mediate inflammation in autoimmune diseases [80, 81]. On the other hand, Th17 cells are critical for mediating immunity against extracellular bacterial and fungal pathogens [82], and in vaccine-induced protection against several mucosal pathogens [83], including *Mtb* [84]. Indeed, our studies were amongst the earliest to show that parenteral vaccine-induced Th17 cells populate the lung and respond rapidly to *Mtb* infection, thus enabling *Mtb* containment [84]. More recently, we have shown that mucosal vaccine-driven protection is dependent on the induction of Th17-derived IL-17, production of chemokines, and formation of organized ectopic B cell follicles facilitating activation of *Mtb*-infected macrophages [64]. In addition, several vaccination strategies have been shown to promote potent, lasting Th17 responses. For example, immunization with antigen *Mtb32* in adjuvant CAF01 [85], and vaccination with the recombinant BCG strain rBCG Δ ureC:Hly in mice [86], both induce strong Th17 responses, which are associated with superior protection to *Mtb* challenge. However, despite the emerging consensus that Th17 cells are critical for vaccine-induced immunity against TB, the exact cytokine and immune requirements that enable Th17-induced recall protection upon *Mtb* challenge remain unclear. Delineating the immune characteristics of Th17 cells that mediate recall protection against TB is critical for targeting Th17 responses for future development of vaccines against TB.

2.1.6 T cell plasticity

Adequate differentiation of T helper cells is required for promotion of either primary protection or vaccine-mediated protection to TB, a process that relies on signals present in the microenvironment at the time of differentiation. The classical paradigm of T helper subsets was that Th1, Th17, Th2 or Tregs are lineages, being terminally differentiated or irreversibly committed to their phenotype. Such a classification of T cell populations facilitated the elucidation of basic immune processes. However, the distinction between subsets is not always obvious and recently, several reports have shown that T cell subsets are not rigid populations, but rather, are plastic and can adapt to changing microenvironments in the host [87]. Given the relevance of Th1 and Th17 responses for anti-mycobacterial immune responses, we will address studies related to plasticity of those particular subsets.

Th17 cells have been found to be a relatively plastic subset, with a number of cytokines, including IL-4 [88], IFN- γ [89, 90], high-dose TGF- β [76], and IL-2 [91], being able of suppressing Th17 differentiation or cytokine secretion. Both in vitro and ex vivo, polyfunctional Th cells co-producing IL-17A and IFN- γ have been described, and have been associated with pathology development in autoimmune conditions [92]. Using a reporter fate mapping mouse system, it was shown that the origin of these polyfunctional Th1/Th17 cells was from Th17 cells acquiring IFN- γ secreting capacity in a mouse model of multiple sclerosis [93]. Similarly, Th17 cells have been shown to acquire IL-4 secreting capacity both in vitro and in vivo during helminth infection [94]. Furthermore, IL-13⁺IL-17⁺ Th cells have been described in mice stimulated with repeated doses of ovalbumin-pulsed dendritic cells [95]. Culture of these dendritic cells in vitro with mouse Th17 cells led to the upregulation of IL-13 production,

indicating that these cells can acquire Th2-like cytokine secretion [95]. Polyfunctional IL-17⁺IL-4⁺ T cells have been described in patients with chronic asthma [96], but the origin of these cells is still under debate. In vitro, human Th17 cells cultured in the presence of IL-4 were able to upregulate IL-4 production, indicating that this cell subset may be plastic both in mice and humans [87].

Th1 cells, however, seem to be a more rigid population, with very limited evidence suggesting that Th1 to Th17 conversion can occur [87]. In vitro culture of Th1 cells under Th17-skewing conditions failed to upregulate ROR γ t or IL-17A, and overall does not seem to happen in C57BL/6 mice [97]. A possible explanation for this is the early downregulation of IL-6 receptor expression on activated T cells [98], which is required for Th17 differentiation. Th1 to Th2 conversion, however, has been described. Th2 polarized LCMV-specific cells transferred to LCMV-infected mice were able to co-express IL-4 and IFN- γ [99]. This ability of Th1 cells to acquire a Th2 cytokine secretion pattern may be affected by the degree of commitment to the Th1 subset, as Th1 cells seem to be less plastic the more rounds of division they undergo [100]. In the context of TB, a chronic disease where patients frequently present with additional comorbidities, the yet unexplored question of T cell plasticity is of particular importance and is being explored in this study.

3.0 REQUIREMENTS FOR TH17-INDUCED RECALL PROTECTION IN TUBERCULOSIS

3.1 SUMMARY

Tuberculosis (TB) vaccine development has focused largely on targeting T helper type 1 (Th1) cells. However, despite inducing Th1 cells, the recombinant TB vaccine MVA85A failed to enhance protection against *Mtb* infection in humans. In recent years, Th17 cells have emerged as key players in vaccine-induced protection against TB. However, the exact cytokine and immune requirements that enable Th17-induced recall protection remain unclear. In this study, we have investigated the requirements for Th17 cell-induced recall protection against *Mtb* challenge by utilizing a tractable adoptive transfer model in mice. Firstly, we show that *Mtb*-specific T1 and Th17 cells are plastic, and can acquire the cytokine secretion properties of other T cell subsets. We demonstrate that adoptive transfer of *Mtb*-specific Th17 cells into naïve hosts, and upon *Mtb* challenge, results in Th17 recall responses that confer protection at levels similar to vaccination strategies. Importantly, while IL-23 is critical, IL-12 and IL-21 are dispensable for protective Th17 recall responses. Unexpectedly, we demonstrate that IFN- γ produced by adoptively transferred Th17 cells impairs long-term protective recall immunity against *Mtb* challenge. This suggests that Th17 plasticity may have a negative effect on vaccine-induced protection to TB. In contrast, CXCR5 expression is crucial for localization of Th17 cells near macrophages within

well-formed B cell follicles to mediate *Mtb* control. Thus, our data identify new immune characteristics that can be harnessed to improve Th17 recall responses for enhancing vaccine design against TB.

3.2 METHODS

Animals

C57BL/6 (B6) animals were purchased from Taconic. *Ifng*^{-/-} mice on the B6 background were purchased from The Jackson Laboratory (Bar Harbor, ME). Early Secretory Antigenic Target-6 (ESAT-6) $\alpha\beta$ TCR Tg mice recognize IA^b/ESAT-6₁₋₂₀ and were provided by G. Winslow (Wadsworth Center, Albany, New York, USA) and D. Woodland (Trudeau Institute, Saranac Lake, New York, USA) [101]. The ESAT-6 TCR Tg mice were crossed and maintained on the *Rag1*^{-/-} background or crossed to Thy1.1 mice for in vivo tracking experiments. ESAT-6.*Rag*^{-/-} mice were further crossed to *Ifng*^{-/-} and *CXCR5*^{-/-} mice to generate ESAT-6 TCR Tg mice deficient in these specific genes. *Il12p35*^{-/-}, *Il21*^{-/-} [102] and *Il23p19*^{-/-} [103] mice were maintained in the animal facility either at the University of Pittsburgh or at Washington University in St. Louis. Experimental mice were age- and sex-matched and used between the ages of 6-8 weeks. All mice were maintained and used in accordance with the approved University of Pittsburgh and Washington University in St. Louis IACUC guidelines.

T cell differentiation and adoptive T cell transfer

Naïve T cells were isolated from ESAT-6 Tg mice using CD4⁺ (L3T4) magnetic bead sorting (Miltenyi Biotec, San Diego, CA). To generate Th17 cells, CD4⁺ T cells were cultured at a 1:1 ratio with BMDCs in the presence of ESAT-6₁₋₂₀ peptide (10 μ g/mL), recombinant (r)-

mouse IL-2 (10 U/mL), r-mouse IL-6 (30 ng/ml R&D Systems), r-mouse IL-23 (50 ng/ml R&D Systems), r-human TGF- β (5 ng/mL R&D Systems), anti-IL-4 antibody (10 μ g/mL), and anti-IFN- γ antibody (10 μ g/mL) in Iscove's Modified Dulbecco's Medium (Life Technologies, Grand Island, NY). For Th1 cells, CD4⁺ T cells were cultured at a 1:1 ratio with BMDCs in the presence of ESAT-6₁₋₂₀ peptide (10 μ g/mL), r-mouse IL-2 (10 U/mL), r-mouse IL-12 (10 ng/ml R&D Systems) and anti-IL-4 antibody (10 μ g/mL) in Iscove's Modified Dulbecco's Medium (Life Technologies, Grand Island, NY). In some experiments, cultured T cells were re-stimulated for 48 hours in the presence of a 1:1 ratio of irradiated splenocytes and ESAT-6₁₋₂₀ peptide (10 μ g/mL) for analysis of cytokine production in the supernatant or by intracellular staining and flow cytometry.

T cell subsets were generated in vitro as described above, purified from infected mice using CD4⁺ magnetic bead sorting or FACS, or IFN- γ -producing CD4⁺ cells were purified from *Mtb*-infected mice using a bead-based strategy (Miltenyi Biotec, San Diego, CA). T cells were laid over irradiated splenocytes (1:1) in the presence of 5 μ g/mL ESAT-6 peptide and 10 U/mL IL-2, in combination with Th1, Th2 or Th17 differentiating cytokines. T cells were incubated for six days at 37°C and 5% CO₂ and supplemented with an equivalent volume of media containing IL-2 (10U/mL) on day 3. After 6 days, supernatants were removed and T cells were restimulated with irradiated splenocytes and 5 μ g/mL ESAT-6 peptide for 48 h. Tissue culture supernatants were then harvested and cells were processed for RNA extraction.

For adoptive transfer, mice received 2×10^6 T cells by intravenous transfer, following which mice were rested for an average of 7 days before exposure to *Mtb*.

Experimental infections

The H37Rv strain of *Mtb* was grown in Proskauer Beck medium containing 0.05% Tween-80 to mid-log phase and frozen in 1mL aliquots at -80°C. For *Mtb* aerosol infections, animals were infected with 100 Colony Forming Units (CFU) of bacteria using a Glas-Col airborne infection system as described previously [104]. Infection with 1×10^6 cfu of BCG Pasteur was performed using the tongue-pull method. Briefly, mice were anesthetized with 3% isoflurane, suspended by their front incisors, and the tongue was extended using forceps. The bacterial suspension was pipetted into the trachea, and the tongue was held until normal breathing resumed. Lung bacterial burden was established by plating out organ homogenates on 7H11 agar plates [104]. For vaccination, 400 μ g of the immunodominant I-A^b-restricted ESAT-6₁₋₂₀ peptide (New England Peptide) were administered subcutaneously in the adjuvant mixture of MPL (monophosphoryl lipid A, Sigma-Aldrich), TDM (trehalose dicorynomycolate, Sigma-Aldrich) and DDA (dimethyl dioctadecylammonium bromide, Eastman Kodak) in a final volume of 200 μ L and mice were challenged after a 30-day period of rest [84].

Lung single-cell preparation and detection of cytokine-producing cells by ELISpot assay

Lung suspensions from *Mtb*-infected mice were prepared as described previously[84] and were used in ELISpot assays as described below. Antigen-specific IFN- γ -producing and IL-17-producing cells were analyzed by ELISpot assay. Multi-screen HA filter plates (Millipore, Billerica, MA) were coated with anti-IFN- γ (BD Biosciences) or anti-IL-17 (R&D Systems) antibodies. Single cell suspensions were added to the plate at a starting concentration of 1×10^5 cells/well and doubling dilutions made. Cells were cultured overnight in the presence of 1×10^6 irradiated splenocytes and 10 μ g/mL ESAT-6₁₋₂₀ peptide and 10 U/mL recombinant mouse IL-2.

The following day, biotinylated anti-IFN- γ or anti-IL-17 antibody (both from eBioscience, San Diego, CA) was added and incubated overnight. Plates were developed by incubation with streptavidin-alkaline phosphatase (Vector Labs, Burlingame, CA) for two hours, followed by incubation with NBT/BCIP (Sigma Aldrich). Spots were enumerated using a CTL-ImmunoSpot analyzer (CTL, Shaker Heights, OH) and the frequency and total number of responding cells calculated as described before [84].

Detection of cytokine-producing cells by flow cytometry

The presence of Thy1.1⁺ congenically labeled ESAT-6 TCR Tg T cells, as well as the presence of cells producing IFN- γ and IL-17 was determined by flow cytometry. Single cell suspensions were stimulated for six hours in the presence of 50 ng/mL phorbol-myristate acetate and 750 ng/mL ionomycin, as well as 5 μ L/mL GolgiStop (BD Biosciences). Cells were treated with Fc Block (anti-CD16/CD32, BD Biosciences) before surface staining for CD3 (clone 500A2, AlexaFluor 700-conjugated, BD Biosciences), CD4 (clone RM4-5, Pacific Blue-conjugated, BD Biosciences) and CD44 (clone IM7, PE-Cy7-conjugated, eBioscience). Cells were then fixed and permeabilized using the Cytofix/Cytoperm fixation permeabilization kit (BD Biosciences) before staining for IL-17 (clone TC11-18H10, PE-conjugated, BD Biosciences) and IFN- γ (clone XMG1.2, APC-conjugated, BD Biosciences). Cell staining was analyzed on an LSR Fortessa (BD Biosciences), and results were processed using FlowJo (Treestar, Ashland, OR).

Determination of protein concentration

ELISA antibody pairs were used to detect cytokine levels (DuoSet; R&D Biosystems) in cell culture supernatants.

Immunohistochemistry

Lung lobes were perfused with 10% neutral-buffered formalin and embedded in paraffin. For immunofluorescent staining, formalin-fixed lung sections were cut, immersed in xylene to remove paraffin, and then hydrated in 96% alcohol, and phosphate-buffered saline. Antigens were unmasked with a DakoCytomation Target Retrieval Solution (Dako, Carpinteria, CA) and non-specific binding was blocked with 5% (v/v) normal donkey serum and Fc block (BD Pharmingen). Endogenous biotin (Sigma-Aldrich) was neutralized by adding avidin followed by incubation with biotin. Sections were probed with anti-B220 to detect B cells (Clone RA3-6B2, BD Pharmingen), anti-CXCL13 (AF470, R&D systems) and anti-CD3 to detect T cells (Clone M-20, Santa Cruz Biotechnology, Santa Cruz, CA). B-cell follicles were outlined with the automated tool of the Zeiss Axioplan 2 microscope (Carl Zeiss, Thornwood, NY) and average size in squared microns was calculated as described before [64].

Statistical analysis

Statistical analysis to determine differences between experimental groups was performed in GraphPad Prism 5 (Graph Pad, La Jolla, CA) using two-tailed Student's *t*-test. Differences between the means of multiple experimental groups were analyzed using one-way ANOVA with Tukey's post-hoc test. Differences were considered significant when $p \leq 0.05$. All analyses were performed using GraphPad Prism Software.

3.3 RESULTS

Th17 recall responses mediate *Mtb* control in an IL-12 and IL-21-independent, but IL-23-dependent manner

Th17 recall responses are associated with vaccine-induced protection against TB [64, 84, 105, 106], but the cytokines and factors that are required for effective Th17 recall responses in vivo upon *Mtb* challenge are not well described. In order to study the requirements for Th17 recall responses in vivo upon *Mtb* challenge, we isolated naïve CD4⁺ T cells from ESAT-6 T cell receptor (TCR) transgenic (Tg) mice and differentiated them in vitro under Th1 or Th17-skewing conditions. As expected, Th17 cells produced high levels of IL-17A (IL-17) and IL-21, but not IFN- γ upon restimulation in vitro, when compared to Th1 cells which produced IFN- γ (Fig 2).

In vitro differentiated Th17 cells were then adoptively transferred into C57BL/6 (B6) hosts and following a period of rest, mice were challenged with low doses of aerosolized *Mtb* H37Rv. We found that adoptive transfer of Th17 cells into B6 hosts resulted in lower lung bacterial burden, when compared with control B6 mice that did not receive cells (published data, [107]). Importantly, the level of protection conferred by adoptive transfer of Th17 cells was comparable to parenteral or mucosal immunization with ESAT-6₁₋₂₀ (published data, [107]), an immunodominant *Mtb* antigen, known to confer vaccine-induced protection upon *Mtb* challenge [84, 105]. Importantly, upon *Mtb* challenge, early IL-17 antigen-specific recall responses were observed in mice that received Th17 cells and mice that were previously vaccinated when compared with unvaccinated mice that did not exhibit early IL-17 responses (published data, [107]). In addition, mucosally vaccinated mice had increased recall protection when compared with parenterally vaccinated mice and this coincided with increased accumulation of early IL-17 responses in the lung upon *Mtb* challenge (published data, [107]). These data suggest that the

Th17 recall response mediated by adoptive transfer of in vitro generated Th17 cells was by itself sufficient to control *Mtb* to levels comparable to prior vaccination. Thus, our model of adoptive transfer of antigen-experienced Th17 cells is a useful tool to study the factors that are required for effective Th17 recall responses in vivo upon *Mtb* challenge.

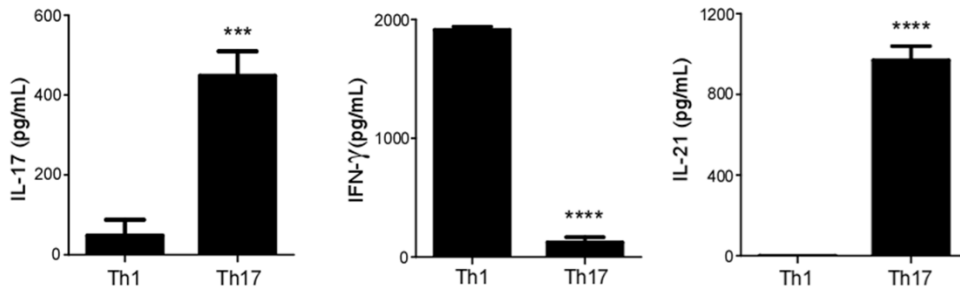


Figure 2. In vitro-differentiated Th17 cells produce high levels of Th17 cognate cytokines, but not IFN- γ .

Th1 or Th17 cells were differentiated in vitro from ESAT-6 TCR Tg mice. Levels of IL-17A, IL-21 and IFN- γ were determined in tissue culture supernatants following a 48-hour restimulation with ESAT-6 peptide. The data points represent the mean (\pm SD) of values from 3 independent samples. *** $p \leq 0.001$, **** $p \leq 0.0001$.

Th17 cell differentiation occurs in the presence of the polarizing cytokines IL-6 and TGF- β [89, 90]. In addition, IL-23 mediates commitment to the Th17 subset [108], while autocrine production of IL-21 induces Th17 differentiation [109]. While much is understood about how Th17 cells differentiate in vitro and during primary immune responses, the requirements for Th17 recall responses in vivo, specifically upon *Mtb* recall challenge have not been well characterized. Thus, using the Th17 cell adoptive transfer model, we then addressed the role of IL-12, IL-23 and IL-21 in mediating effective Th17 recall responses and conferring protection upon *Mtb* challenge. IL-12 is a polarizing cytokine required for differentiation of Th1 responses [110, 111], and is thus critical for protective immunity against TB [112]. Accordingly, IL-12p35-

/- control mice were more susceptible to *Mtb* challenge when compared to B6 control mice (Fig 3A). Similar to B6 mice that received Th17 cells, adoptive transfer of Th17 cells into IL-12p35^{-/-} mice resulted in reduction in lung *Mtb* burden (Fig 3A), suggesting that although IL-12 is required for protective primary immunity against TB, IL-12 is not required for protective Th17 recall responses upon *Mtb* challenge. Interestingly, IL-12p35^{-/-} mice that received Th17 cells also exhibited increased ESAT-6-specific IFN- γ -producing T cells (Fig 3B), and increased ESAT-6-specific IL-17-producing cells (Fig 3C), when compared to cytokine-production in naïve B6 mice (published data, [107]). IL-21 is a cytokine that is involved in the induction of Th17 cells [109]. As previously described [102], IL-21^{-/-} mice challenged with *Mtb* did not have increased bacterial burden compared to B6 control mice (Fig 3D). Interestingly, Th17 adoptive transfer into IL-21^{-/-} mice improved *Mtb* control, when compared to IL-21^{-/-} mice that did not receive cells (Fig 3D). These results indicate a dispensable role for IL-21 in both primary immunity [102] as well as protective Th17 recall responses in TB. The protection afforded in the IL-21^{-/-} mice coincided with generation of efficient *Mtb*-specific IFN- γ -producing (Fig 3E) and IL-17-producing (Fig 3F) T cell responses. Interestingly, when we transferred in vitro-differentiated Th17 cells into IL-23p19^{-/-} mice and evaluated their ability to confer protection upon *Mtb* challenge, we found that IL-23 was required for Th17-induced protection (Fig 3G). As shown before [104], IL-23p19^{-/-} control mice are not more susceptible to *Mtb* infection, when compared to B6 control mice (Fig 3G). However, IL-23p19^{-/-} mice that received Th17 cells had comparable lung bacterial burdens to IL-23p19^{-/-} mice that did not receive T cells (Fig 3G), suggesting that despite a dispensable role for IL-23 in primary immunity to *Mtb* infection, IL-23 has a critical role in Th17 recall response mediated protection against *Mtb* infection. Incidentally, IL-23p19^{-/-} mice that received Th17 cells and did not mediate early *Mtb* control also exhibited defective IL-

17 responses (Fig 3I), although ESAT-6-specific IFN- γ responses were robust and at levels comparable to B6 *Mtb*-infected mice (Fig 3H). These data together project a critical role for IL-23, but not IL-12 or IL-21 in Th17 recall responses in response to *Mtb* infection. In addition, these data clearly show that Th17 cells generated in vitro in the presence of IL-23, still required the presence of IL-23 for effective Th17 recall response following *Mtb* challenge.

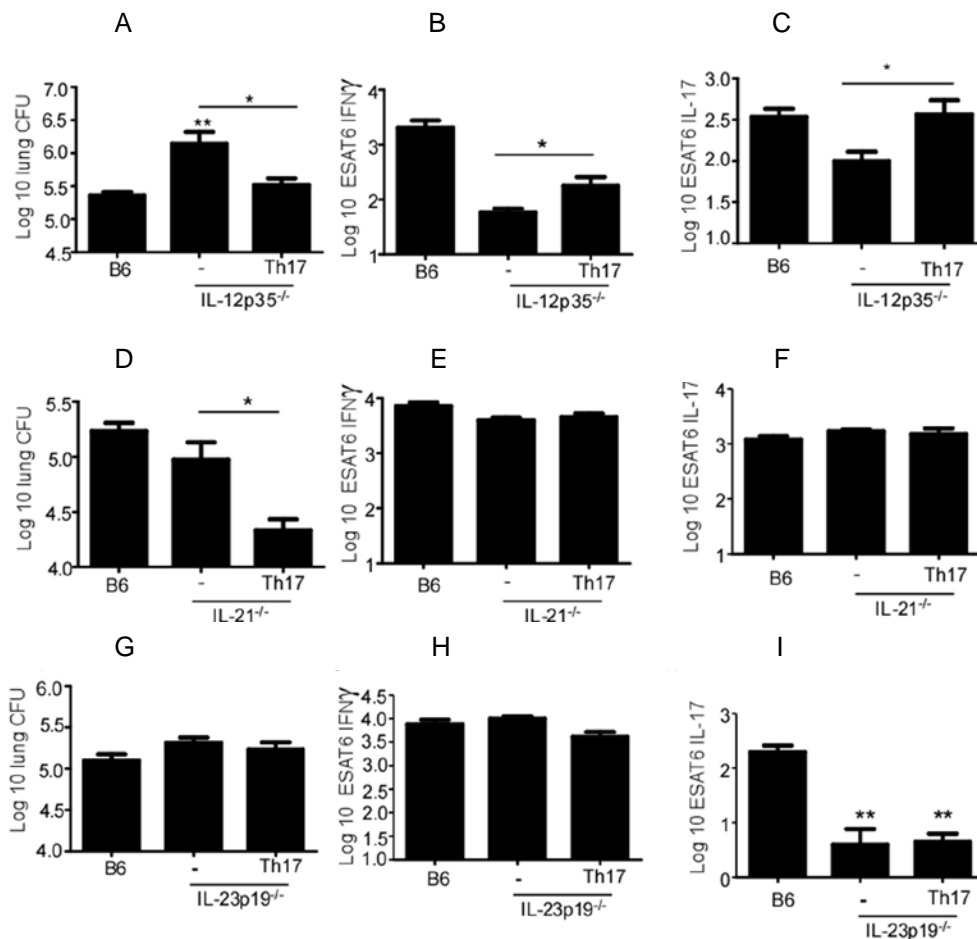


Figure 3. Th17 recall responses mediate *Mtb* control through an IL-12 and IL-21-independent but IL-23-dependent mechanism.

C57BL/6 (B6), IL-12p35^{-/-}, IL-21^{-/-}, or IL-23p19^{-/-} mice were left untreated (-) or received 2x10⁶ ESAT-6 TCR Tg Th17 cells by i.v. route, and were aerosol challenged with 100 CFU *Mtb* H37Rv. (A, D, G) Lung bacterial burden at 40 dpi and (B, E, H) the number of IFN- γ or (C, F, I) IL-17-producing ESAT-6-specific CD4⁺ T cells were

determined via peptide-driven ELISpot. The data points represent the mean (\pm SD) of values from 4 to 8 mice. * $p \leq 0.05$, ** $p \leq 0.01$, *** $p \leq 0.001$.

Transferred Th17 recall responses occur early upon *Mtb* challenge and produce both IFN- γ and IL-17

To further understand the immune features of Th17 recall responses, we tracked Thy1.1⁺ Th1 or Th17 cells upon adoptive transfer in B6 Thy1.2⁺ congenic hosts. We found that adoptively transferred Th17 cells preferentially migrated to, and were retained in the lung compartment, when compared to similarly transferred Th1 cells (published data, [107]). To further delineate the early kinetics of Th17 recall responses upon *Mtb* challenge, we adoptively transferred naïve undifferentiated Thy1.1⁺ Th0 cells, in vitro generated Thy1.1⁺ Th17 cells or Th1 cells into B6 Thy1.2⁺ congenic mice, rested mice and then challenged them with *Mtb*, and early Thy1.1⁺ *Mtb*-specific recall responses were assessed on days 10, 12 and 14 post *Mtb* infection. Consistent with our observation that Th17 cells accumulate and are retained in the lung upon adoptive transfer and prior to *Mtb* challenge (published data, [107]), we observed that the number of Th17 cells increased in the lungs between days 12 and 14 post *Mtb* challenge (published data, [107]). This was in contrast to B6 mice that received Th0 cells or Th1 cells, where significantly fewer ESAT-6-specific Th cells were detected in the lungs at these early time points (published data, [107]). This is consistent with previous studies which have shown that *Mtb*-specific Th0 cells take 13-18 days to accumulate in the *Mtb*-infected lungs [101, 113, 114]. Interestingly, in vitro differentiated Th17 cells which were primarily IL-17-producers at the time of transfer, produced IFN- γ following *Mtb* challenge, with or without IL-17 expression (published data, [107]). The majority of the adoptively transferred *Mtb*-specific Th17 cells were activated as detected by expression of CD44, suggesting that the ability to co-produce IFN- γ is

not due to in vivo priming of undifferentiated adoptively transferred T cells (published data, [107]). These data together show that antigen-experienced *Mtb*-specific Th17 cells accumulate early in the lungs following *Mtb* challenge when compared to naïve Th0 cells or antigen-experienced Th1 cells. In addition, our new data demonstrate that in vitro differentiated Th17 recall responses which confer protection upon *Mtb* challenge (Fig 3), can acquire the ability to co-produce IFN- γ during early recall responses.

***Mtb*-specific Th cell subsets exhibit variable plasticity in an in vitro setting.**

Given the ability of Th17 cells to co-produce IL-17 and IFN- γ , we hypothesized that *Mtb* specific CD4⁺ T cells are plastic and can change their cytokine production in response to external cytokine stimuli. Thus, we assessed the plasticity of *Mtb*-specific in vitro generated T cell subsets. For this, CD4⁺ T cells purified from ESAT-6 TCR Tg mice [101], which recognize the immunodominant *Mtb* ESAT-6₁₋₂₀ antigen, were in vitro polarized to the Th1, Th2, Th17 or Tfh subsets and subsequently exposed to differentiation conditions that drive different Th subsets. We found that the in vitro generated Th17 and Tfh subsets constituted highly plastic subsets, with the potential to acquire IFN- γ secretion upon exposure to Th1 cytokines (Fig 4A). In addition, both in vitro generated Tfh as well as Th17 subsets increased IL-17 (Fig 4B) and IL-21 production (Fig 4C) upon incubation under Th17 or Tfh skewing conditions, respectively. Additionally, in vitro-differentiated Th1 cells were less plastic, as they increased IL-21 production in response to Tfh cytokines (Fig 4C), but did not upregulate IL-17 production under Th17 conditions (Fig 4B). Th2 cells only upregulated IL-21 under Tfh conditions (Fig 4C), but were unable to acquire IFN- γ (Fig 4A) or IL-17 production (Fig 4B) upon exposure to Th1 or Th17 skewing conditions. These data together indicate that in vitro primed *Mtb*-specific T cell

subsets are plastic, yet differ in their ability to acquire the cytokine secretion patterns of other subsets, with Th17 and Tfh cells demonstrating the most plasticity.

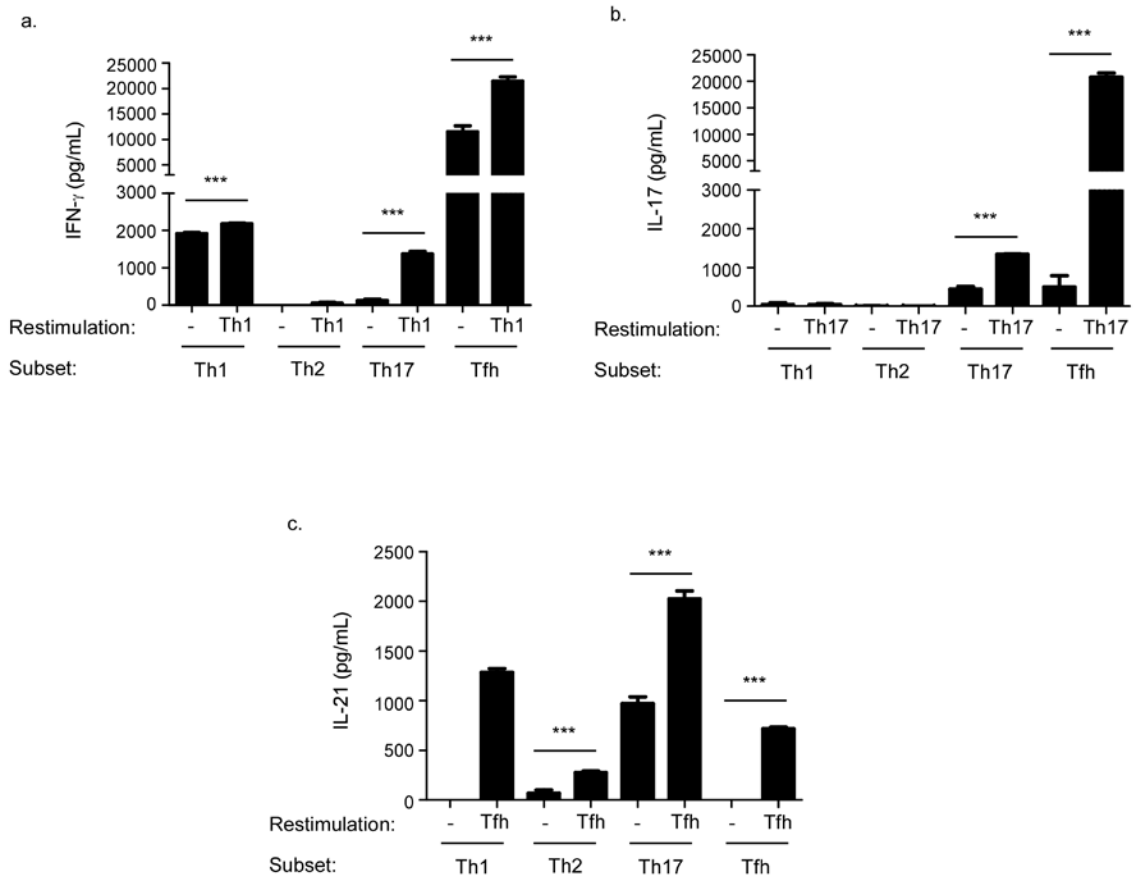


Figure 4. *Mtb*-specific T cell subsets exhibit variable plasticity in an in vitro setting.

ESAT-6 TCR Tg Th1, Th2, Th17 and Tfh cells were differentiated from naïve CD4⁺ T cells *in vitro* using cytokine cocktails (indicated as subset below the graph). Cells were then incubated with cDMEM (-), IL-12 (Th1 conditions); TGF- β , IL-6 and IL-23 (Th17 conditions); or IL-21 (Tfh conditions) for 6 days (indicated as restimulation below the graph). Cells were washed, incubated for 48 h with anti-CD3/CD28 beads and culture supernatants assessed to determine (A) IFN- γ , (B) IL-17 and (C) IL-21 protein levels. The data points represent the mean (\pm SD) of values from 3-5 samples. *** $p \leq 0.0005$.

In vivo primed, *Mtb*-specific T cell populations are plastic.

We next addressed if in vivo differentiated lung CD4⁺ Th cells induced following chronic *Mtb* infection will also demonstrate plasticity and can respond to cytokine changes in the microenvironment. Thus, we purified CD4⁺ T cells from the lungs of *Mtb*-infected wild type C57BL/6 mice and ex vivo exposed them to different Th cell subset-skewing cytokine cocktails. We found that, in the absence of additional stimuli (Untreated), these cells produced IFN- γ , low levels of IL-17 and undetectable production of IL-4 (Fig 5A), suggestive of a Th1 subset [102]. In support of our hypothesis, exposure to Th2-skewing cytokines led to the inhibition of IFN- γ production and to the upregulation of IL-4 production (Fig 5A), indicating that under the right conditions, in vivo generated *Mtb*-specific T cells can also acquire the ability to produce IL-4. Additionally, these cells were able to acquire IL-17 production in response to Th17 cytokines (Fig 5A). Interestingly, such an increase in IL-17 production was accompanied by a coincident increase in IFN- γ production (Fig 5A). Such plasticity was observed at varying points during chronic infection, as analysis on day 30 and day 50 post *Mtb* infection revealed similar results (data not shown). Since total lung CD4⁺ T cells were used in these assays, it is possible that an undifferentiated T cell population was contributing to the plasticity observed. To address whether changes observed in cytokine production was due to plasticity of the Th1 subset or due to differentiation of uncommitted CD4⁺ T cells, we enriched CD4⁺ cells for IFN- γ -producing population by using a magnetic-activated cell sorting (MACS) approach. We observed that the enriched IFN- γ -producing CD4⁺ T cells were potent producers of IFN- γ , and upon exposure to the Th2 skewing cocktail, downregulated IFN- γ production and increased IL-4 production (Fig 5B). However, the ability to produce IL-17 upon incubation with Th17-skewing conditions was lost in the IFN- γ -producing CD4⁺ T cell population, but was retained in the sorted IFN- γ

negative CD4⁺ T cell population (Fig 5B). To further confirm our findings using a highly pure IFN- γ -producing CD4⁺ T cell population, we infected IFN- γ -YFP reporter mice with *M.bovis* BCG via oropharyngeal aspiraton, and sorted CD4⁺CD44⁺YFP⁺ lung cells using a flow cytometric approach. Using this strategy, we obtained a ~90.1% pure IFN- γ -producing CD4⁺ T cell population, which upon exposure to Th2-skewing cytokine cocktail resulted in reduction in IFN- γ production accompanied by an increase in IL-4 production (Fig 5C). IL-17 production was undetectable after incubation under Th17 conditions, suggesting that IL-17 production in CD4⁺ T cells upon exposure to Th17-skewing conditions was likely from a naïve undifferentiated or a differentiated but IFN- γ negative CD4⁺ T cell population (Fig 5B). Taken together, our results indicate that mycobacteria antigen-specific CD4⁺ T cells, although predominantly committed to the Th1 subset in vivo, can be stimulated to acquire the cytokine secretion pattern of Th2 cells ex vivo. In addition, *Mtb*-specific Th17 cells differentiated in vitro can upregulate IFN- γ production in response to signals in the microenvironment. Implicating these findings to an in vivo setting, these results suggest that changes to the lung microenvironment that favor Th2 cell development may redirect the commitment of *Mtb*-specific Th1 cells to a subset with reduced ability to contain the infection. Similarly, Th17 cells may act as bifunctional T cells, producing both IL-17 and IFN- γ .

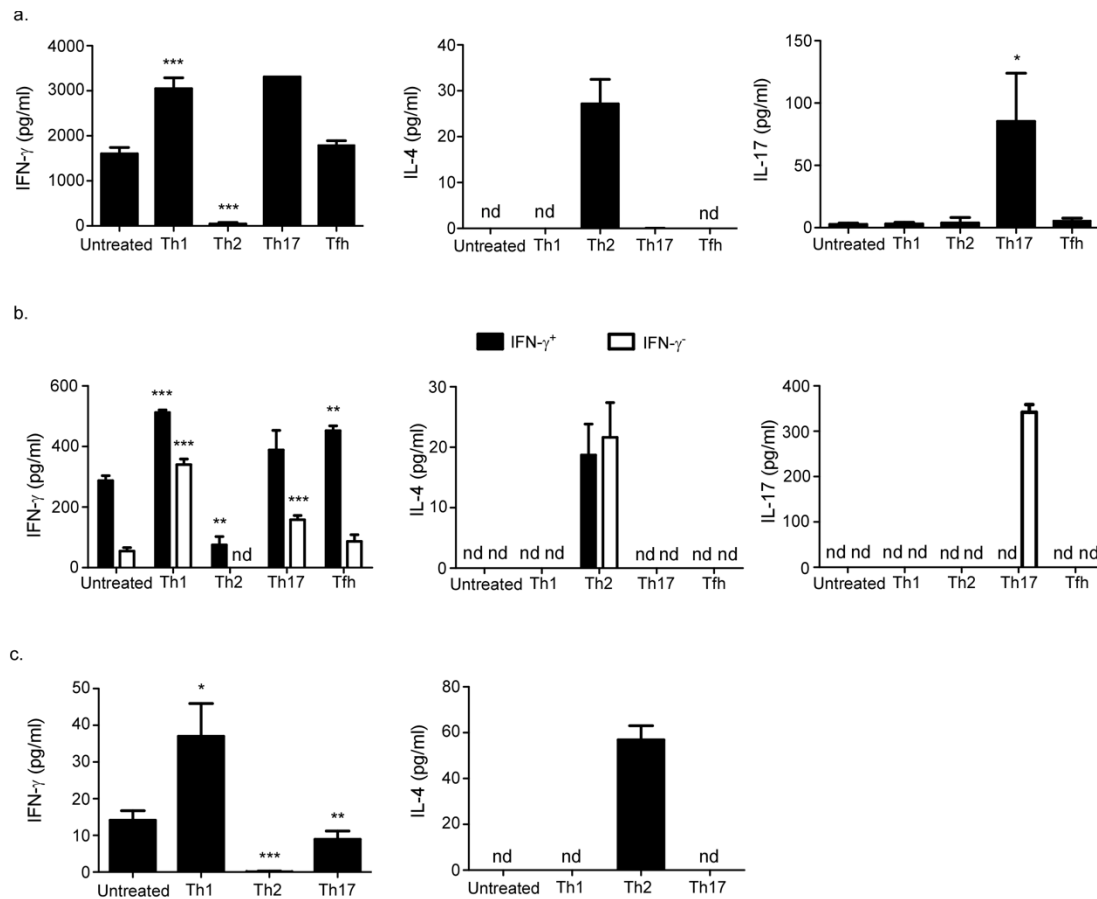


Figure 5. In vivo primed, *Mtb*-specific T cell populations are plastic.

(A) C57BL/6 mice were aerosol infected with ~100 cfu H37Rv *Mtb* and lung CD4⁺ T cells were purified 30 days post-infection. Cells were incubated with cDMEM for 6 days, in the presence of subset-skewing cytokine cocktails, ESAT-6 peptide and IL-2. Cells were washed, restimulated for 48 h with irradiated splenocytes and ESAT-6 peptide and culture supernatants assessed to determine IFN- γ , IL-4 and IL-17 protein levels. (B) IFN- γ -YFP (Yeti) reporter mice were aerosol infected with ~100 cfu H37Rv *Mtb* and lung CD4⁺ T cells were purified on day 50 post-infection. Subsequently, IFN- γ -secreting cells were enriched, leading to a 50% pure population. This IFN- γ^+ cell population, as well as the remaining IFN- γ^- cells, were cultured with cDMEM for 6 days, in the presence of subset-skewing cytokine cocktails, ESAT-6 peptide and IL-2. Cells were washed, restimulated for 48 h with irradiated splenocytes and ESAT-6 peptide and culture supernatants assessed to determine IFN- γ , IL-4 and IL-17 protein levels. (C) IFN- γ reporter mice were i.t. infected with BCG and lung CD4⁺ T cells were purified on day 30 post-infection. Subsequently, CD4⁺CD44⁺IFN- γ^+ cells were purified by FACS, leading to a 91.1% pure population. This IFN- γ^+ cell population was cultured with cDMEM for 6 days, in the presence of different subset-skewing cytokine

cocktails, Ag85 and IL-2. Cells were washed, restimulated for 48 h with irradiated splenocytes and ESAT-6 peptide and culture supernatants assessed to determine IFN- γ and IL-4 protein levels. The data points represent the mean (\pm SD) of values from 3-5 samples. * $p \leq 0.05$, ** $p \leq 0.01$, *** $p \leq 0.001$, ND-not detectable.

IFN- γ production by Th17 cells decreases the potency of recall protection against *Mtb* challenge

Given the ability of adoptively transferred Th17 antigen-experienced cells to co-produce IFN- γ (published data, [107]) and the capacity of in vitro-differentiated Th17 cells to produce IFN- γ in response to IL-12 treatment (Fig 4A), we next sought to determine whether IFN- γ or IL-17 production by Th17 cells was mediating the control upon *Mtb* challenge. Thus, we transferred ESAT-6 TCR Tg IFN- γ -deficient Th17 cells into IL-12p35^{-/-} mice which lack IFN- γ responses (Fig 3B), and determined lung bacterial burden following *Mtb* challenge. Surprisingly, not only was IFN- γ dispensable for Th17-induced protection, but IFN- γ deficiency in Th17 cells further increased protection in IL-12p35^{-/-} mice, when compared to adoptive transfer of IFN- γ -sufficient Th17 cells (Fig 6A). Our recent work has demonstrated a critical role for IL-17 in induction of CXCL-13 and formation of ectopic lymphoid structures in the lung for early *Mtb* control [102, 115]. Consistent with these findings, we found that adoptive transfer of IFN- γ -deficient Th17 cells more efficiently induced localized CXCL-13 protein expression within lymphoid follicles (Fig 6B) and triggered the formation of well-organized B cell follicles in the lungs (Fig 6B,C), when compared to lungs of IL-12p35^{-/-} mice that received IFN- γ -sufficient Th17 cells.

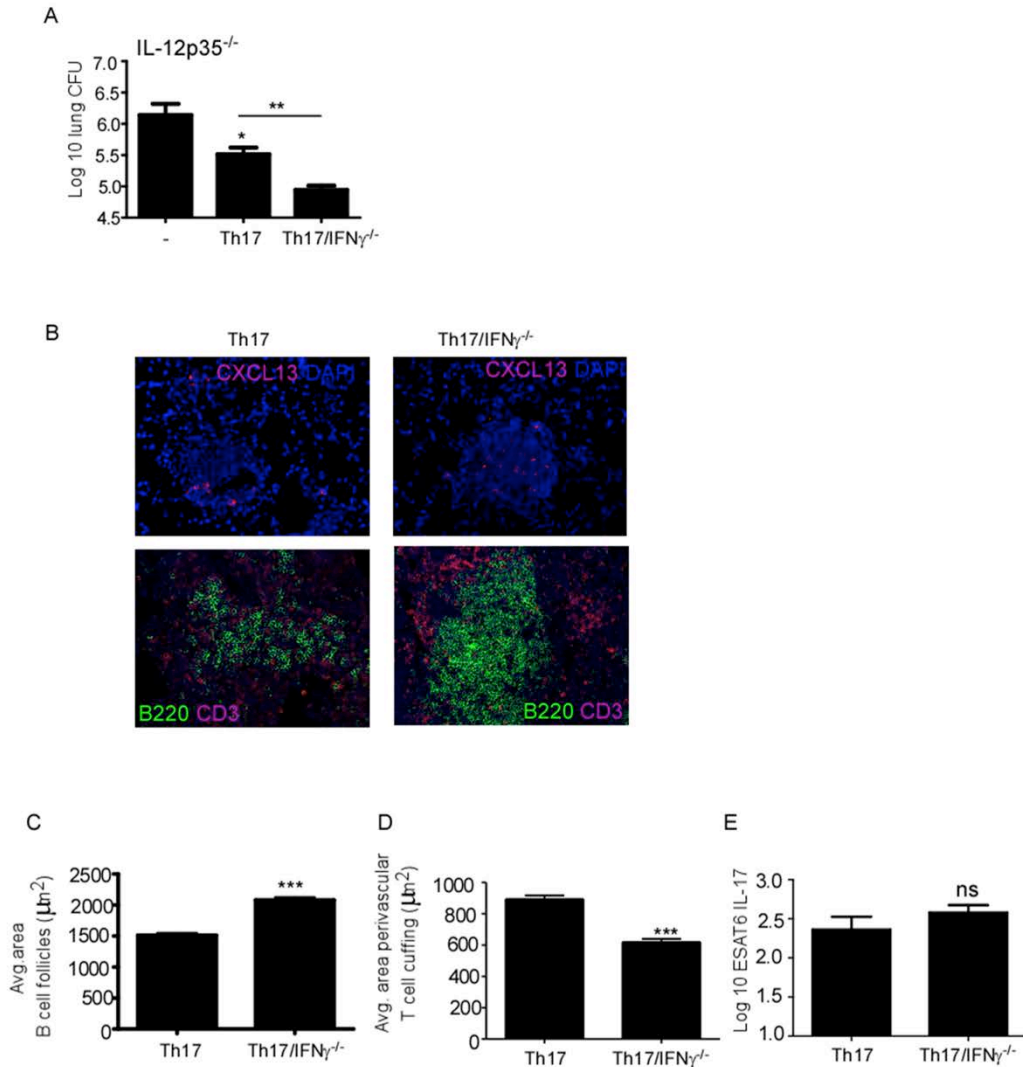


Figure 6. IFN- γ production in Th17 cells decreases the potency of recall protection against *Mtb* challenge.

Th17 cells were differentiated in vitro from IFN- γ -sufficient and IFN- γ -deficient ESAT-6 TCR Tg mice. IL-12p35^{-/-} mice received 2×10^6 ESAT-6 TCR Tg Th17 or IFN- γ -deficient Th17 cells i.v. or were left untreated (-), rested, and aerosol infected with *Mtb*. (A) Lung bacterial burden at 40 dpi was determined by plating on 7H11 agar plates. (B) Formalin-fixed, paraffin-embedded (FFPE) serial lung sections from the above groups were processed for immunofluorescence using antibodies specific for CXCL-13 or B220 and CD3. (C) The average (Avg.) size of B-cell follicles and (D) the average (Avg.) area occupied by perivascular T-cell cuffing were calculated using the morphometric tool of the Zeiss Axioplan microscope. (E) IL-17-producing ESAT-6-specific CD4⁺ T cells were determined via peptide-driven ELISpot. The data points represent the mean (\pm SD) of values from 5 to 8 mice. * $p \leq 0.05$, ** $p \leq 0.01$, *** $p \leq 0.001$, NS, not significant.

Increased ectopic B cell follicle formation also coincided with a reduction in T cell perivascular cuffing (Fig 6D), which is indicative of migration of T cells to areas containing *Mtb*-infected macrophages [102]. These findings together project that not only is IFN- γ production by Th17 cells dispensable for T cell recall immunity against TB, but in fact, presence of early IFN- γ is detrimental to recall immunity against *Mtb* challenge.

M.bovis BCG, the current vaccine against TB, confers protection against pediatric cases of disseminated TB, but its efficacy against adult pulmonary TB ranges from 0 to 80%. Defining the requirements for induction of long-lasting protective immunity is therefore a key parameter in the development of more efficacious vaccines against TB. Thus, we next determined whether Th17-induced protection observed in the IL-12p35^{-/-} mice (Fig 6) was prolonged and whether the absence of IFN- γ in adoptively transferred cells conferred any long-term advantage to *Mtb* control in hosts. Accordingly, we found that although IL-12p35^{-/-} mice that received Th17 cells had short-term protection (Fig 6A), the IL-12p35^{-/-} hosts that received Th17 cells lost the protective effects around 100 days post-challenge (Fig 7A). This was despite the fact that IL-12p35^{-/-} hosts which received Th17 cells had significantly larger B cell follicles (Fig 7B, C), increased localization of CXCL13 protein within follicles (Fig 7C), and decreased T cell perivascular cuffing (Fig 7D), when compared to IL-12p35^{-/-} mice that did not receive Th17 cells.

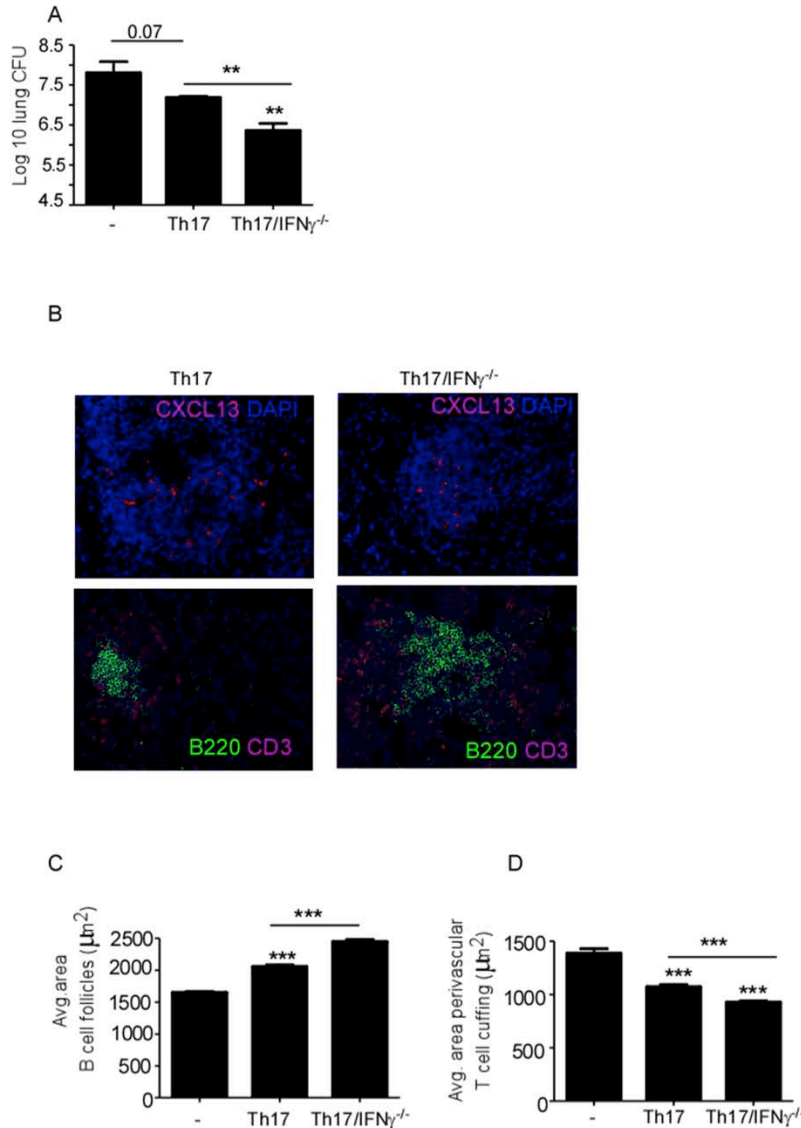


Figure 7. IFN- γ -deficient adoptively transferred Th17 cells induce long-lasting protection against *Mtb* challenge.

IL-12p35^{-/-} mice received 2x10⁶ ESAT-6 TCR Tg Th17 or IFN- γ -deficient Th17 cells i.v. or were left untreated (-), rested, and aerosol infected with *Mtb*. (A) Lung bacterial burden at 100 dpi was determined by plating on 7H11 agar plates. (B) FFPE serial lung sections from the above groups were processed for immunofluorescence using antibodies specific for CXCL-13, and B220 and CD3. (C) The average size of B-cell follicles and (D) the average area occupied by perivascular T-cell cuffing were calculated using the morphometric tool of the Zeiss Axioplan microscope. The data points represent the mean (\pm SD) of values from 5 to 8 mice. **p \leq 0.01, ***p \leq 0.001.

Importantly, transfer of IFN- γ -deficient Th17 cells conferred sustained long-term protection in IL-12p35^{-/-} mice (Fig 7A), and this coincided with significantly larger ectopic lymphoid follicles (Fig 7B,C) and decreased T cell perivascular cuffing (Fig 7D), indicating that the establishment of a certain threshold B cell follicle size may be required for long term *Mtb* containment. These data together for the first time suggest that the ability to produce IFN- γ by Th17 cells may compromise long-term protective ability of T cell recall responses following *Mtb* challenge.

CXCR5 expression on adoptively transferred Th17 cells is critical for the protective recall responses against TB.

We have recently demonstrated that CXCL-13 is a critical chemokine that is necessary for migration of CXCR5-expressing T cells into the lung parenchyma to localize in apposition to *Mtb*-infected macrophages [102]. Using *Cxcr5*^{-/-} ESAT6 TCR Tg Th17 cells, we next determined whether expression of this receptor was required for Th17-driven protection in recall responses to *Mtb* challenge. Thus, we adoptively transferred either no cells, Th17 cells, IFN- γ -deficient Th17 cells or CXCR5-deficient Th17 cells into B6 mice and following a period of rest, challenged mice with low doses of *Mtb*. We found that similar to our data with IL-12p35^{-/-} mice that received IFN- γ -deficient Th17 cells (Fig 6,7), absence of IFN- γ in Th17 cells conferred better recall protection even in B6 mice, when compared to B6 mice that received IFN- γ -sufficient Th17 cells (Fig 8). Most importantly, we found that B6 mice that received CXCR5-deficient Th17 cells exhibited impaired *Mtb* control, while B6 mice that received CXCR5-sufficient Th17 cells conferred protection (Fig 8), suggesting that expression of CXCR5 on Th17

cells is critical for the protective recall responses mediated by Th17 cells. *Cxcr5*^{-/-} mice do not form ectopic lymphoid structures and are more susceptible to *Mtb* challenge [102]. Thus, we next addressed if adoptive transfer of CXCR5-sufficient Th17 cells is sufficient to rescue ectopic structure formation and confer protective recall responses in *Cxcr5*^{-/-} mice. We found that adoptive transfer of ESAT6 TCR Tg Th17 cells into *Cxcr5*^{-/-} mice resulted in improved *Mtb* control (published data, [107]), suggesting that presence of CXCR5 on adoptively transferred Th17 cells was necessary to mediate recall responses in CXCR5-deficient hosts. This was associated with improved B cell follicle formation and diminished T cell perivascular cuffing (published data, [107]). Taken together, these results indicate that CXCR5 expression on Th17 cells during recall responses is necessary for correct localization of T cells within the lung parenchyma near infected macrophages to mediate *Mtb* control.

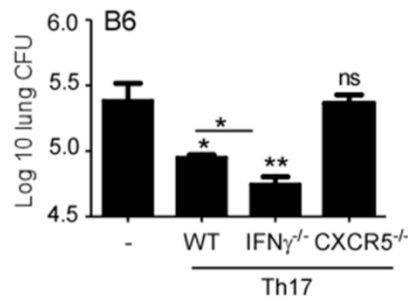


Figure 8. CXCR5 expression on Th17 cells is critical to mediate protective recall responses following *Mtb* challenge.

C57BL/6 (B6) mice received 2×10^6 ESAT-6 TCR Tg wild-type (WT), IFN- γ -deficient or CXCR5-deficient Th17 cells i.v. or were left untreated (-), rested, and aerosol infected with *Mtb*. Lung bacterial burden at 40 dpi was determined by plating on 7H11 agar plates. The data points represent the mean (\pm SD) of values from 5 to 8 mice.

* $p \leq 0.05$, ** $p \leq 0.01$, NS, not significant.

3.4 DISCUSSION

The recent emergence of drug resistant *Mtb* strains [67], the spread of the HIV-TB co-epidemic [67] and the disappointing efficacy data from the recent human clinical trials with MVA85A [71], together highlight the big gaps in our understanding of how protective recall responses function during *Mtb* challenge. If we want to reach the deadline of elimination of TB as a public health problem by 2050, the development of safe and more effective vaccines against TB is urgent and an area of top priority. Early studies projected Th1 responses and the cytokine IFN- γ in primary protection against TB [116], where it plays a role in the potentiation of macrophage killing mechanisms. Thus, most vaccines in the past have used induction of IFN- γ responses as a correlate for vaccine efficacy [117]. However, recent studies have demonstrated that while vaccine-induced protection occurs in the absence of IFN- γ , vaccine-induced recall protection is lost in the absence of IL-17 [64, 84, 105, 106]. Thus, it is now becoming clear that targeting Th17 cells rather than Th1 cells to improve vaccine-induced immunity may enhance the efficacy of future vaccine strategies against TB [117]. However, in order to improve Th17 recall responses, we need to first understand the immune characteristics of Th17 recall responses that confer protection against *Mtb* challenge. Thus, using a Th17 cell transfer model, we have identified that Th17 recall responses are dependent on IL-23, while endogenous IL-12 and IL-21 are not required for effective Th17 recall responses. In addition, we demonstrate that upon *Mtb* challenge, Th17 recall responses appear earlier than naïve or Th1 cells and acquire the ability to produce IFN- γ . This was in line with our demonstration that, in vitro, *Mtb*-specific Th17 cells are plastic, and can increase IFN- γ production in response to culture under Th1 conditions. Importantly, the ability to produce IFN- γ is in fact detrimental to long term protective recall

responses against TB, while expression of CXCR5 by Th17 cells is necessary to mediate strategic positioning of Th17 recall responses within the lung to promote early *Mtb* control. Thus, identification of new immune characteristics of Th17 cells as described in this paper, are critical to harness novel pathways to enhance Th17 recall responses for design of more effective vaccines against TB.

Our new data show that adoptive transfer of ESAT-6-specific Th17 cells into naïve hosts followed by a period of rest and *Mtb* challenge, results in similar levels of protection as prior parenteral vaccination with ESAT-6₁₋₂₀ antigen in adjuvant. IL-23 is as an important factor in differentiation of effector Th17 cells [108]. Accordingly, our early work showed that IL-23p19^{-/-} mice vaccinated with parenteral *Mtb* antigen vaccine had reduced priming of Th17 responses and demonstrated loss of vaccine-induced protection upon *Mtb* challenge, suggesting that IL-23 was critical for initiation of vaccine-induced Th17 responses [84]. However, because IL-23p19^{-/-} vaccinated hosts have defects in initiation of Th17 responses, we cannot use IL-23 deficient hosts to specifically address if IL-23 has a role to play in Th17 recall responses upon *Mtb* challenge. Thus, our studies in the present paper demonstrate for the first time that Th17 cells primed in vitro in the presence of IL-23 also require the presence of IL-23 for effective Th17 recall responses that contribute to protection upon *Mtb* challenge. This is consistent with a recent study that showed an important role for IL-23 in activation of memory Th17 cells in a model of Experimental Autoimmune Encephalomyelitis (EAE) [118]. Interestingly, immune pathways that are important for primary immunity against TB such as IL-12 and IFN- γ are dispensable for Th17 recall responses. Thus, our data show a critical role for IL-23, but not IL-12 and IL-21, in activation of Th17 recall responses for protection against *Mtb* challenge, projecting IL-23 as a

key target pathway in both generation of Th17 responses [84] and activation of Th17 recall responses upon *Mtb* challenge.

Our previous data showed that parenteral vaccination induces a population of antigen-specific Th17 cells in the lungs, which are required for vaccine-induced protection against *Mtb* challenge [84]. Our current data support these findings as they show that adoptive transfer of Th17 cells also results in accumulation and persistence of Th17 cells in the lung compartment, suggesting that specific chemokine receptor expression such as CCR4 on Th17 cells [84], may regulate the preferential accumulation in mucosal compartments. Consistent with these findings, improving lung Th17 populations by mucosal immunization strategies enhances protection against *Mtb* challenge [64, 106]. Our data show that upon *Mtb* challenge, accumulation of Th17 recall responses occurs prior to accumulation of either Th1 recall responses or Th0 cells in the lungs of *Mtb*-infected mice, suggest that the preferential location of Th17 cells in the mucosal compartment may serve an advantage and improve protection upon pulmonary *Mtb* challenge. In addition, although it is interesting that the early accumulation of Th17 recall responses upon *Mtb* challenge coincides with production of IFN- γ , this is not a completely unexpected finding. Several recent studies have projected Th17 cells as inherently plastic and have shown that they can readily acquire the ability to co-produce IFN- γ , especially in inflammatory models [97, 118, 119]. In agreement with our findings, in observing long term vaccine-induced Th17 recall responses to *Mtb* challenge, it was found that not only did IL-17-producing CD4⁺ T cells accumulate in the lung earlier than IFN- γ -producing T cells, but IL-17-producing CD4⁺ T cells also co-produced IFN- γ [85]. However, it is surprising that adoptive transfer of IFN- γ -deficient Th17 cells into host mice results in more protective and long-term control of *Mtb*, suggesting a detrimental role for IFN- γ in recall responses against *Mtb* challenge. As IFN- γ production has

been shown to limit IL-17 production in T cells [120], it is thus possible that IFN- γ deficiency in Th17 recall responses improves IL-17 production and downstream induction of chemokines and enhancement of *Mtb* control. In addition, the increased protection afforded by adoptive transfer of IFN- γ -deficient Th17 cells holds true irrespective of whether IFN- γ -deficient Th17 cells are transferred into B6 mice or IL-12 deficient mice, suggesting that early IFN- γ production by Th17 recall responses is detrimental to *Mtb* control. Our findings are supported by a recent study that used both experimental and mathematical approaches to demonstrate that the control of *Mtb* burden in the lung was not immediate after onset of IFN- γ responses in the lung [121]. As IFN- γ production has been conventionally used as a correlate for vaccine efficacy against TB, our findings instead project an important role for targeting IL-17 while limiting IFN- γ in vaccine design for TB, and as such needs to be explored in different preclinical vaccine models.

IL-17 induces expression of the homeostatic chemokines CCL-19 and CXCL-13 [122], which orchestrate the formation of ectopic B-cell follicles within inducible Bronchus-Associated Lymphoid Tissue (iBALT). Similarly, our recent findings in vaccine models of TB demonstrate that early vaccine-induced Th17 cells produce IL-17 to mediate expression of CXCL-13 in lung stromal cells, enabling CXCR5-expressing T cells to localize near *Mtb*-infected macrophages [64]. Accordingly, our data show that effective Th17 recall responses coincide with localized CXCL-13 expression within lymphoid follicles, improved T cell localization and B cell follicle formation for enhanced *Mtb* control, while CXCR5 deficiency on Th17 cells abrogates the protective effects of Th17 recall immune responses. Similarly, although IL-17 and IL-23 are dispensable for primary immunity against lab adapted strains such as *Mtb* H37Rv, long-term control of *Mtb* is dependent on IL-23, and failure to contain *Mtb* infection in IL-23-deficient mice is associated with reduced B cell follicle formation [123]. More recently, we have shown

that IL-17 is required for protective primary immunity and formation of B-cell follicles upon challenge with emerging clinical strains of *Mtb*, i.e. hypervirulent W-Beijing strains [124], suggesting that design of vaccines for emerging *Mtb* strains must target the generation of Th17 cells for effective long term protection against TB. However, excess IL-17 production has been associated with severe lung pathology during TB [125, 126]. Thus, optimization of antigen delivery strategies that promote the generation and maintenance of lung resident Th17 cells, while minimizing potentially pathological effects of IL-17 should be carefully evaluated in preclinical models. In addition, our T cell plasticity studies demonstrate that Th1 cells primed in vivo during mycobacterial infections can acquire Th2 cytokine production upon ex vivo restimulation. These findings highlight the interesting notion that a Th2-dominant environment, such as that which arises during helminth infection, may alter Th1 responses and bacterial containment. This will be explored in the next chapter.

In conclusion, given the urgency for the development of safe and effective vaccines against TB, identification of immune characteristics of Th17 recall responses as described here can provide novel insights into pathways that can be targeted to improve vaccine design against TB. Our studies suggest that targeting Th17 cells, enhancing expression of CXCR5, or suppressing IFN- γ production in Th17 recall responses may all provide novel avenues and pathways to improve Th17 cell function and improve vaccine efficacy against TB.

3.5 ACKNOWLEDGEMENTS

The author would like to thank Javier Rangel-Moreno, PhD (University of Rochester, NY) for immunofluorescence processing and analysis, Alison Logar for technical assistance with

fluorescence-activated cell sorting and Kristin Griffiths, Samantha Slight and Yinyao Lin for performing the additional experiments referenced but not shown here, which are published in the paper [107]. An additional thanks is offered to Samantha Slight and Radha Gopal for their assistance and instruction during my initial phases in the Khader lab. This work was supported by Children's Hospital of Pittsburgh of UPMC, Washington University in St. Louis, NIH grant HL105427 to S.A. Khader, Children's Hospital of Pittsburgh Research Advisory Committee Grant from Children's Hospital of Pittsburgh of the UPMC Health System to L. Monin, American Lung Association Senior Research Training Fellowship RT-30592, Department of Molecular Microbiology, Washington University in St. Louis, and Alexander and Gertrude Berg Fellowship to K.L. Griffiths. J. Rangel-Moreno was supported by funds of the Department of Medicine, University of Rochester, and U19 AI91036.

4.0 CO-INFECTIONS SHAPE DISEASE OUTCOME DURING TB

4.1.1 Co-endemicity of diseases with TB

The immune requirements for primary control of TB and the optimal responses for vaccine-mediated immunity remain incompletely understood. However, an additional layer of complexity is added by the fact that TB in natural human populations rarely occurs in isolation [127]. For example, in sub-Saharan Africa, HIV, malaria, TB and multicellular parasite infections each cause significant morbidity and mortality [127]. This highlights the notion that in many regions of the world, individuals may display concurrent immune responses to several pathogens, which can affect one another.

Perhaps the best studied co-infection between *Mtb* and another pathogen is the HIV-TB syndemic [128]. HIV infection is the major risk factor for progression to active TB, increasing the risk for TB reactivation by 20 to 30-fold [14]. In turn, TB is the most common single cause of death in individuals with AIDS, accounting for 26% of AIDS-related deaths [129]. It has been estimated that about 14 million individuals are co-infected with HIV and *Mtb* [130], which greatly adds to the mortality and impact of each individual pandemic. The reduction of CD4⁺ cell counts associated with progression to AIDS contributes to the increased reactivation rates in HIV-*Mtb* co-infected individuals [131, 132]. Additional immune changes, such as impairment of CD8⁺ T cell responses, up-regulation of *Mtb* receptors in macrophages [133], changes in

macrophage killing capacity [134] and impaired chemotactic mechanisms [135] may all contribute to less efficient TB control in HIV-infected individuals.

Malaria causes approximately 200 million new infections and over 500 000 deaths every year. It is an arthropod-borne disease, spread by female mosquitoes of the genus *Anopheles*, and can be caused by five species of parasites of the genus *Plasmodium* [136]. Similar to TB, it is endemic in tropical and developing regions of the world, and its effect on *Mtb* control has been explored in several studies. Co-infection between *Mtb* and *Plasmodium* exacerbated *Mtb* bacterial burden and led to increased mortality in a mouse model [137]. More recently, a different study showed that *Plasmodium* infection increased *Mtb* bacterial burden, while enhancing lung pathology and dysregulating T cell responses in mice [138]. Importantly, a study conducted in a hospital in Guinea-Bissau showed that increasing preventive measures for malaria, including bed nets, vector control and anti-malaria prophylaxis reduced the mortality in TB patients [139]. Together, these findings indicate that malaria may hinder TB control and promote reactivation in co-infected patients.

The outcome of co-infection on TB disease control, however, is not always detrimental to the host. *Helicobacter pylori*, which infects the gastric mucosa and epithelial lining of the stomach, and is the leading cause of gastric cancer and peptic ulcers, infects about 80% of individuals in TB-endemic regions [140]. Similar to *Mtb*, *H. pylori* induces the secretion of numerous proinflammatory cytokines, including IFN- γ , TNF- α , IL-1 β and IL-6 [141]. In addition, high IL-12 production leads to the differentiation of Th cells to the Th1 subset [142]. Interestingly, a recent study has shown that a cohort of individuals from California who were seropositive for *H.pylori* and PPD positive had enhanced IFN- γ production in response to TB antigens. In addition, *H. pylori*-infected individuals were less likely to progress to active TB in a

separate Gambian cohort, and these findings were validated in a NHP model [143]. Together, these results suggest that *H. pylori* co-infection may play a beneficial role in *Mtb* containment.

4.1.2 Helminth modulation of host immune responses

Helminth parasites constitute a broad group of organisms that can cause pathology in vertebrate hosts. It is estimated that approximately 1 billion people living in developing regions of the world are infected with one or more helminths [144]. Although rarely lethal, helminths tend to establish chronic infections, which limit cognitive development and lead to stunted growth in children [145], and contribute to morbidity in adults. Their complex life cycle involves invasion of intermediate and definitive hosts, which in humans often occurs via the oral or skin route. Following invasion, parasites can establish themselves in different organs of the definitive host, which can range from the gastrointestinal tract, to the lungs, liver, circulatory system and brain [146].

However, despite evolutionary divergence, immune responses against such parasites are strikingly conserved, and greatly differ from those induced by viruses and bacteria. Adaptive immune responses against helminths are characterized by the activation of Th2 cells, which secrete IL-4, IL-5 and IL-13 and antagonize Th1 responses [147]. These mediators lead to the activation of several effector mechanisms, including antibody class switch to IgE, activation of eosinophils, mast cells and basophils, increased smooth muscle contractility and mucus secretion [146]. The relative contribution of each mechanism to host defense against helminths varies depending on the specific infecting species.

In addition, although these responses are well adapted to parasite elimination, they often contain a regulatory component, elicited by the parasite, which compromises clearance of the

parasite but protects the host from excessive damaging immunopathology [147, 148]. This is particularly important as helminths generally establish chronic infections, each individual worm having a lifespan that can range from months (in the case of gastrointestinal nematodes) to decades (in the case of schistosomes). Regulation of inflammation is one of the mechanisms through which these parasites can ensure their continued survival in their definitive host, and this can occur at multiple levels. Macrophages acquire an alternatively activated phenotype in response to helminth molecules, which is characterized by increased Arginase-1, Ym-1 (chitinase-3-like-3) and RELM- α (resistin-like molecule α) expression [147]. Together, these molecules can regulate tissue repair processes, and are involved in extracellular matrix repair, wound healing and fibrosis. In addition, alternatively activated macrophages (AAMs) can secrete anti-inflammatory cytokines, including IL-10 and TGF- β . Unlike classic macrophage activation, AAMs possess decreased iNOS expression, inhibit T cell proliferation *in vitro* and mediate fibrosis. Helminth products similarly affect other cells of the innate immune system. DCs exposed to helminth antigens possess decreased expression of costimulatory molecules, including CD40, CD80 and CD86, and preferentially drive Th2 and Treg differentiation [149]. Further, parasite-specific T cell responses are inhibited in chronic helminth infections, as evidenced by the antigen-specific hyporesponsiveness of blood T cells following *in vitro* restimulation PBMCs of patients with Schistosomiasis [150]. Interestingly, such effects were reversible, and dependent on parasite persistence, as antihelminthic drug treatment abolished the inhibition [150]. Finally, helminths can lead to the activation and accumulation of several regulatory cell types, including Foxp3⁺ Tregs [151], IL-10-producing Tr1 cells [152] and regulatory B cells (Bregs) [153] in *Schistosoma* infections.

4.1.3 Tuberculosis and helminth co-infections

As we described in the previous section, helminth parasites skew the immune response to a Th2 response and simultaneously limit the establishment of immune responses that would lead to their elimination. These immune changes, however, are not confined to parasite-specific responses, as helminth infections have been linked to impaired immune responses to vaccines [154] and co-infecting pathogens [155]. Interestingly, these regulatory mechanisms can be beneficial in conditions of pathologic inflammation, including allergy [153] and autoimmunity [156, 157].

The single factor that most strongly impacts efficacy of the BCG vaccine is geographical latitude. Indeed, protection from adult pulmonary TB is lowest in developing countries found within 30 degrees latitude of the equator. In addition, the death rates from TB during the first 2 months of antibiotic regime initiation are high in developing countries. Despite the presence of confounding factors, including co-infection with HIV, difficulty in access to health care and disease severity at the time of diagnosis, death rates remain higher even when these factors are taken into account. Among the proposed hypotheses to explain this phenomenon is modulation of anti-mycobacterial immune responses by co-infecting helminths. Indeed, several studies suggest that infection with parasitic worms hinders the ability to mount efficient anti-mycobacterial responses.

Human studies on co-infected individuals suggest that infection with helminths compromises protection conferred by *M. bovis* Bacillus Calmette-Guerin (BCG) vaccination [158-160], and may be associated with increased TB reactivation rates in HIV-infected patients [161]. In addition, antihelminthic treatment of individuals who were immunized with BCG vaccination resulted in increased proliferation and IFN- γ production by peripheral blood

mononuclear cells (PBMC) in response to PPD stimulation [162]. In experimental models, mice chronically infected with *Schistosoma mansoni* have increased susceptibility to *M. bovis* BCG systemic infection, accompanied by decreased *M. bovis* BCG-specific Th1 responses [163]. Additionally, *S. mansoni*-infected mice vaccinated with *M. bovis* BCG demonstrate reduced protection upon subsequent *Mtb* systemic challenge [164]. In a mouse model of *Mtb* infection, repeated infections with *Nippostrongylus brasiliensis* led to a significant increase in bacterial burden. This effect correlated with AAM accumulation, but T cell responses were unaltered [165]. Thus, the prevailing models suggest that Th2 responses or their effector mechanisms, induced due to helminth co-infections, impair Th1 immune responses and *Mtb* control.

4.1.4 *Schistosoma mansoni*

Approximately one billion people are infected with one or more helminths, of which schistosomiasis, caused by trematodes of the genus *Schistosoma*, affects about 207 million individuals [166]. *S. mansoni* leads to about 130,000 deaths ever year and is a significant cause of morbidity in many infected individuals, causing diarrhea in 780,000 individuals, blood in stool in 4.4 million and hepatomegaly in 8.5 million [167]. Two main clinical conditions can be observed in *S. mansoni*-infected individuals- acute or chronic schistosomiasis. The former, also known as Katayama fever, occurs during the first 6 to 8 weeks of infection, and is characterized by elevated levels of serum TNF, IL-1 and IL-6. Interestingly, it most frequently presents in individuals who are traveling to endemic areas and mount strong Th1 rather than Th2-skewed immune responses [168]. Chronic schistosomiasis, in turn, can present in its most severe form as hepatosplenic disease with hepatic fibrosis, hepatosplenomegaly and portal hypertension, which arises from persistent immune granulomatous responses to *S. mansoni* eggs that become lodged

in the liver [169, 170]. Efforts to control this disease include elimination of the snail intermediate host, the prevention of sewage waste contamination of freshwater, avoiding human contact with water containing infected snails and treatment of infected individuals. In this regard, praziquantel is the most widely used drug against *S. mansoni*. Several factors have contributed to its widespread use, including its effectiveness after only one oral dose, lack of toxicity and low cost (US\$ 0.15 per child and US\$ 0.30 per adult) [171]. Its exact mechanism of action remains unknown, but is thought to involve activation of calcium channels and disruption of adenosine absorption from the host, a process that is essential for parasite survival. In addition, praziquantel has been shown to increase antigen expression on the worm surface, increasing *S. mansoni* targeting by host antibodies [171].

Flukes of the *Schistosoma* genus differ from other helminths in four ways: they have only two hosts, are non-hermaphroditic, they infect their definitive hosts through breaching the skin barrier rather than via ingestion, and reside in the circulatory system [168]. *Schistosoma mansoni*'s life cycle is shown in Figure 9. *Schistosoma mansoni* eggs are eliminated in the feces of infected individuals, which can reach freshwater reservoirs if there is contamination with human sewage (Fig 9A). These eggs hatch, releasing miracidia (Fig 9B), which can swim by ciliary movement until they invade an intermediate snail host (Fig 9C). Within the snails, miracidia develop into sporocysts, which have the potential of giving rise to thousands of cercariae (Fig 9D). Cercariae are then liberated into freshwater, where they can then swim and penetrate the skin of a definitive vertebrate host (Fig 9E). Upon entry, these parasites shed their tails and become schistosomulae, and migrate predominantly to the mesenteric veins of the large intestine and develop into male or female adult parasites (Fig 9F). Upon pairing, adult males and females reproduce, each couple producing up to 300 eggs per day (Fig 9G). The released eggs

pierce their way through the intestinal wall into the lumen and are excreted in the feces (Fig 9H), thereby completing the cycle.

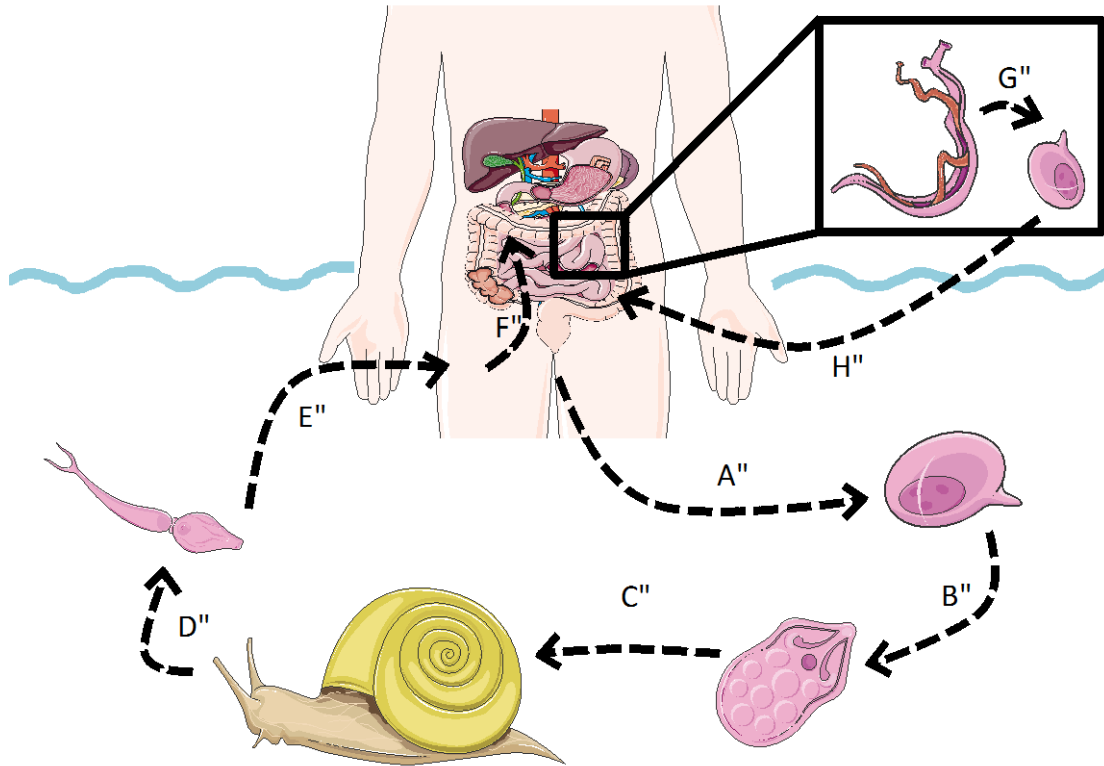


Figure 9. *Schistosoma mansoni* life cycle.

(A) *S. mansoni* eggs are eliminated in the feces of infected individuals, which can reach freshwater reservoirs if there is contamination with human sewage. (B) These eggs hatch, releasing miracidia, which swim by ciliary movement (C) until they invade an intermediate snail host. (D) Within the snails, miracidia develop into sporocysts, which have the potential of giving rise to thousands of cercariae. (E) Cercariae are then liberated into freshwater, where they can then swim and penetrate the skin of a definitive vertebrate host. (F) Upon entry, cercariae shed their tails, becoming schistosomulae, which migrate predominantly to the mesenteric veins of the large intestine and develop into male or female adult parasites. (G) Upon pairing, adult males and females reproduce, each couple producing up to 300 eggs per day. (H) The released eggs pierce the intestinal wall into the lumen and are excreted in the feces, thereby completing the cycle. Figure was produced using Servier Medical Art (www.servier.com).

The nature of the immune response to *S. mansoni* is thought to proceed through three phases [168]. During the initial 3-5 weeks, prior to the development of adult worms, T cells mainly develop into the Th1 subset. However, at the onset of egg production between 5-6 weeks post-infection, the immune response switches toward a Th2 type. Interestingly, egg deposition has been shown to trigger this Th2 differentiation, and numerous studies have used *Schistosoma* egg antigens (SEA), an egg lysate, to explore the mechanisms driving this immune response in the absence of the tissue damage caused by the presence of the live parasite. Subsequently, as the infection reaches its chronic phase, a regulatory component arises, dampening Th2 inflammation.

In this work, we have studied the effect of *S. mansoni* infection on a subsequent *Mtb* infection using a mouse model. Our previous findings showed that T cells in *Mtb* infection are plastic, with *Mtb*-specific Th1 cells being able to acquire Th2 cytokine production after in vitro treatment under Th2-skewing conditions. In addition, several studies have shown that innate immune cells differ between *Mtb* and helminth infections. This suggests that immune changes induced by helminth infections may reduce the effectiveness of anti-*Mtb* immune responses. Importantly, this posits the interesting notion that deworming may serve as a simple, cost-effective strategy to improve *Mtb* control and limit TB reactivation in individuals living in areas of high TB and helminth co-endemicity.

5.0 THE EFFECT OF SCHISTOSOMA MANSONI CO-INFECTION AND ANTIGENS ON TUBERCULOSIS

5.1 SUMMARY

Helminths are endemic in populations where tuberculosis (TB) prevalence is highest. Human studies suggest that helminth co-infections contribute to increased susceptibility to TB and increased rates of TB reactivation. The prevailing models suggest that Th2 responses induced due to helminth co-infections impair Th1 immune responses and limit *Mycobacterium tuberculosis* (*Mtb*) control. Using a pulmonary mouse model of *Mtb* infection, we show that *Schistosoma mansoni* co-infection or treatment with *S.mansoni* egg antigens can reversibly impair *Mtb*-specific T cell responses without affecting macrophage mediated *Mtb* control. Instead, *S. mansoni* infection results in accumulation of high arginase-1-expressing macrophages in the lung, forming type 2 granulomas and mediating exacerbated inflammation in *Mtb*-infected mice. In a *Mtb*-infected genetically diverse mouse population, increased lung inflammation is also associated with enhanced arginase-1 activity. Most importantly, increased serum activity of arginase-1 in human pulmonary TB patients correlates with lung damage, and serum arginase-1 activity is increased in TB patients co-infected with helminths. Thus, helminth co-infections induce arginase-1-expressing type 2 granulomas and increase inflammation and TB disease severity; effects that can be reversed by treatment with anti-helminthics. Thus, our data provide

novel insights into the mechanisms by which helminth co-infections drive increased susceptibility, disease progression and severity in TB.

5.2 METHODS

Human tissue samples and patient diagnosis.

Fresh blood samples from ATB patients were obtained from patients recruited to the Tuberculosis Outpatient Clinic, INER, Mexico or NIH-NIRT-ICERT, Chennai, India. Serum samples from all patients with ATB were collected prior to anti-*Mtb* treatment and did not present co-morbidities such as diabetes, HIV, cancer and COPD. For ATB patients, chest radiographs were assessed for the presence, distribution and extent of pulmonary abnormalities, such as airway consolidation and fibrosis, lung distortion, traction bronchiectasis, irregular interfaces and parenchymal bands. We developed a quantitative scale for measuring the degree of lung damage, according to the profusion of pulmonary abnormalities. The pulmonary parenchyma was evaluated in four quadrants with the division between the upper and lower lung in both sides being arbitrarily set at the carina section. Each quadrant was scored from 0 to 5, where 0 denotes absence of lesions and 5 is the maximum affection. The score represented the percentage of lung parenchyma involvement. The maximum score for the four lung zones was 20 [126]. The images were blinded and the same image was read twice separately by an experienced observer (pulmonologist researcher). The reported score is the mean of two measurements.

Buffy coats from 20 mL of EDTA anticoagulated peripheral blood from ATB and LTB patients, who signed an informed consent letter, were obtained at the Tuberculosis clinic of the INER. Total peripheral blood mononuclear cells (PBMCs) were obtained by density gradient

centrifugation using Lymphoprep (Axis-Shield, Oslo, Norway). CD14⁺ monocytes were purified using magnetic beads (Miltenyi, Auburn, CA, USA). Purity of isolated monocytes was assessed by flow cytometry using anti-human monoclonal antibodies: CD14-FITC and CD3-PE-Cy7 (BioLegend, San Diego, CA, USA), obtaining > 97% purity. Total RNA was isolated from monocytes for real time RT-PCR expression assays using validated TaqMan assays.

In samples collected from NIH-NIRT-ICER, Chennai, India, we studied a group of 44 individuals with active pulmonary TB, 22 of whom were infected with the helminth *Strongyloides stercoralis*. Active pulmonary TB was diagnosed microbiologically on the basis of being at least culture positive for *Mtb* by solid cultures in LJ medium (some were also sputum smear positive). *Strongyloides* infection was diagnosed by the presence of IgG antibodies to the 31-kDa recombinant NIE antigen by the Luciferase Immunoprecipitation System Assay, as described previously [172].

Animals.

C57BL/6 mice were purchased from Taconic Labs, and IFN- γ -YFP reporter mice were obtained from Dr. Markus Mohrs, Trudeau Institute [173]. ESAT-6 (Early Secreted Antigenic Protein 6) transgenic (Tg) mice, expressing the $\alpha\beta$ TCR specific for the IAb-presented ESAT-6₁₋₂₀ peptide were kindly provided by Dr. G. Winslow (Wadsworth Center, Albany, NY) and Dr. D. Woodland (Trudeau Institute, Saranac Lake, NY) [101]. The ESAT-6 TCR Tg mice were maintained on the *Rag1*^{-/-} background. Yarg (Arginase-1 eYFP reporter mice), C57BL/6.SJL and DO mice were purchased from Jackson Labs. *Tie2*^{Cre}*Arg1*^{flox/flox} bone marrow as well as *Arg1*^{flox/flox} (WT) mice were used as before [174]. Mice strains were bred and maintained in house either at the University of Pittsburgh or Washington University in St.Louis. Experimental mice were age-and sex-matched and used between the ages of 6-8 wks in accordance with

Animal Care and Use Committee guidelines.

***Mtb* aerosol infection, *S.mansoni* infection and and immunizations.**

Mtb strain H37Rv was cultured in Proskauer Beck medium containing 0.05% Tween 80 to mid-log phase and frozen in 1 ml aliquots at -80°C. For *Mtb* infections, animals were aerosol infected with ~100 Colony Forming Units (CFU) of bacteria using a Glas-Col airborne infection system. At given time points, organs were harvested, homogenized and serial dilutions of tissue homogenates plated on 7H11 agar plates supplemented with OADC. Additionally, lung samples were processed for RNA extraction, histology and cytokine determination. For *S. mansoni*, *Mtb* co-infections, mice were infected by percutaneous exposure to 55 *S. mansoni* cercariae (Puerto Rican strain, Naval Medical Research Institute) 6 weeks prior to *Mtb* aerosol challenge. *S.mansoni* liver egg burden was determined by overnight digestion of the liver in 4% KOH at 37°C. Eggs were enumerated by microscopic observation of the liver suspensions. SEA was prepared as described before [175]. For immunizations, 50µg of SEA, BSA or PPD were subcutaneously administered to mice as described before [175].

Antihelminthic treatment.

S.mansoni treatment was performed by oral gavage with 6.25 mg of praziquantel in a volume of 300µL [176]. *S.mansoni*, *Mtb* co-infected mice received 3 doses of praziquantel, 24, 72 and 120 hrs following *Mtb* infection. Control mice instead received 300µL of PBS.

Generation of BMC mice.

To generate BMC mice, we treated C57BL/6.SJL mice with Sulfamethoxazole and Trimethoprim (Hi-Tech Pharmacal) in the drinking water for 2 weeks prior to irradiation. Mice

were sublethally irradiated with 1000 rad and were reconstituted with $5-10 \times 10^6$ bone marrow cells from either WT control ($Arg1^{flox/flox}$) or $Tie2^{cre} Arg1^{flox/flox}$ mice via i.v. injection as before [102]. Mice were allowed to reconstitute for 6 weeks while continuing to receive antibiotic water, after which they were used in experimental procedures. Bone marrow reconstitution was verified by flow cytometric analysis of peripheral blood cells.

Modified Cornell mouse model of latent tuberculosis.

C57BL/6 mice were aerosol infected with ~100 CFU of *Mtb* H37Rv using a Glas-Col airborne infection system and rested for 30 days. Mice were subsequently treated for 6 weeks with rifampicin (100mg/L) and isoniazid (200mg/L) in the drinking water [126]. After a 2 week period, mice received either 2 subcutaneous immunizations of 50 μ g SEA or PBS. Lung and spleen bacterial burden was determined 2 weeks after the second immunization, as described above.

CD4⁺ T cell isolation, in vitro T cell differentiation and restimulation.

Single cell suspensions from DNase/collagenase-treated lung tissue or spleen were prepared as previously described [84]. CD4⁺ T cells from secondary lymphoid organs of ESAT-6 TCR Tg mice or from the lungs of *Mtb*-infected mice were isolated using magnetic CD4⁺ beads (GK1.5, MiltenyiBiotech), according to the manufacturer's instructions. For SEA treatment, cells were incubated in the presence of irradiated splenocytes, 5 μ g/ml ESAT-6 peptide, 10U/mL IL-2 with 50 μ g/ml SEA. T cells were incubated for six days at 37°C and 5% CO₂ and supplemented with an equivalent volume of media containing IL-2 (10U/ml) on day 3. Control cells were incubated using the same peptide and cytokine concentrations in the absence of SEA. After 6 days, T cells were restimulated with irradiated splenocytes and 5 μ g/mL ESAT-6 peptide for 48h.

Tissue culture supernatants were then harvested and used in ELISA, while cell pellets were processed for RNA extraction.

Arginase-1 activity determination.

Arginase-1 activity in serum or lung homogenates was determined using the QuantiChrom Arginase Assay Kit (BioAssays Systems, Hayward, CA). For serum samples, urea was eliminated by performing 2 washes with PBS through Amicon Ultra 0.5 (10kDa cutoff, Millipore). For lung homogenates, protein concentration was adjusted to 100 μ g/mL. 40 μ L of sample was incubated at 37°C for 120 minutes in the presence or absence of 10 μ L of 5X assay reagent. Urea levels were subsequently detected and calculated according to the manufacturer's instructions. Arginase-1 activity is expressed as U/L of sample.

Cytokine and chemokine protein determination.

Culture supernatants or lung homogenates were generated and cytokine and chemokine concentrations were determined by sandwich ELISA (Mouse DuoSet ELISA-R&D Systems) or Luminex (Millipore), according to the manufacturer's instructions.

Flow cytometry.

Single-cell lung suspensions from lung tissue were stained with fluorochrome-labeled antibodies specific for CD3 (145-2C11), CD4 (RM4-5), CD44 (IM7), CD11c (HL3), CD11b (M1/70), MHC class II (M5/114.15.2) or isotype control antibodies (BD Biosciences). For intracellular cytokine staining, lung cell suspensions were stimulated with 50ng/mL PMA (Sigma-Aldrich), 750ng/mL ionomycin (Sigma-Aldrich) and GolgiStop (BD Biosciences) for 5 hours at 37°C. Following Fc block incubation (BD Biosciences), surface staining was carried out. Cells were then permeabilized with Cytofix-Cytoperm solution (BD Biosciences), and stained with anti-IFN- γ (XMG1.2) or anti-IL-4 (11B11) (BD Biosciences). Cells were analyzed

using a Becton Dickinson LSR II flow cytometer using FACS Diva software. Cells were gated based on their forward by side scatter characteristics and the frequency of specific cell types was calculated using FlowJo (Tree Star, CA). Mean fluorescence intensity was also determined to define expression levels of different molecules using FlowJo.

Real-time PCR.

RNA was extracted using the RNeasy kit (Qiagen) and cDNA was then amplified with FAM-tagged probes and PCR primers on a Vii7 thermocycler. Specific gene expression was calculated relative to *Gapdh* expression. Primer and probe sequences targeting specific genes were commercially purchased (ABI Biosystems).

Detection of IFN- γ -producing cells by ELISpot.

ESAT-6₁₋₂₀-specific IFN- γ -producing CD4⁺ T cells from infected lungs were quantified using peptide-driven ELISpot. Briefly, 96-well ELISpot plates were coated with monoclonal anti-mouse IFN- γ (R46A2, eBioscience) in phosphate-buffered saline and blocked with media supplemented with 10% FBS. Cells from lungs were plated at an initial concentration of 5×10^5 cells/well and serial two-fold dilutions were made. Restimulation was carried out in the presence of 1×10^6 cells/well C57BL/6 irradiated splenocytes, ESAT-6₁₋₂₀ peptide (10 μ g/mL) and mouse rIL-2 (10U/mL). After 24 hours, plates were washed and probed with biotinylated anti-mouse IFN- γ (XMG1.2, eBioscience). Spots were enumerated using a CTL-immunospot S5 MicroAnalyzer. No spots were detected in cultures lacking antigen.

RNA seq.

Total RNA was isolated using the RNEasy Mini kit (Qiagen, Hilden, Germany) and RNA integrity was determined with the Agilent 2100 Bioanalyzer (Carlsbad, CA). Briefly, mRNA was purified from 2–5 μ g of total RNA using Sera-Mag Oligo(dT) Beads, fragmented with

magnesium-catalyzed hydrolysis and reverse transcribed into cDNA using random primers (Superscript II; Invitrogen). Then, cDNA underwent end repair with T4 DNA polymerase and Klenow DNA polymerase, followed by the addition of 'A' bases to the 3' end, and ligation to adaptor oligos. Products from the ligation were run on a 2% agarose gel. A gel slice consisting of the 200 bp region (+/-25 bp) was excised and used as a template for PCR amplification. The final PCR product was purified, denatured with 2 N NaOH, and diluted to 10–12 pM prior to cluster amplification on a single-read flow cell v4, as outlined in the Single Read Cluster Generation Kit v4 (Illumina). The flow cell was sequenced on an Illumina Genome Analyzer II.

We mapped reads to *Mus musculus* (mm9) reference transcriptome from GenBank using the bwa alignment tool. For sample-wise data normalization, we applied DESeq using R statistical software. To achieve more reliable results, we applied 3 popular methods for detecting differentially expressed genes (DEGs) using RNAseq data: edgeR, DESeq and baySeq. We considered genes detected by at least 2 methods as DEGs when they had a q-value (FDR) less than 0.05. Pathway analysis was performed using Ingenuity IPA. P-values from Fisher's exact test were adjusted by Benjamini-Hochberg multiple testing correction.

Morphometric analysis and Immunofluorescence.

Lungs from *Mtb*-infected mice were inflated with 10% neutral buffered formalin and paraffin embedded. Lung sections were stained with H&E stain (Colorado Histo-Prep) and processed for light microscopy. To visualize collagen deposition, Gomori's trichrome staining (Sigma Aldrich, MO) was performed according to the manufacturer's instructions. Mucus was detected by Periodic acid-Schiff (PAS) stain. Slides were prepared for immunofluorescent staining by deparaffinization and subsequent rehydration by washes with xylene, alcohol and PBS. Antigen retrieval was performed using a DakoCytomation Target Retrieval Solution,

followed by blocking with 5% (v/v) normal donkey serum and Fc block (5ug/mL, 2.4G27). Endogenous biotin was neutralized with avidin followed by biotin (Sigma-Aldrich). Sections were stained with goat anti-mouse CD3ε (M-20; Santa Cruz Biotechnology), rat anti-mouse B220 (RA3-6B2; BD Pharmingen), inducible NO synthase (goat anti-mouse, M-19; Santa Cruz Biotechnology), F4/80 (MCA497GA, Serotec), Arginase-1 (rabbit anti-Arginase I, H-52, Santa Cruz Biotechnology) and biotin monoclonal mouse anti-mouse Muc5AC (45M1; Abcam). Primary antibodies were detected with secondary antibodies conjugated to Alexa fluor 568 for iNOS and CD3 (A-11057, Life Technologies). Donkey anti-rat Ab conjugated to Alexa Fluor 488 was used to visualize B220 (A-21208, Life Technologies), donkey anti-rabbit conjugated to FITC was used to visualize Arginase-1 (711-095-152, Jackson Immunoresearch laboratories). Streptavidin-Alexa Fluor 488 was used to visualize Muc5AC (Life Technologies). Slow fade gold antifade with DAPI (Life Technologies) was used to counterstain tissues and to detect nuclei. Images were obtained with a Zeiss Axioplan 2 microscope and were recorded with a Zeiss AxioCam digital camera. Caudal lobes underwent morphometric analysis in a blinded manner using the morphometric tool of Zeiss Axioplan microscope, which determines the area defined by the squared pixel value for each granuloma and B cell follicle [102].

In vitro *Mtb*-killing assay.

Bronchoalveolar lavage was performed on euthanized naïve C57BL/6 mice with sterile PBS containing 0.2 mM EDTA. Following centrifugation, cells were incubated for 1 h at 37°C, after which adherent cells were used for subsequent studies. CD4⁺ T cells from *Mtb*-infected mice were sorted as previously described and treated in the presence or absence of SEA for 6 days. Following restimulation, T cells were washed extensively and then layered over *Mtb*-infected alveolar macrophages (MOI 1:1) for 6 days. At the end of the culture period,

macrophages were washed twice with PBS, lysed by a 5 min incubation with 0.05% SDS. Following SDS neutralization with 10% BSA, intracellular *Mtb* burden was determined by plating of serial dilutions on 7H11 plates.

Detection of nitrites by the Griess reaction.

Culture supernatants were assessed for nitrite production by using the Griess Reagent System Kit (Promega, Madison, WI), according to the manufacturer's instructions.

Statistical Analysis.

Differences between the means of multiple experimental groups were analyzed using one-way ANOVA with Tukey's post-hoc test. For all other analyses, we used the two-tailed Student's t-test. Correlation between variables was determined by calculating Pearson's coefficient using a two-tailed analysis. Differences were considered significant when $p \leq 0.05$. For all figures, data represent mean \pm SD. All analyses were performed using GraphPad Prism Software.

Study approval.

All individuals were examined as part of a clinical research protocol approved by the Institutional Review Board of the Tuberculosis Outpatient Clinic, INER, Mexico or NIH-NIRT-ICERT, Chennai, India and informed written consent was obtained from all participants. All mice were used following the National Institutes of Health guidelines for housing and care of laboratory animals and in accordance with University of Pittsburgh and Washington University in St. Louis Institutional Animal Care and Use Committee guidelines. All efforts were made to minimize suffering and pain as described in these approved protocols.

5.3 RESULTS

***S. mansoni* co-infection induces lung fibrosis and exacerbates inflammation during TB**

Although helminth co-infections are thought to increase susceptibility to *Mtb* infection, the mechanisms underlying this association remain poorly understood. To experimentally model helminth and *Mtb* co-infection, we infected C57BL/6 Arginase-1 Yellow Fluorescent Protein (YFP) reporter mice (Yarg mice) with *S. mansoni* and allowed helminth infection to progress for 6 weeks, a period associated with induction of potent Th2 responses [177]. Following this, mice were infected with low doses of aerosolized *Mtb* and TB disease progression was monitored. Mice co-infected with *S. mansoni* and *Mtb* had larger inflammatory granulomas in the lungs (Fig 10A and 11A-upper panel), which contained both eosinophils and neutrophils (Fig 11A-lower panel). In contrast, smaller and more lymphocytic granulomas were detected in the lungs of *Mtb*-infected mice (Fig 10A and 11A). The increased inflammatory response coincided with a significant increase in the number of arginase-1-expressing macrophages in *S. mansoni*, *Mtb* co-infected mice, when compared to *Mtb*-infected mice (Fig 10B). In addition, increased pulmonary mRNA expression for *Arg1*, and increased arginase-1 activity in the serum of *S. mansoni*, *Mtb* co-infected mice was detected, when compared to *Mtb*-infected mice (Fig 10B). Interestingly, in co-infected lungs, we found that type 2 granulomas containing high arginase-1 expressing macrophages were distinct (55% of granulomas) and in close proximity to type 1 granulomas (45% of granulomas) typically containing macrophages expressing high inducible nitric oxide synthase (iNOS) (Fig 10C,D), while no type 2 granulomas were observed in *Mtb*-infected lungs.

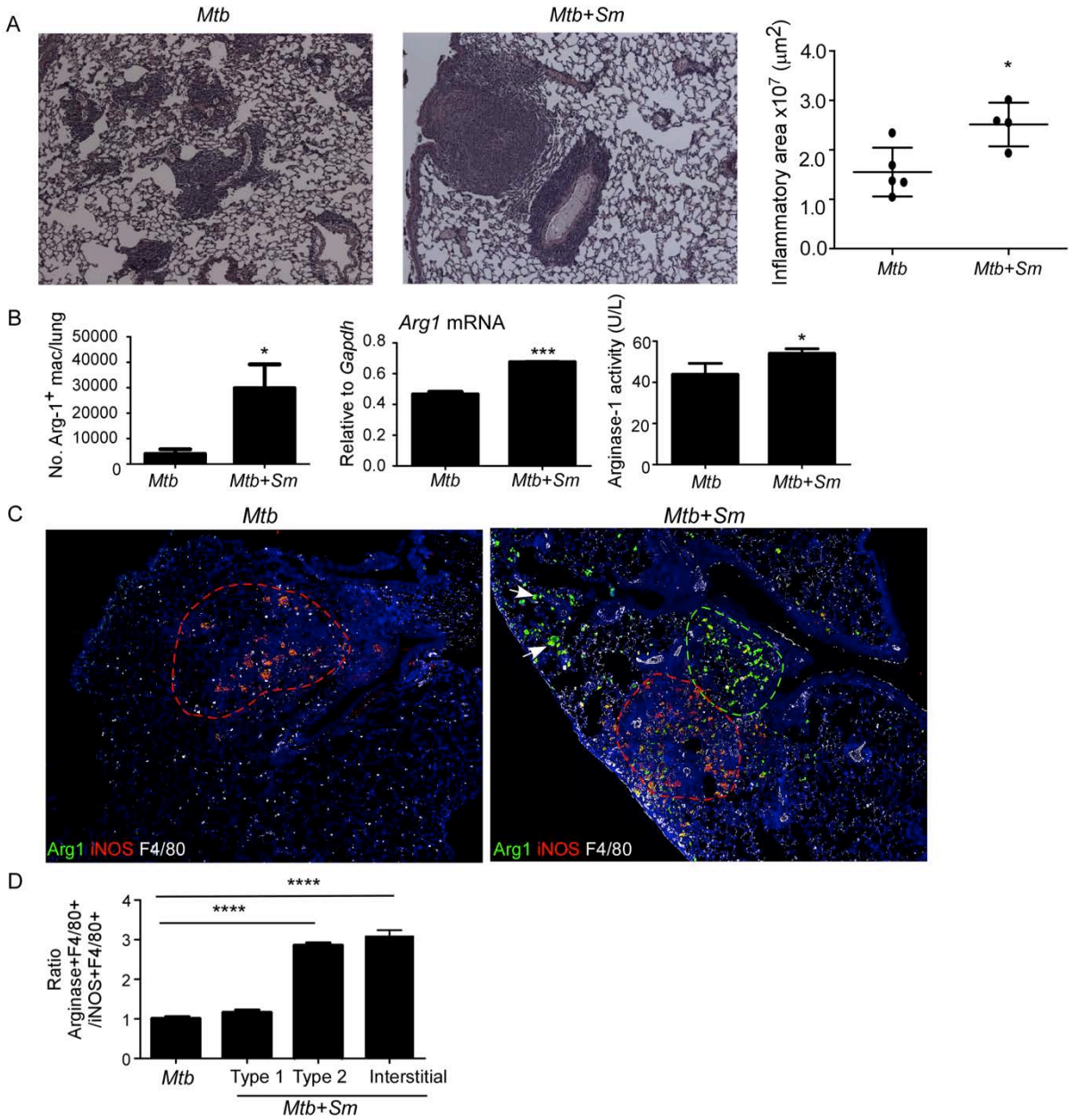


Figure 10. *S. mansoni* induces arginase-1-expressing type 2 granulomas and exacerbates inflammation during co-infection with *Mtb*.

S. mansoni-infected (*Mtb+Sm*) or control Yarg mice (*Mtb*) were aerosol infected with *Mtb*. (A) On D30 post infection, pulmonary inflammation was assessed on FFPE lung sections stained with H&E. 100X magnification. Total area occupied by inflammatory lesions per lobe was quantified. (B-left panel) Arginase-1 reporter expression in lung macrophages was detected by flow cytometry. (B-middle panel) *Arg1* mRNA expression in total lung was assessed by RT-PCR and expression relative to *Gapdh* expression shown. (B-right panel) Arginase-1 activity was

quantitated in the serum of infected mice. (C) FFPE sections from infected mice underwent immunofluorescence staining using antibodies specific for arginase-1, iNOS and F4/80. 4X4 mosaics of 200X magnification fields are shown. “Type 1” granulomas (red selection), “type 2” granulomas (green selection) and interstitial macrophages (arrows) are shown. (D) The number of high iNOS⁺ and high arginase-1-expressing F4/80⁺ cells per 200X field were counted and ratio of high arginase-1-expressing cells to high iNOS-expressing cells per field is shown. n=4-5 mice per group. Lungs of all mice were included in the analysis, one representative image per group is shown. Lungs of all mice were included in the analysis, one representative image per group is shown. *p≤0.05, ***p≤0.001, ****p≤0.0001 unpaired, two-tailed Student’s *t*-test (A, B) or one-way ANOVA with post-hoc Tukey (D). Results are representative of 3 independent experiments.

In addition, arginase-1-expressing macrophages were also localized within the lung interstitium of *S. mansoni Mtb*-co-infected mice, but not in the lungs of *Mtb*-infected mice (Fig 10C,D). Interestingly, mice infected with *S. mansoni* alone also exhibited increased inflammation, when compared to either uninfected lungs or *Mtb*-infected lungs and exhibited increased accumulation of arginase-1-expressing macrophages (Fig 11B,C). Together, these data demonstrate that *S. mansoni* infection results in accumulation of arginase-1-expressing macrophages in the lung, and upon infection with *Mtb* promotes exacerbated inflammation and increased TB disease severity.

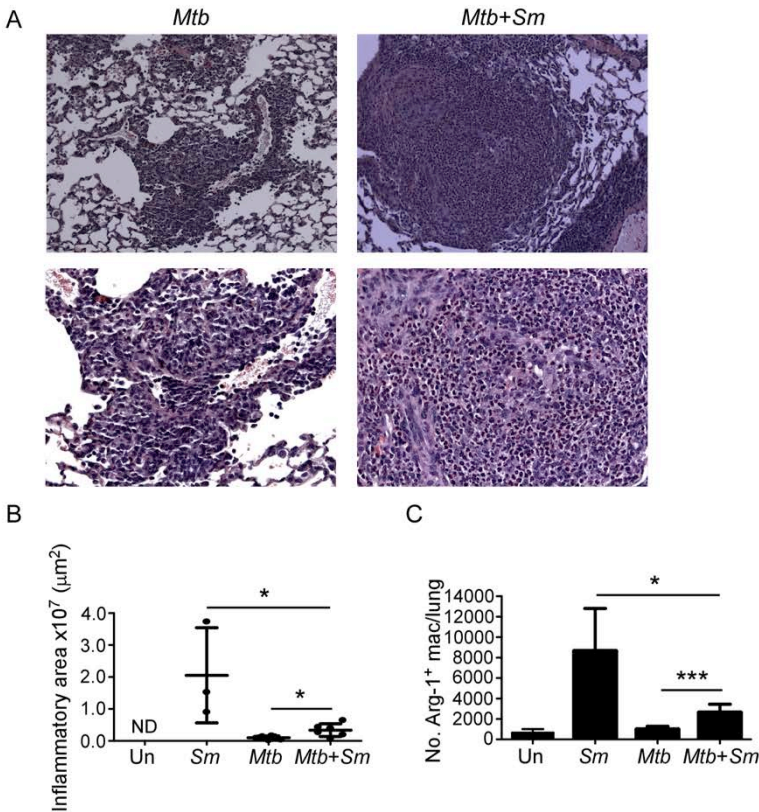


Figure 11. *S. mansoni* co-infection leads to increased lung pathology during TB.

S. mansoni-infected or control Yarg mice were either left untreated or aerosol infected with *Mtb*. (A) On day 30 post-infection, pulmonary inflammation in *Mtb*-infected (*Mtb*) or co-infected (*Mtb+Sm*) mice was assessed on FFPE lung sections stained with H&E. Upper panel, 200X magnification, lower panel, 400X magnification. (B) Additional FFPE lung sections from uninfected (Un), *S. mansoni* (*Sm*)-infected, *Mtb*-infected or co-infected mice were stained with H&E. Total area occupied by inflammatory lesions per lobe was quantified. (C) Arginase-1 reporter expression in lung macrophages was determined by flow cytometry. n=4-5 mice. Lungs from all mice were included in the analysis, one representative image per group is shown. *p<0.05, ***p<0.001, ND-not detectable, one-way ANOVA with post-hoc Tukey.

Coincident with increased accumulation of arginase-1-expressing macrophages, we also found increased expression of Th2 cytokines such as *Il4* and *Il13* mRNA in the lungs of *S. mansoni*, *Mtb* co-infected mice (Fig 12A). This also coincided with increased expression of mRNA for matrix metalloproteases such as *Mmp13*, and neutrophil derived products such as

myeloperoxidases (*Mpo*) in *S. mansoni*, *Mtb* co-infected lungs (Fig 12A). Furthermore, lungs from *S. mansoni*, *Mtb* co-infected mice showed increased numbers of Muc5AC⁺ goblet cells, increased staining for mucins and glycogen in Periodic acid-Schiff (PAS) stained lung sections, as well as increased collagen deposition within type 2 granulomas (Fig 12B). These data together suggest that helminth infection drives accumulation of high arginase-1-expressing macrophages inside type 2 granulomas and interstitial areas, induces mucus production, local fibrosis, and exacerbates pulmonary inflammation in *Mtb* co-infected mice.

Our recent studies have demonstrated that in TB, protective granulomas contain distinct B cell lymphoid follicles harboring T cells and macrophages, while inflammatory granulomas lack well-formed B cell containing lymphoid follicles, and instead contain neutrophils that mediate inflammation [102, 126]. Thus, we next measured the area occupied by lymphoid B cell follicles and found that *S. mansoni* co-infection in *Mtb*-infected mice, resulted in decreased and poorly formed B cell follicles (Fig 12C). Consistent with reduced B cell follicle formation, we also found that T cell accumulation was decreased within the lymphoid follicles, and T cells instead formed perivascular cuffs (Fig 12D). These data suggest that the majority of granulomas formed in *S. mansoni*, *Mtb* co-infected lungs are preferentially composed of granulocytes, and loosely organized B cell lymphoid follicles, a feature associated with non-protective inflammatory granulomas [102].

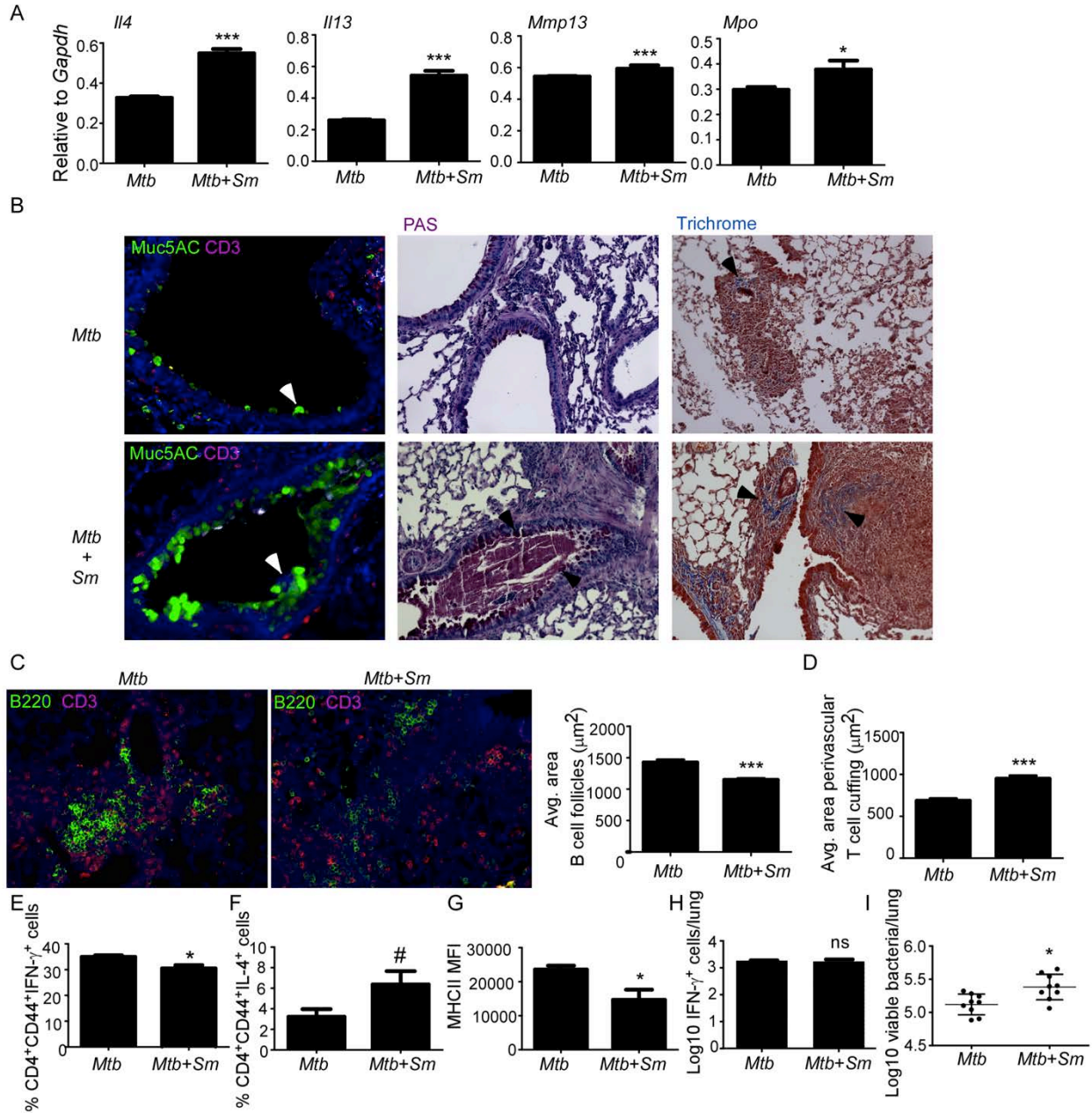


Figure 12. *S. mansoni* co-infection leads to increased lung pathology, impaired Th1 responses and increased susceptibility to *Mtb* infection.

S. mansoni-infected (*Mtb+Sm*) or control Yarg mice (*Mtb*) were infected with *Mtb*. (A) On D30 post-infection, lung expression of *Il4*, *Il13*, *Mmp13* and *Mpo* mRNA relative to *Gapdh* was determined by RT-PCR. (B) FFPE sections were processed for immunofluorescence using antibodies for Muc5AC and CD3; mucus and glycogen accumulation by the PAS stain, and collagen deposition by Gomori's Trichrome stain. 200X magnification. Arrows indicate areas of positive staining. (C) Immunofluorescence staining for B220 and CD3 was also performed. 200X magnification.

The average size of B cell follicles within granulomas and (D) the average area of perivascular T cell cuffing were calculated. (E) The percentage of IFN- γ - and (F) IL-4-producing activated T cells (CD4⁺CD44⁺IFN- γ ⁺ and CD4⁺CD44⁺IL-4⁺, respectively) were determined by flow cytometry. (G) MHC class II expression on lung macrophages was determined by flow cytometry. (H) The percentage of ESAT-6₁₋₂₀-specific, IFN- γ -producing cells in the lungs was determined by antigen-driven ELISpot. (I) Lung bacterial burden was determined by plating. n=4-9 mice per group. Lungs from all mice were included in the analysis, one representative image per group is shown. #p=0.0616, *p \leq 0.05, ***p \leq 0.001, ns-not significant, unpaired, two-tailed Student's *t*-test (A, C-I). Results are representative of 2 independent experiments.

***S. mansoni* co-infection reversibly impairs Th1 responses and limits *Mtb* bacterial control**

Accumulation of IFN- γ -expressing Th1 cells is critical for protective immunity against *Mtb* infection [116]. We found that accumulation of IFN- γ -producing activated CD4⁺ T cells was impaired in *S. mansoni*, *Mtb* co-infected lungs (Fig 12E), and this coincided with a trend in the increase in IL-4-producing CD4⁺ T cells (Fig 12F), and no differences in accumulation of Foxp3-expressing T regulatory cells (data not shown). In addition, the impaired Th1 response was associated with decreased activation of macrophages, as measured by MHC Class II expression (Fig 12G). Interestingly, the small but significant impairment in production of IFN- γ by lung CD4⁺ T cells in *S. mansoni* *Mtb*-co-infected mice was reversible, as the number of *Mtb*-specific IFN- γ -producing CD4⁺ T cells measured by in vitro overnight antigen-driven ELISpot assay was comparable between *S. mansoni*, *Mtb* co-infected mice and *Mtb*-infected mice (Fig 12H). Furthermore, we found that the impairment in Th1 responses ex vivo coincided with a significant but slight increase in lung *Mtb* burden in *S. mansoni*, *Mtb*-co-infected mice, when compared to *Mtb*-infected mice (Fig 12I). Unexpectedly, our data thus suggest that the Th2

responses induced by helminth infection have reversible effects on Th1 immunity and minimal effect on mycobacterial control, but more prominently affect lung inflammation.

Treatment of *S. mansoni*, *Mtb* co-infected mice with an anti-helminthic can reverse TB disease severity

Praziquantel is an anti-helminthic used for treatment of human schistosomiasis [178]. Thus, we next addressed if treatment with an anti-helminthic such as praziquantel can be used to limit disease severity in *S. mansoni*, *Mtb* co-infected mice. Mice were infected with *S. mansoni* and co-infected with *Mtb*, following which one group was treated with praziquantel, while the control co-infected group was treated with PBS. Treatment with praziquantel resulted in significantly decreased *S. mansoni* egg burden in the liver (Fig 14A). As before, *S. mansoni*, *Mtb* co-infected control mice exhibited increased disease severity (Fig 13A,B) and increased collagen deposition (Fig 14B), when compared to *Mtb*-infected mice. Importantly, co-infected mice treated with praziquantel significantly reversed exacerbated inflammation (Fig 13A,B), decreased collagen deposition within pulmonary granulomas (Fig 14B), decreased staining for Muc5AC⁺ goblet cells as well as decreased accumulation of mucins and glycogen (Fig 14C,D). The decreased inflammation in praziquantel treated co-infected mice coincided with a reduction in serum arginase-1 activity (Fig 13C), and decreased accumulation of high arginase-1-expressing macrophages within the type 2 granulomas in the lungs (Fig 13D,E). This also coincided with increased activation of lung macrophages (Fig 13F) and improved *Mtb* control (Fig 13G) in praziquantel treated co-infected mice, when compared to control co-infected mice. Together, these data provide formal evidence that use of anti-helminthics can reverse the

accumulation of arginase-1-expressing macrophages in the lung to prevent exacerbated inflammation and decrease disease severity in *S. mansoni*, *Mtb* co-infected hosts.

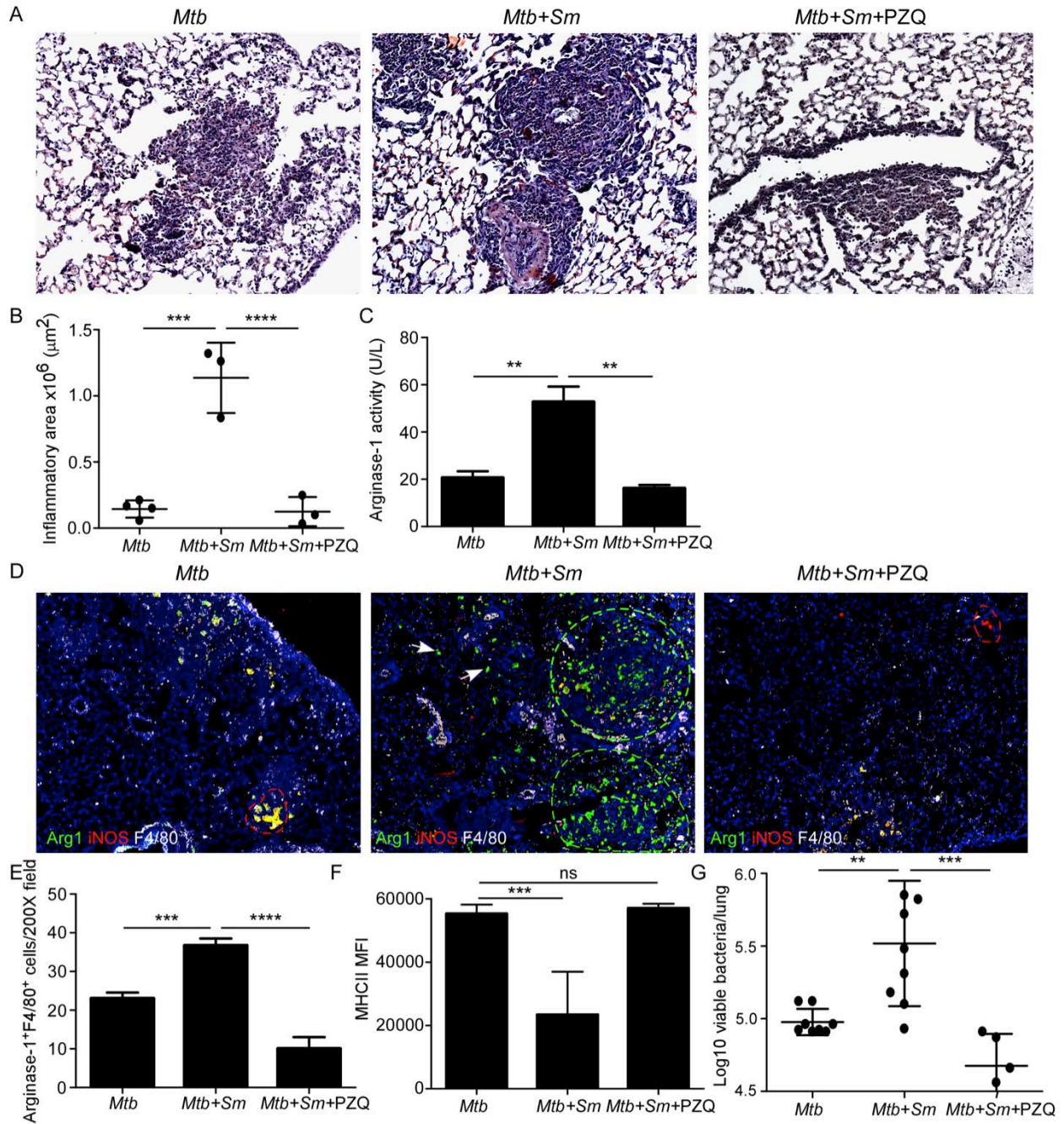


Figure 13. Praziquantel treatment of *S.mansoni* infection reverses the increased inflammation seen in *Mtb-S. mansoni* co-infected mice.

S. mansoni-infected (*Mtb+Sm*) or control C57BL/6 mice (*Mtb*) were aerosol infected with *Mtb* and treated with praziquantel (*Mtb+Sm+PZQ*). (A) On D30 post infection, pulmonary inflammation was assessed on FFPE lung sections stained with H&E. 200X magnification. (B) Total area occupied by inflammatory lesions per lobe was quantified. (C) Arginase-1 activity was quantitated in the serum of infected mice. (D) FFPE sections from infected mice underwent immunofluorescence staining using antibodies specific for arginase-1, iNOS and F4/80. 4X4 mosaics of 200X magnification fields are shown. “Type 1” granulomas (red selection), “type 2” granulomas (green selection) and interstitial macrophages (arrows) are shown. (E) The number of high arginase-1-expressing F4/80⁺ cells per 200X field was determined. (F) MHC class II expression on lung macrophages was determined by flow cytometry. (G) Lung bacterial burden was determined by plating. n=4-5 mice per group. Lungs from all mice were included in the analysis, one representative image per group is shown. **p≤0.01, ***p≤0.001, ****p≤0.0001, ns-not significant, one-way ANOVA with post-hoc Tukey (B,C,E-G).

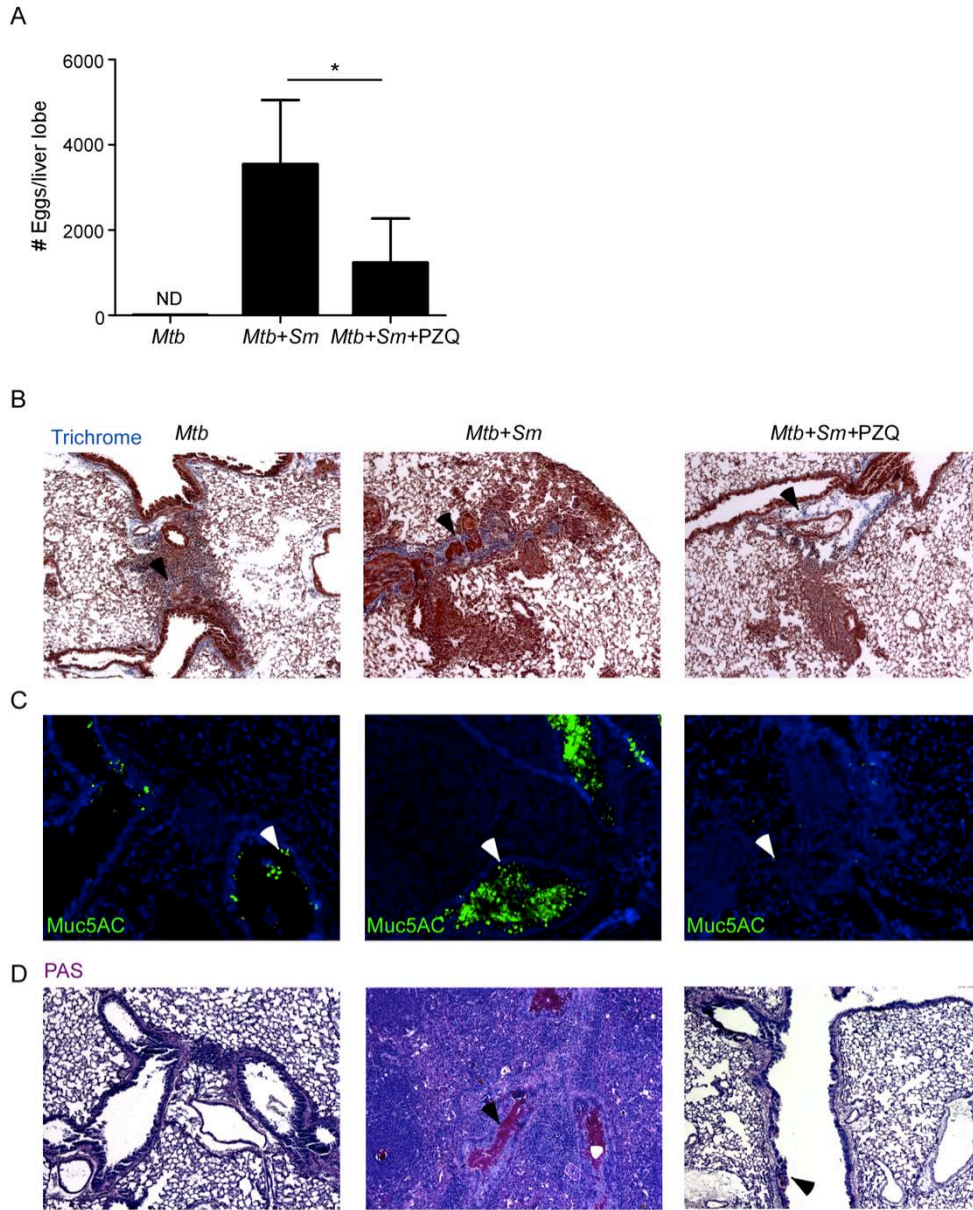


Figure 14. Praziquantel treatment of *Mtb-S.mansoni* co-infected mice reduces *Schistosoma* egg burden and leads to decreased lung pathology upon *Mtb* infection.

S. mansoni-infected (Mtb+Sm) or control C57BL/6 mice (Mtb) were infected with *Mtb* and treated with praziquantel (Mtb+Sm+PZQ) or PBS. (A) Liver *Schistosoma* egg burden was determined. (B) FFPE sections were processed for collagen deposition analysis using Gomori's Trichrome stain. 100X magnification. (C) FFPE sections were processed for immunofluorescence using antibodies for Muc5AC. 100X magnification. (D) Mucus and glycogen accumulation were evaluated by the PAS stain. 100X magnification. Arrows indicate areas of positive

staining. n=4-5 mice per group, one representative image per group is shown. *p≤0.05, one-way ANOVA with post-hoc Tukey (A), ND-not detectable.

Arginase-1 expression drives exacerbated inflammation in helminth *Mtb* co-infected hosts

Our data thus far suggest that *S. mansoni* infection induces the accumulation of arginase-1 expressing macrophages within the lung, which upon *Mtb* infection mediate exacerbated inflammation and increased TB disease. To mechanistically address if arginase-1 expression in macrophages mediates the exacerbated disease seen in helminth *Mtb* co-infected mice, we then generated bone marrow chimeric mice (BMC). C57BL/6.SJL host mice received either WT bone marrow (WT BMC-*Arg1*^{fllox/fllox}) or bone marrow from arginase-1-deficient mice where macrophages are devoid of arginase (*Tie2*^{cre} *Arg1*^{fllox/fllox} BMC) [174]. Upon complete reconstitution, BMC mice were infected with *S. mansoni*, followed by co-infection with *Mtb* as before. Under these conditions both WT BMC and *Tie2*^{cre} *Arg1*^{fllox/fllox} BMC co-infected mice exhibited a slight but significant increase in bacterial burden when compared to *Mtb*-infected WT BMC mice (Fig 15A). In contrast, *Tie2*^{cre} *Arg1*^{fllox/fllox} BMC co-infected mice exhibited decreased lung inflammation (Fig 15B,C), increased formation of protective B cell follicles within TB granulomas (Fig 15D), and decreased T cell perivascular cuffing when compared to WT BMC co-infected mice (Fig 15E). This coincided with the absence of arginase-1-expressing macrophages within the lungs of *Tie2*^{cre} *Arg1*^{fllox/fllox} co-infected mice, when compared to accumulation of high arginase-1-expressing macrophages in lungs of WT BMC co-infected mice (Fig 15F). These new data provide direct evidence that accumulation of arginase-1-expressing macrophages in the lungs following *S. mansoni* infection mediates exacerbated inflammation and disease severity during *Mtb* co-infection, without affecting mycobacterial control.

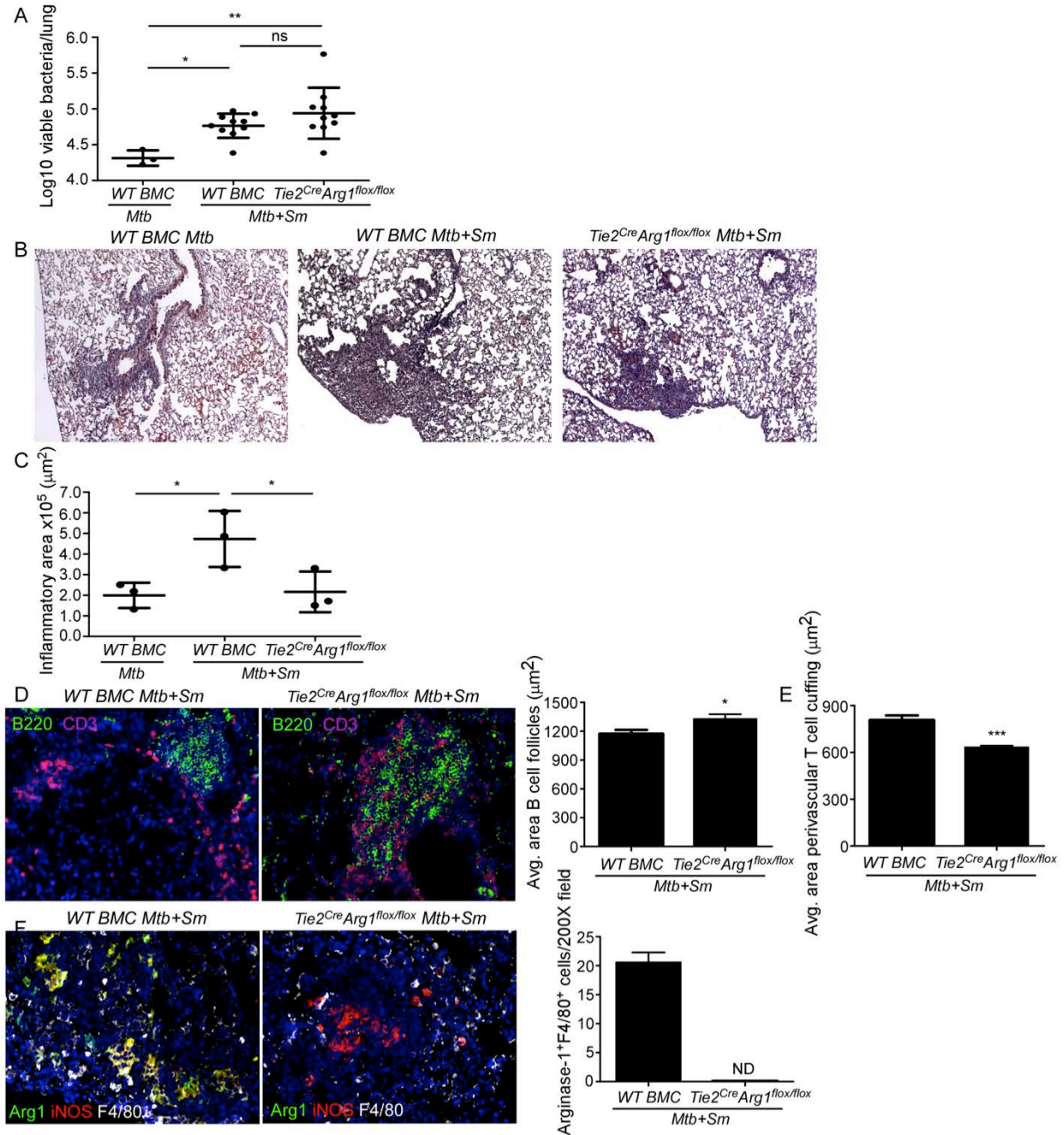


Figure 15. *Tie2^{Cre} Arg1^{flox/flox}* BMC co-infected mice have reduced lung pathology.

WT BMC or *Tie2^{Cre} Arg1^{flox/flox}* BMC mice were *S.mansoni*-*Mtb*-co-infected (*Mtb+Sm*) or infected with *Mtb* alone (*Mtb*). (A) On D25 post-infection, lung bacterial burden was determined by plating. (B) Pulmonary inflammation was assessed on FFPE lung sections stained with H&E. 100X magnification. (C) Total area occupied by inflammatory lesions per lobe was quantified. (D) FFPE sections were processed for immunofluorescence using antibodies for B220 and CD3. 200X magnification. The average size of B cell follicles within granulomas was

determined. (E) The average area of perivascular T cell cuffing in B220 and CD3-stained sections was calculated. (F) FFPE sections were stained with antibodies specific for arginase-1, iNOS and F4/80. 200X magnification. The number of high arginase-1-expressing F4/80⁺ cells per 200X field was determined. n=3-10 mice per group. Lungs of all mice were included in the analysis, one representative image per group is shown. *p≤0.05, **p≤0.01, ***p≤0.001, ns-not significant, ND-not detectable, one-way ANOVA with post-hoc Tukey (A, C), unpaired, two-tailed Student's *t*-test (D-F).

SEA immunization exacerbates lung inflammation during *Mtb* infection

In addition to the generation of type 2 granulomas, *S. mansoni* co-infection in *Mtb*-infected mice may also alter tissue architecture due to the physical presence of the parasite and thus exacerbate lung pathology. Thus, we sought to determine whether exposure to the helminth product *S. mansoni* egg antigen (SEA), which contains the major antigens that induce Th2 responses during infection [177], is by itself sufficient to exacerbate lung inflammation in TB. Thus, C57BL/6 mice were aerosol infected with low doses of *Mtb* and were immunized with SEA at day 15 post infection, a time when *Mtb*-specific T cell responses are initiated in the mouse model of TB [114]. We found that mice that were SEA immunized and *Mtb* infected, demonstrated increased lung inflammation (Fig 16A), and type 1 granulomas harbored fewer iNOS-expressing macrophages (Fig 16B). In contrast to *S. mansoni*, *Mtb*-infected lungs, we did not observe distinct arginase-1-expressing macrophage containing type 2 granulomas in the lungs of SEA-immunized *Mtb*-infected mice (data not shown), but nevertheless found increased expression of *Arg1* mRNA in sorted lung CD11c⁺ cells from SEA immunized *Mtb*-infected mice (Fig 16C). Similarly, we found that the formation of B cell follicles was reduced and less organized in SEA immunized *Mtb*-infected mice (Fig 16D), and this coincided with decreased accumulation of T cells within lymphoid follicles, which instead accumulated as T cell perivascular cuffs (Fig 16E).

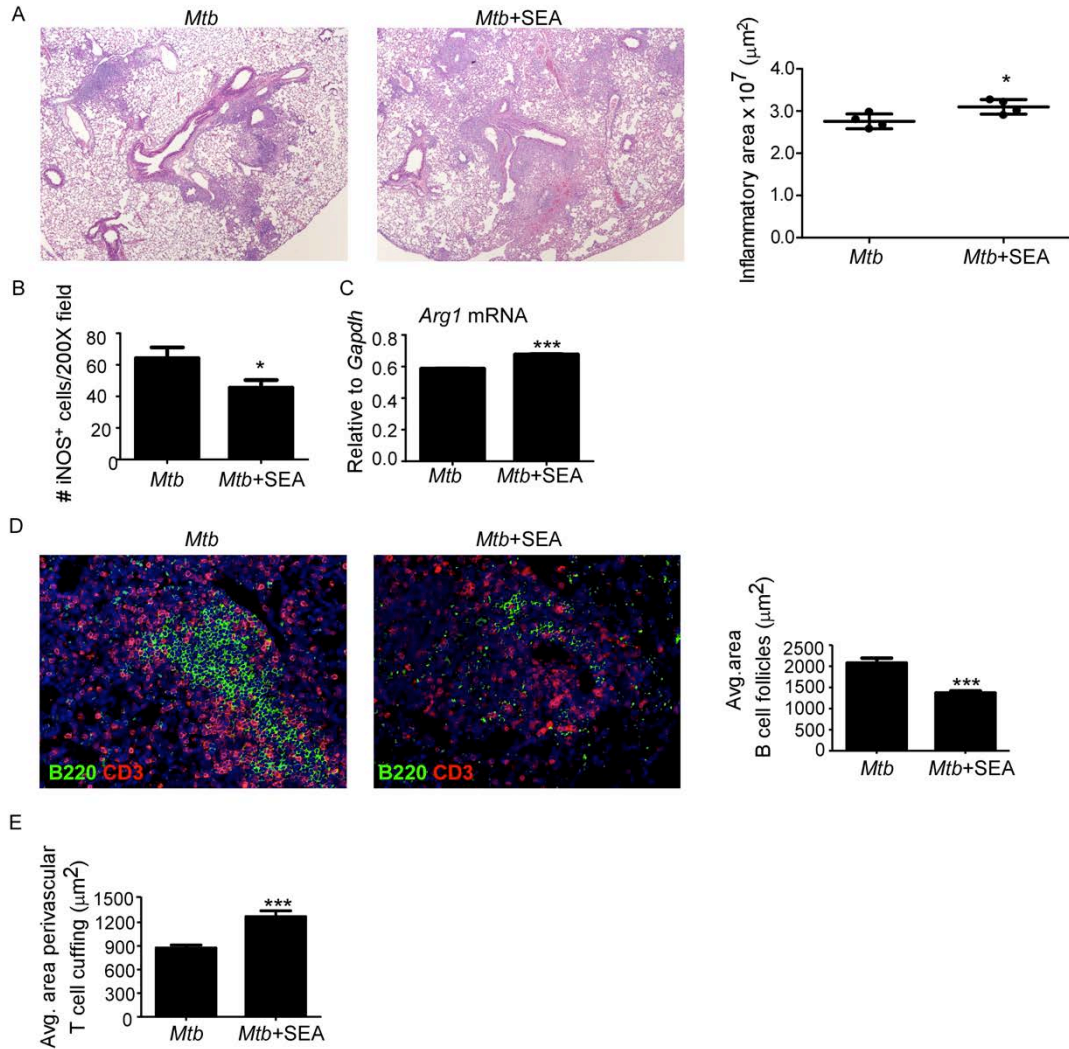


Figure 16. SEA immunization increases susceptibility to *Mtb* infection.

C57BL/6 mice were aerosol infected with *Mtb* and immunized with SEA (*Mtb+SEA*) or saline (*Mtb*) on D15 post-infection. (A) Pulmonary inflammation was assessed on D30 post-infection on H&E stained FFPE lung sections. 40X magnification for H&E sections. Total area occupied by inflammatory lesions per lobe was quantified. (B) FFPE sections from infected lungs were processed for immunofluorescence using antibodies specific for iNOS and F4/80, and the number of iNOS-expressing F4/80⁺ cells per 200X field was counted. (C) CD11c⁺ cells were sorted from the lungs of SEA-treated, *Mtb*-infected mice, as well as *Mtb*-infected mice and level of *Arg1* mRNA relative to *Gapdh* was determined by RT-PCR. (D) FFPE lung sections were also stained using antibodies specific for B220 and CD3. 200X magnification. The average size of B cell follicles within granulomas, as well as (E) the average area occupied by perivascular T cell cuffing were calculated. n=4-8 mice per group. Lungs of all mice were included

in the analysis, one representative image per group is shown. * $p \leq 0.05$, *** $p \leq 0.001$, unpaired, two-tailed Student's *t*-test (A-E). Results are representative of 2 independent experiments.

Importantly, mice similarly immunized with a control antigen such as Bovine Serum Albumin (BSA) or a Th1 promoting antigen such as Purified Protein Derivative (PPD) did not promote lung inflammation, instead limiting inflammation (Fig 17A,B). In addition, mice immunized with either BSA or PPD did not affect *Mtb* burden (Fig 17C). Together, these data suggest that exacerbated lung inflammation and decreased formation of protective B cell follicles can be recapitulated by immunization with SEA in *Mtb*-infected mice, suggesting that the inflammatory effects of the co-infection are due to the presence of *Schistosoma* antigens, and likely not due to tissue alterations caused by the physical presence of the helminth parasite.

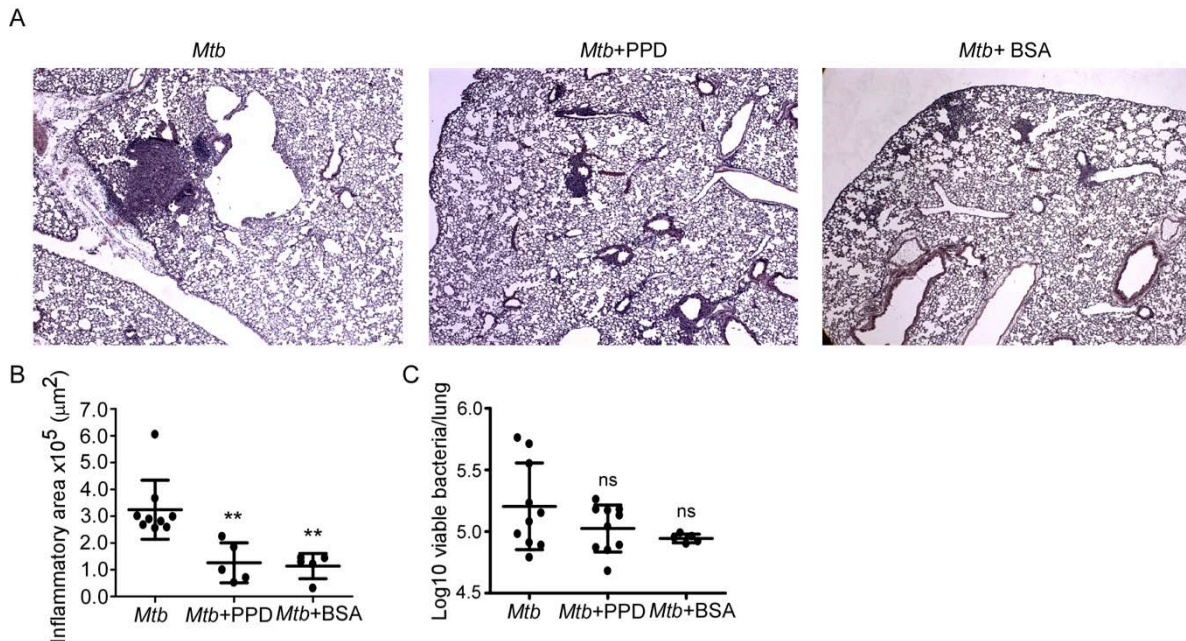


Figure 17. PPD and BSA immunization of *Mtb*-infected mice does not exacerbate lung inflammation and *Mtb* control.

C57BL/6 mice were aerosol infected with *Mtb* and immunized with saline (*Mtb*), PPD (*Mtb*+PPD) or BSA (*Mtb*+BSA). (A) Pulmonary inflammation was assessed on D30 post-infection on H&E stained FFPE lung sections. 50X magnification. (B) Total area occupied by inflammatory lesions per lobe was quantified. (C) Lung bacterial

burden was determined on D30 post-infection. n=5 mice per group. Lungs of all mice were included in the analysis, one representative image per group is shown. *p≤0.05, **p≤0.01, ns-not significant, one-way ANOVA with post-hoc Tukey (B, C).

SEA mediated inhibition of Th1 responses in *Mtb* infection is reversible

Aerosol infection of mice with *Mtb* results in a chronic pulmonary infection which induces a predominantly Th1 immune response in the lung [114]. Consistent with this, we found that CD4⁺ T cells isolated from the lungs of chronically *Mtb*-infected wild type C57BL/6 mice strongly expressed mRNA for *Ifng*, *Tnf*, *Stat1* and *IL12rb2*, which are associated with the Th1 cell pathway (Table 1), but not canonical Th2 (*Gata3*, *IL4ra*), or Th17 genes (*IL17a*, *Rorc*).

In vitro treatment of such isolated CD4⁺ T cells with SEA in the presence of irradiated APCs, inhibited both polyclonal (anti-CD3/CD28 bead stimulated) and *Mtb*-specific IFN- γ production (Fig 18A), without detectable IL-4 production in culture supernatants (data not shown). Upon analysis of gene expression in these cell pellets, we found genes associated with Th1 function (*Ifng*, *Tbx21*, *Cxcr3*), T cell signaling (*Lck*, *Cd3g*, *Zap70*, *Lat*), T cell costimulation (*Cd40lg*, *Icos*, *Cd28*) and T cell activation (*Il2ra*) were downregulated in SEA-treated cells (Table 2, Fig 18B), while expression of the Th2 cytokines *Il4*, *Il5* and *Il13* was below the threshold of detection.

Table 1. Induction of genes associated with Th1 cell function in CD4⁺ T cells during *Mtb* infection.

Gene	Un 1	Un 2	Un 3	<i>Mtb</i> 1	<i>Mtb</i> 2	<i>Mtb</i> 3	Fold Change	edgeR	DESeq	baySeq
<i>Ifng</i>	95.9	261	281	3700	2810	2620	14.3	3.18E-34	6.14E-25	0.000025

<i>Il12rb1</i>	86.5	139	106	501	568	517	4.79	1.26E-34	8.01E-24	0.00000218
<i>Il12rb2</i>	71.5	56.5	60.1	395	320	301	5.4	6.74E-32	1.42E-19	0.00000178
<i>Stat1</i>	32.9	21.9	27.3	102	94	96.9	3.57	8.17E-12	0.0000029	0.0000256
<i>Tnf</i>	4.7	1.82	12	73.2	86.4	82.5	13	1.73E-22	3.36E-13	0.00000897
<i>Il1a</i>	57.4	149	102	1110	870	897	9.32	2.36E-39	2.52E-35	0.0000056
<i>Gata3</i>	638	458	447	79	71.7	75.3	-6.83	2.69E-40	8.31E-14	0.0000011
<i>Il4ra</i>	3320	3550	2980	1940	2280	2080	-1.56	0.0000301	0.00488	0.00542
<i>Il13ra1</i>	532	645	529	1430	1240	1370	2.36	3.74E-16	3.69E-10	0.0000211
<i>Il17a</i>	4.7	9.11	4.01	13.5	4.9	3.2	1.21	0.837	0.957	0.23
<i>Rorc</i>	70.5	72.9	79.4	30.8	14.7	17.6	-3.53	4.97E-10	0.00000137	0.000117
<i>Il17ra</i>	3630	2210	2110	842	906	907	-2.99	1.75E-13	0.00157	0.0000757
<i>Il6ra</i>	2140	1180	1130	272	387	411	-4.17	1.58E-15	0.00241	0.000816
<i>Il21</i>	0	0	3.21	19.3	9.36	14.4	13.4	0.00000309	0.00607	0.00356
<i>Il10</i>	4.7	10.9	8.02	63.6	61.5	61.6	7.89	4.5E-17	2.14E-09	0.00000538
<i>Tgfb1</i>	1600	1450	1100	1240	1660	1480	1.06	0.732	0.501	0.305
<i>Ccl4</i>	56.4	164	192	3830	3840	3490	27.1	7.07E-47	8.56E-110	0.000000605
<i>Ccl7</i>	30.1	31	42.5	1410	767	821	29	3.52E-69	9.38E-10	0.000000908
<i>Cxcl3</i>	5.64	1.82	9.62	214	148	138	29.2	2.28E-39	1.8E-16	0.00000314
<i>Cxcl9</i>	16.9	23.7	24.1	1780	1540	1510	74.8	7.97E-179	6.30E-127	2.31E-09
<i>Cxcl10</i>	23.5	56.5	48.9	1810	1400	1150	33.8	2.83E-87	1.53E-25	0.00000114

Table 2. Top down- and upregulated genes in CD4⁺ T cells from *Mtb*-infected mice following ex vivo treatment with SEA.

Gene	<i>Mtb</i>			<i>Mtb</i> + SEA			Fold Change	edgeR	DESeq	baySeq
	1	2	3	1	2	3				
Top downregulated genes										
<i>Klrc1</i>	36.7	33.6	47.1	1.01	0	0	-116	2.13E-24	3.72E-15	0.000353
<i>Ccl1</i>	316	263	367	4.05	1.4	3.49	-106	5.46E-114	6.33E-53	4.53E-07
<i>Ifng</i>	4400	3370	3150	38.5	43.5	36.1	-92.5	0	2.38E-54	3.84E-13
<i>Themis</i>	273	249	265	2.03	2.1	4.66	-89.5	9.08E-133	4.88E-94	2.57E-08
<i>Rgs16</i>	1160	1310	1120	22.3	14.7	5.82	-83.8	0	1.39E-191	3.07E-08
<i>Cxcr6</i>	2320	2110	2210	37.5	23.8	31.4	-71.6	0	0	7.12E-12
<i>Klrc2</i>	11.5	15.5	22.1	0	0.70	1	-70	5.99E-11	6.92E-06	0.00735
<i>Gzmc</i>	22.9	34.7	10.6	1.01	0	0	-67.3	1.27E-09	1.34E-04	0.0518
<i>Trat1</i>	57.3	39	43.3	1.01	0	1.16	-64.1	4.51E-25	1.23E-16	1.58E-04
<i>Lck</i>	22.9	26.7	29.8	0	1.4	0	-56.6	2.61E-17	3.02E-09	6.63E-04
<i>Apol7e</i>	91.6	66.7	70.2	3.04	1.4	0	-51.5	1.57E-39	6.47E-26	2.08E-05
<i>Cd40lg</i>	156	106	105	2.03	2.81	2.33	-51.2	1.82E-51	7.97E-21	1.18E-06
<i>Ccr8</i>	36.7	28.3	35.6	2.03	0	0	-49.6	3.93E-19	1.2E-11	0.000532
<i>B4galnt4</i>	199	245	226	5.06	3.51	5.82	-46.6	6.82E-101	5.18E-77	2.19E-08
<i>Mmp3</i>	1050	4.27	377	21.3	4.91	4.66	-46.5	1.13E-07	2.18E-01	0.00000104
<i>Fasl</i>	128	115	114	6.08	3.51	0	-37.2	1.01E-59	1.45E-38	5.51E-07
<i>Cd5</i>	559	629	631	18.2	12.6	19.8	-35.9	5.47E-213	1.92E-169	2.88E-09
<i>Ms4a4b</i>	1630	1460	1480	48.6	37.9	43.1	-35.2	0	2.58E-308	1.28E-10
<i>Icos</i>	887	734	797	26.3	21.7	21	-35	3.58E-231	4.64E-126	8.72E-09

<i>Il18rap</i>	314	288	270	12.2	6.31	6.99	-34.3	1.87E-119	1.52E-88	1.78E-08
Top upregulated genes										
<i>Notch3</i>	4.58	5.87	4.81	39.5	21.7	24.5	5.61	4.23E-07	4.33E-04	2.30E-03
<i>Mospd4</i>	0	4.27	2.89	11.1	11.9	15.1	5.34	3.99E-04	1.16E-01	2.89E-02
<i>Slc32a1</i>	4.58	9.61	3.85	23.3	40	28	5.06	1.41E-06	5.86E-04	5.18E-03
<i>Rpph1</i>	0	11.7	4.81	25.3	28.8	25.6	4.81	1.55E-05	1.29E-02	6.24E-03
<i>Bfsp2</i>	2.29	3.2	3.85	9.11	21	11.6	4.47	2.39E-03	4.03E-02	6.41E-02
<i>Vpreb3</i>	11.5	16	9.62	47.6	49.1	43.1	3.77	3.24E-09	1.39E-04	5.08E-04
<i>Tecta</i>	6.87	8.54	0.96 2	17.2	27.4	16.3	3.72	1.54E-03	2.43E-02	5.35E-02
<i>Myh14</i>	6.87	2.67	2.89	21.3	11.2	11.6	3.55	4.44E-03	4.37E-02	5.40E-02
<i>Dusp13</i>	4.58	10.1	11.5	29.4	34.4	28	3.49	6.12E-06	7.75E-03	2.56E-03
<i>Cgn</i>	2.29	9.08	5.77	23.3	17.5	16.3	3.33	1.80E-03	1.30E-01	2.79E-02
<i>Lingo4</i>	4.58	5.87	7.7	19.2	23.1	17.5	3.3	4.64E-04	4.22E-02	8.67E-03
<i>Hspa5</i>	9.16	39.5	20.2	59.8	91.9	67.5	3.18	2.04E-05	1.42E-02	5.97E-02
<i>Rtn4r</i>	6.87	8.54	5.77	16.2	28.1	22.1	3.13	7.61E-04	3.75E-02	1.90E-02
<i>Dnah2</i>	59.6	71	58.7	209	198	165	3.02	2.29E-19	5.51E-13	9.18E-05
<i>Gm11166</i>	6.87	8.01	16.4	25.3	30.2	36.1	2.93	2.62E-04	1.53E-02	1.54E-02
<i>Cyp4f18</i>	667	838	785	1870	2590	2160	2.89	3.03E-35	4.24E-09	1.37E-04
<i>Hspa5</i>	16	46.4	31.8	73.9	121	72.2	2.84	2.05E-05	4.79E-02	1.39E-01
<i>Kctd19</i>	22.9	16.6	17.3	49.6	65.9	45.4	2.84	5.60E-07	9.42E-05	2.59E-03
<i>Axdnd1</i>	6.87	9.08	13.5	26.3	22.4	32.6	2.77	1.04E-03	5.27E-02	1.93E-02

To further address if the inhibition of IFN- γ production occurs in *Mtb*-specific Th cells, we adoptively transferred naive CD4⁺ T cells isolated from the *Mtb* Early Secretory Antigenic target 6 (ESAT-6) T Cell Receptor (TCR) transgenic (Tg) mice into *Cd4*^{-/-} mice, infected the mice with low doses of aerosolized *Mtb*, and isolated in vivo expanded Th cells from the lungs

on day 30 post infection. Consistent with our previous data, these isolated Th cells produced IFN- γ upon restimulation with ESAT-6, but in vitro SEA treatment in the presence of APCs inhibited the production of IFN- γ (Fig 18C), without inducing detectable levels of IL-4 (data not shown).

Next, we assessed whether similar to *Schistosoma* infection, SEA immunization affects Th1 immunity in vivo. We found that total IFN- γ levels in lung homogenates were reduced in SEA immunized *Mtb*-infected mice when compared to *Mtb*-infected lungs (Fig 18D). Next, to assess the effect of SEA at the cellular level, using IFN- γ reporter mice (Yeti mice), we found that SEA immunization decreased both the accumulation of activated IFN- γ -producing CD4⁺ T cells in *Mtb*-infected animals (Fig 18E), and levels of IFN- γ reporter expression by activated CD4⁺ Th cells in the lungs of *Mtb*-infected mice (Fig 18F). Strikingly, assessment of IFN- γ *Mtb*-specific T cell responses by restimulation with *Mtb* antigen in ELISpot assays, or following stimulation with PMA/Ionomycin, showed no differences between SEA treated and *Mtb*-infected groups (Fig 18G,H). These data together suggest that SEA-mediated inhibition of IFN- γ expression in CD4⁺ T cells evident in vitro (in cultured Th cells with SEA and APCs) and ex vivo (as assessed by reporter expression), can be reversed by in vitro culture in the absence of SEA (as assessed by ELISpot and intracellular staining). These data suggest that the effects of SEA on Th cell cytokine production and activation profile can be potent in in vitro cultures, but the effects are reversible upon removal of SEA. Additionally, activation of lung macrophages as measured by MHC-II expression, was reduced in SEA treated *Mtb*-infected mice (data not shown). Incidentally, decreased Th1 responses and decreased macrophage activation, coincided with a small but significant increase in bacterial burden in the lungs of SEA immunized *Mtb*-infected mice (Fig 18I). Interestingly, immunization with SEA on day 15 but not day 1 in *Mtb*-

infected mice, coincided with increased susceptibility to TB, suggesting that the presence of SEA during initiation of *Mtb*-specific T cell responses, but not earlier, affects protective outcomes during *Mtb* infection (Fig 18I).

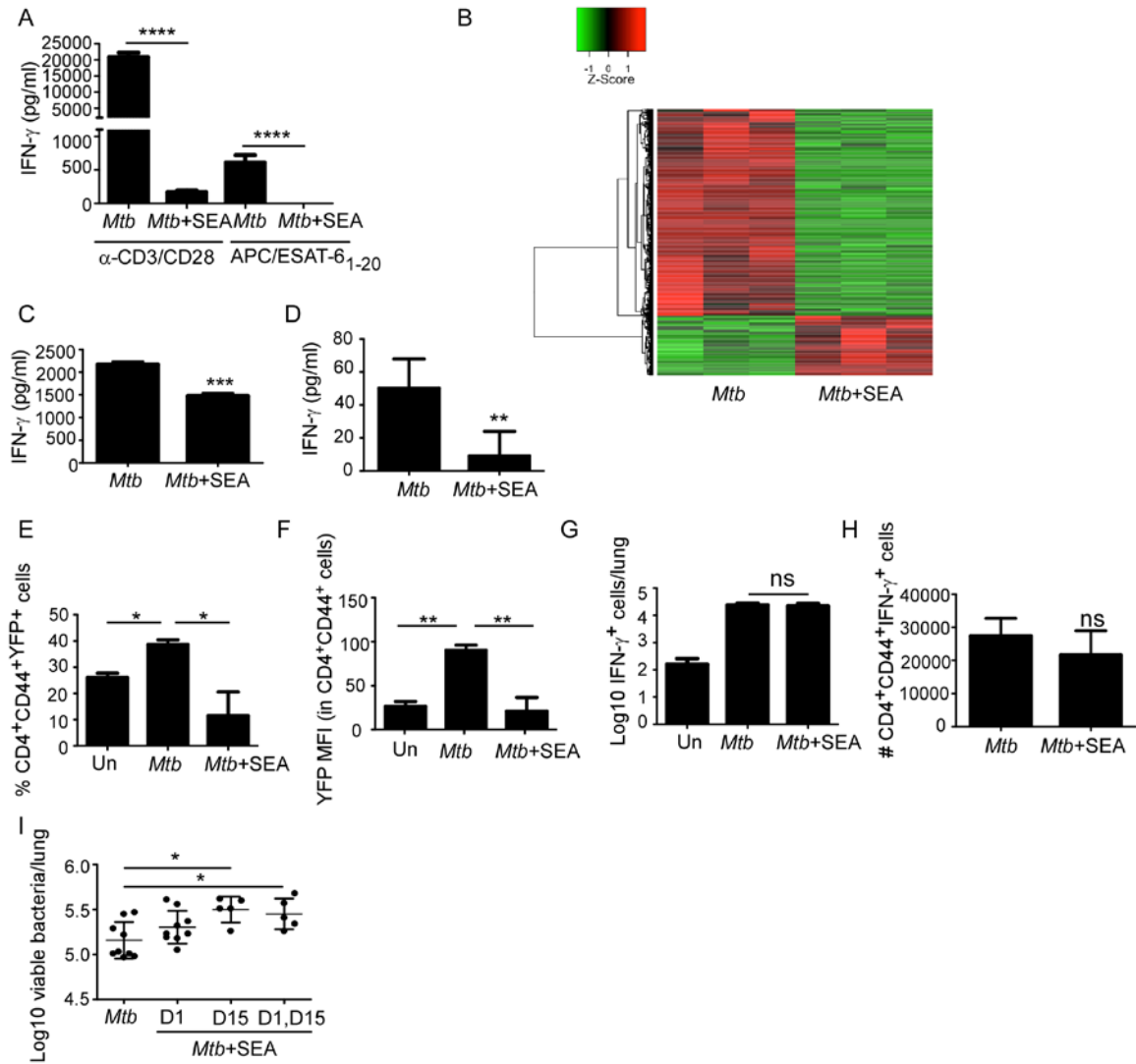


Figure 18. SEA treatment impairs *Mtb*-driven Th1 responses and increases susceptibility to *Mtb* infection.

(A) Lung CD4⁺ T cells were purified from D30 *Mtb*-infected mice and incubated with (*Mtb*+SEA) or without SEA (*Mtb*) and APCs. Cells were restimulated with anti-CD3/CD28 beads or irradiated splenocytes and ESAT-6₁₋₂₀ peptide and supernatant IFN- γ levels assessed. (B) Overall gene expression changes induced by SEA in cell pellets from (A) were assessed by RNAseq. Heat-map representation of significant genes is shown. (C) CD4⁺ cells sorted from ESAT-6 TCR Tg mice were transferred to Cd4^{-/-} mice, which were *Mtb*-infected. On D30 post-infection, lung CD4⁺ cells were sorted, treated with SEA and restimulated with irradiated splenocytes and ESAT-6₁₋₂₀ peptide.

Supernatant IFN- γ levels were determined. (D) In some experiments, *Mtb*-infected C57BL/6 mice were immunized with SEA or saline on D15 post-infection. D30 lung IFN- γ levels were determined. (E) *Mtb*-infected Yeti mice were immunized with SEA on D15 post-infection and the percentage of lung CD4⁺CD44⁺YFP⁺ cells was determined by flow cytometry on D30. (F) IFN- γ MFI (YFP) within CD4⁺CD44⁺ T cells was determined. (G) The number of lung ESAT-6₁₋₂₀-specific, IFN- γ -producing cells was determined by ELISpot. (H) Lung CD4⁺CD44⁺IFN- γ ⁺ cell numbers following PMA/ionomycin stimulation were determined. (I) C57BL/6 mice were infected with *Mtb* and immunized with SEA or saline on D1, D15 or both D1 and D15 post-infection and D30 lung bacterial burden determined. n=3 samples (A,B) or n=5-9 mice per group (C-I). *p \leq 0.05, **p \leq 0.01, ***p \leq 0.001, ****p \leq 0.0001, ns-not significant, one-way ANOVA with post-hoc Tukey (A,E,F,G,I) or unpaired, two-tailed Student's *t*-test (C,D,H). One experiment of two shown, Un- Uninfected controls.

In vitro SEA treated CD4⁺ T cells from *Mtb*-infected lungs which demonstrated impaired T cell activation and IFN- γ production (Fig 18A,B), upon subsequent washes to remove SEA and further incubation with *Mtb*-infected alveolar macrophages, could now produce IFN γ and activate macrophages to induce iNOS (Fig 19A,B), which coincided with control of *Mtb* infection in infected alveolar macrophages, albeit not to the same level as CD4⁺ T cells isolated from *Mtb*-infected lungs (Fig 19C). Not surprisingly, naive lung CD4⁺ T cells isolated from uninfected mice, which demonstrated poor induction of IFN- γ production in T cells (Fig 19A) and decreased induction of iNOS (Fig 19B), exhibited reduced *Mtb* control in alveolar macrophages (Fig 19C). These data together with the improved *Mtb* control observed in praziquantel-treated co-infected mice (Fig 13G), indicate that although the presence of helminth antigens is sufficient to dampen *Mtb*-specific Th1 responses, these effects are reversible upon removal of the parasite and/or its products.

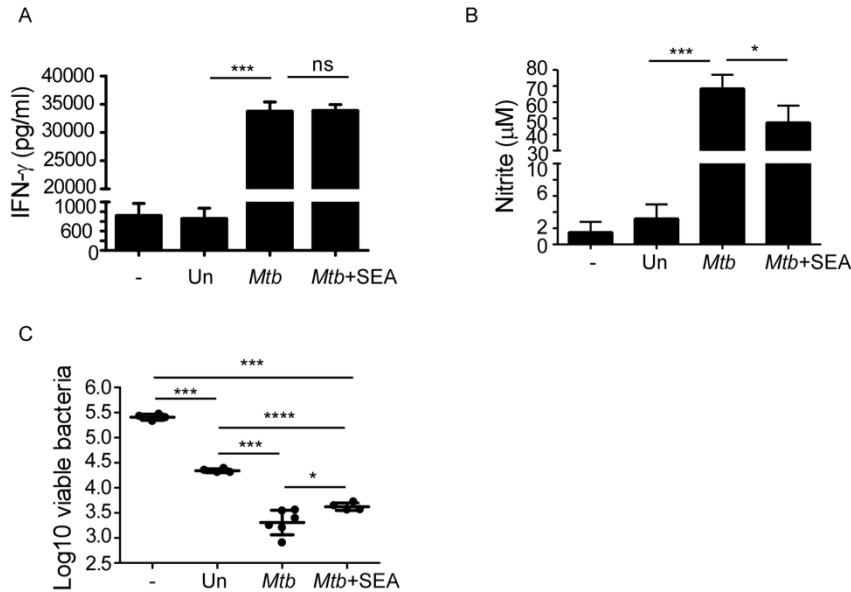


Figure 19. Impairment of Th1 responses in SEA treated Th cells is reversible.

C57BL/6 mice were aerosol infected with *Mtb* and pulmonary CD4⁺ T cells were purified on D30 post-infection. Cells were then incubated for 6 days, alone (*Mtb*) or in the presence of SEA (*Mtb*+SEA) along with APCs. Cells were washed multiple times and restimulated for 48h with irradiated splenocytes and ESAT-6₁₋₂₀ peptide and then layered over *Mtb*-infected alveolar macrophages (MOI of 1) for 6 days. Alveolar macrophages that did not contain T cells (-) and alveolar macrophages incubated with T cells isolated from uninfected mice (Un) were included as controls. (A) Culture supernatants were assessed to determine IFN- γ levels and (B) nitrite production by macrophages was determined using the Griess reaction. (C) At the end of the culture period, macrophages were washed, lysed and intracellular *Mtb* burden determined by plating. n=4-6 samples. *p \leq 0.05, ***p \leq 0.001, ****p \leq 0.0001, ns-not significant, one-way ANOVA with post-hoc Tukey (A-C).

Helminth infections are associated with increased TB reactivation rates in HIV-infected patients [161]. Thus, based on our data that *S. mansoni* infection or immunization with SEA can exacerbate lung inflammation and increase *Mtb* susceptibility, we then tested whether SEA immunization would affect disease progression in mice undergoing TB reactivation. Using the Cornell model of *Mtb* reactivation [179], chronically *Mtb*-infected mice were treated with isoniazid and rifampicin until no cultivable lung bacteria were recovered [126], and mice were

immunized with SEA and spontaneously allowed to reactivate *Mtb* infection. We found that SEA immunized mice had higher lung and spleen bacterial burden when compared to control mice that also reactivated *Mtb* infection (Fig 20). These data for the first time provide experimental evidence that TB reactivation can be accelerated due to the presence of helminth products such as SEA, likely due to its effect on both Th1 responses, as well as due to decreased formation of lymphoid follicle-containing lung granulomas.

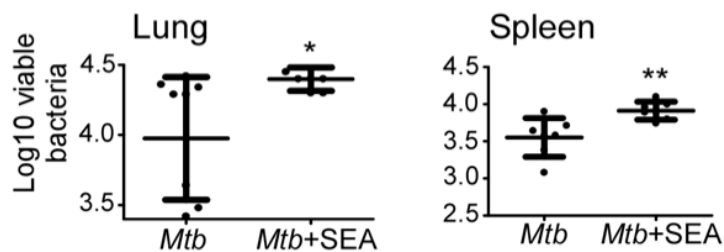


Figure 20. SEA treatment increases TB reactivation in mice.

C57BL/6 mice were aerosol infected with *Mtb* for 30 days, and were subsequently treated with rifampicin and isoniazid in the drinking water for 6 weeks. 2 and 4 weeks after antibiotic treatment cessation, mice were immunized with SEA (*Mtb*+SEA) or saline (*Mtb*) and lungs and spleen were harvested 2 weeks later. Lung and spleen bacterial burden were determined by plating on 7H11 agar plates. n=7 mice per group. * $p \leq 0.05$, ** $p \leq 0.01$, unpaired, two-tailed Student's *t*-test.

Arginase-1 expression is associated with exacerbated inflammation in TB

Our data demonstrate that arginase-1 induced in response to *S. mansoni* infection and SEA immunization exacerbates inflammation in inbred C57BL/6 *Mtb*-infected mice. Inbred mice do not exhibit the heterogeneity in inflammatory responses seen in human TB. Thus, we recently used the Diversity Outbred (DO) mouse population to model heterogeneity in lung inflammatory and protective outcomes upon *Mtb* infection [126]. We next addressed if arginase-1 expression in

Mtb-infected DO hosts, even in the absence of helminth co-infection, was associated with exacerbated lung inflammation. Thus, we carried out RNA sequencing on lungs of individual genetically diverse DO mice that had severe inflammation (SI) and compared their transcriptional expression profile to individual DO mice that had enhanced control (EC), which coincided with formation of lymphoid follicle-containing granulomas and decreased *Mtb* burden [126]. Interestingly, we found that *Arg1* mRNA was among the top 10 genes differentially expressed in mice with severe inflammation, when compared to genes expressed in lungs of mice with enhanced *Mtb* control (Table 3, Fig 21A). In support of recently published studies [126, 180], mRNA for inflammatory molecules such as *S100a8* and *S100a9*, and chemokines associated with neutrophilic accumulation were also significantly increased in the lungs of mice with severe inflammation at the mRNA level (Table 3).

Table 3. Top 15 genes upregulated in lungs of DO mice with severe inflammation (SI) compared to mice with enhanced mycobacterial control (EC).

Gene	SI1	SI2	SI3	EC1	EC2	EC3	EC4	Fold Change
<i>Asprv1</i>	3.25701	39.9014	86.26	1.2504	0.645684	0.937151	1.76856	-5.228739831
<i>Alb</i>	14.4631	0.43517	0.218826	0.578426	0.0779802	0.0296708	0.0543738	-4.766670836
<i>Sifa211</i>	19.0143	85.6295	392.37	5.72234	10.4689	7.36957	2.73549	-4.655391684
<i>Slfn4</i>	8.08829	50.7014	13.174	0.232605	0.930751	1.13256	1.59585	-4.62380979
<i>Cxcl2</i>	10.383	64.7287	129.571	3.29095	2.76533	2.26271	3.2902	-4.555087448
<i>Pscs</i>	1.00759	36.4841	0.113578	0.523481	0	0	1.63579	-4.537356052
<i>Arg1</i>	11.1046	26.8485	149.778	10.0835	1.71299	1.59227	0.315004	-4.191061053
<i>Niacr1</i>	32.5266	173.235	96.2922	5.97616	10.0292	9.74134	10.8565	-3.45980135
<i>S100a9</i>	153.772	720.948	1968.91	26.5317	49.9857	223.773	76.2103	-3.332046807
<i>S100a8</i>	322.557	643.468	1746.02	86.289	32.8266	198.995	47.2137	-3.307168991
<i>Cd16311</i>	0.06745	3.01754	2.17326	0	0.0564829	0.658925	0.124513	-3.061294999

	05							
<i>Il1b</i>	99.8531	232.153	436.031	18.2768	17.5145	47.7993	40.5069	-3.044739449
<i>Ccl3</i>	167.375	692.047	436.08	40.2995	96.735	32.3074	56.8208	-2.933115825
<i>Il1a</i>	28.2172	54.4466	45.7485	3.11797	9.1227	4.55808	6.35482	-2.886514335
<i>Gzmb</i>	54.0801	93.7295	62.1257	15.5687	11.7763	13.6951	6.64021	-2.55351675

The increased expression of *Arg1* mRNA was confirmed by RT-PCR (Fig 21B). Importantly, arginase-1 activity in lung homogenates of individual DO mice correlated with increased pulmonary inflammation (Fig 21C). Thus, we then addressed whether arginase-1 could be an inflammatory marker that correlates with the extent of lung damage in human ATB patients in a TB endemic setting. We found that levels of arginase-1 activity in the serum from ATB patients showed a positive linear correlation with the extent of lung inflammatory damage as assessed by chest radiographs (Fig 21D). This also coincided with increased relative expression of *ARG1* mRNA in CD14⁺ monocytes isolated from peripheral blood of ATB patients, when compared to LTB patients (Fig 21E). Importantly, we also found increased serum arginase-1 activity in ATB patients with helminth co-infections, when compared to ATB patients without helminth co-infections (Fig 21F). These data provide new evidence that despite the well-known role for arginase-1 in impairing Th1 responses, arginase-1 may have a new emerging role to play in mediating pulmonary inflammation in TB.

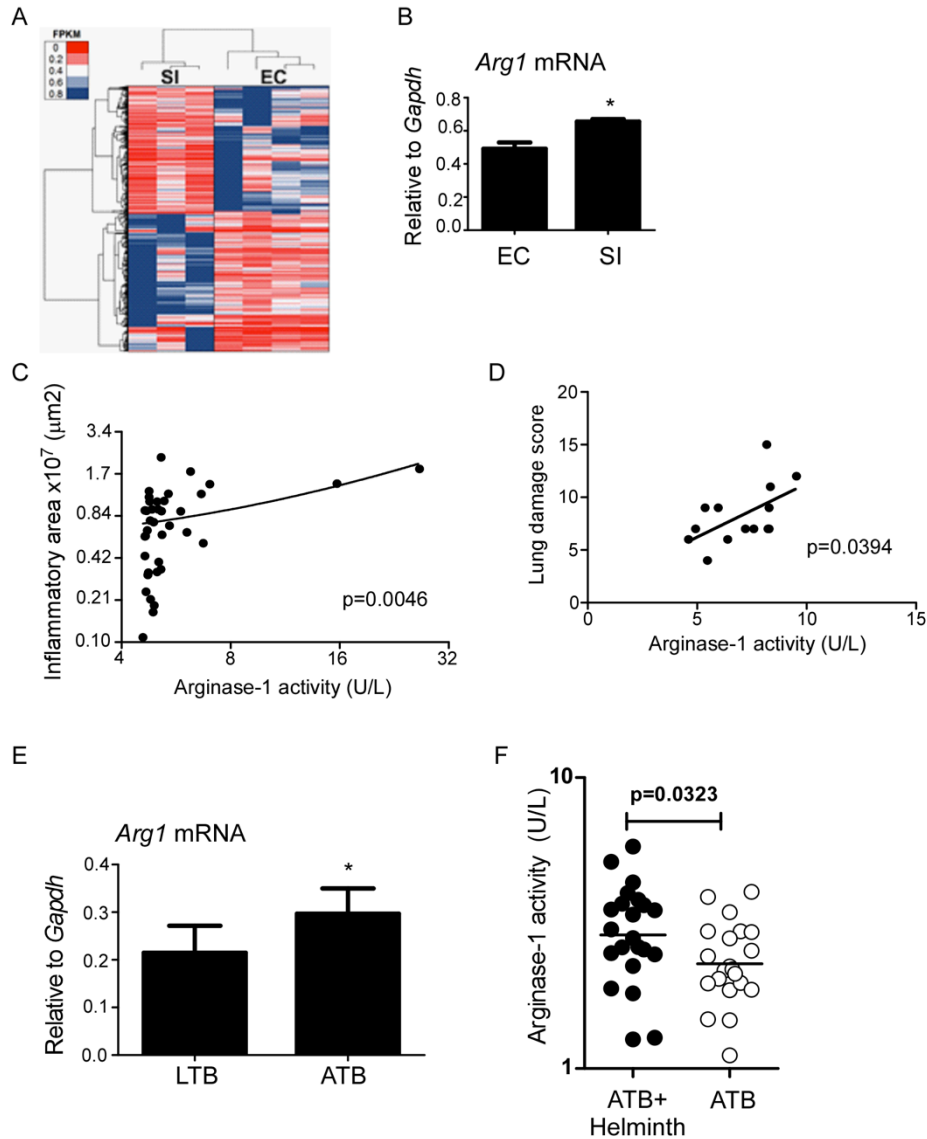


Figure 21. Arginase-1 expression during *Mtb* infection in genetically diverse mice and in humans correlates with increased inflammation and lung damage.

Individual DO (n=40) mice were aerosol infected with *Mtb* and lung bacterial burden on D50 post-infection was determined. Total area occupied by inflammatory lesions per lobe was quantified in H&E stained FFPE lung sections. RNAseq was performed on lung RNA from individual DO mice with the most severe inflammation (SI) and individual DO mice with enhanced control (EC), which also correlated with improved formation of lymphoid follicles within the granulomas. (A) Heat-map representation of significant genes. (B) The levels of *Arg1* mRNA expression relative to *Gapdh* in lungs of individual DO mice with SI or EC was determined by RT-PCR. (C) Arginase-1 activity was determined in lung homogenates of individual DO and linear correlation between arginase-1

activity and lung inflammatory area was determined (Pearson's correlation, log₂ scale). (D) Linear correlation analysis of arginase-1 activity in serum of patients with ATB and their lung damage score was carried out (Pearson's correlation, n=13). (E) The levels of *ARG1* mRNA expression relative to *GAPDH* in blood monocyte cDNA derived from LTB (n=5) and ATB (n=6) human donors were determined. (F) Arginase-1 activity in serum from ATB patients with helminth co-infection and those without helminth co-infections was measured (n=22 each). *p≤0.05, unpaired, two-tailed Student's *t*-test (B,E,F).

5.4 DISCUSSION

TB remains one of the largest global health threats, and it is estimated that, 5-10% of infected individuals will progress to ATB. However, the mechanisms leading to TB reactivation in otherwise immunocompetent individuals are largely undefined. As such, co-infection with helminths is considered a risk factor associated with increased TB reactivation rates and increased susceptibility to TB. However, thus far, the mechanisms behind this association remain poorly defined. In this study, we demonstrate that co-infection with *S. mansoni*, or presence of *S. mansoni* products such as SEA, can reversibly impair Th1 immune responses, but its effects on *Mtb* control are minimal. Unexpectedly, our data demonstrate that the more prominent effect of helminth infection during TB is the accumulation of high arginase-1-expressing macrophages within type 2 granulomas in the lung, mediating exacerbated inflammation and lung pathology during coinfection. Importantly, the effects driven by helminth-induced arginase-1-expressing macrophages on inflammation are reversible, as treatment with anti-helminthics can improve TB disease outcome. Our data in genetically diverse DO mice infected with *Mtb*, and humans with ATB, also show that increased arginase-1 activity correlates with increased inflammatory damage and disease severity during TB. Furthermore, helminth co-infection in ATB patients increases arginase-1 activity in serum. Together, our data suggest that contrary to the well-known anti-inflammatory role for arginase-1 and its inhibitory effects on Th1 responses [181], arginase-1 has a new prominent role in driving inflammation and mediating lung damage during TB.

Evidence suggests that a skewed Th2 response caused due to *S. mansoni* infection compromises protection conferred by *M. bovis* BCG vaccination in humans [158-160], and in mice systemically infected with *Mtb* [164]. Similarly, other models of helminth co-infections

such as *Nippostrongylus brasiliensis*, a rodent intestinal helminth that migrates to the lung, also drives Th2 responses and generation of alternatively activated macrophages in the lung, resulting in impaired resistance to *Mtb* [182]. Interestingly, while helminth co-infections increase *M. bovis* BCG [163] and *Mtb* [182] lung burden, the increase in mycobacterial burden is often transient [182], and moderate (about one log higher in co-infected hosts) [163] [182], suggesting that the effect of helminth co-infections on *Mtb* control is not profound enough to fully explain the increased severity of TB in helminth co-infected individuals observed in TB endemic regions. Furthermore, in some models of helminth *Mtb* co-infection, there are no differences observed in overall mycobacterial control [183, 184]. Our results support these published studies, as *S. mansoni* co-infection or immunization with SEA resulted in increased *Mtb* burden in the lung, but this effect was not profound, suggesting that *Mtb* control mechanisms are not completely suppressed in co-infected hosts. Furthermore, while some evidence suggests that *Mtb*-specific Th1 responses are impaired due to helminth co-infection [158, 163, 185], other studies have found that *Mtb*-specific Th1 responses are unaltered in the presence of helminth infections [182, 184]. Our studies show that *Mtb* infection induces a potent Th1 signature in in vivo primed T cells isolated from the infected lung, and that in vitro treatment with SEA has an inhibitory effect on Th1 immune responses, as well as on cell activation pathways. Similarly, presence of SEA or *S. mansoni* during *Mtb* infection in vivo results in a significant inhibition of IFN- γ production in T cells. This was associated with a trend towards increased levels of Th2 cells in co-infected mice, but no acquisition of a Th2 phenotype by *Mtb*-specific Th1 cells in vitro upon exposure to SEA. Whether these Th2 cells are *S.mansoni*-specific, or whether conversion of *Mtb*-specific Th1 cells to the Th2 subset occurs could be determined by transferring sorted Th1 cells from *Mtb*-infected ESAT-6 TCR Tg mice into uninfected or *S.mansoni*-infected controls. IL-4 is a

cytokine driving differentiation of Th cells upon priming, and its combination with IL-2 signaling is sufficient for differentiation [186]. A previous study focusing on Th1 to Th2 plasticity during *Nippostrongylus brasiliensis* infection established that conversion was enhanced, but not dependent on IL-4 signaling [187]. Whether this is also the case during *Mtb-S.mansoni* co-infection could be addressed by co-infecting IL-4-deficient mice. Our in vitro studies revealed a marked suppression of gene expression associated with Th1 commitment and TCR signaling in *Mtb*-specific Th1 cells treated with SEA. This is reminiscent of the marked degradation of cytosolic RNA by the RNase omega-1, one of the main components of SEA, in DCs. Omega-1-driven RNA degradation in DCs leads to Th2 differentiation due to decreased TCR signal strength [188]. Whether in vitro, omega-1 is responsible for the marked suppression of Th1 function upon SEA treatment, and whether it participates in Th1 to Th2 conversion in vivo, will be addressed in future studies.

In addition, we demonstrate that these effects on cytokine production by Th1 cells are transient and reversible, as evidenced by their comparable ability to produce IFN- γ following in vitro restimulation. In addition, removal of SEA restores IFN- γ production and the ability to activate alveolar macrophages to control *Mtb* infection. The discrepancy between our ex vivo flow cytometric analysis using reporter mice and our ELISpot results highlights the importance of directly analyzing immune cell function in the absence of additional restimulation in vitro. The differential assays used in the various studies, may in part be responsible for the variability in the impairment of *Mtb*-specific Th1 responses observed due to helminth infections across studies [158, 163, 182, 185]. Nonetheless, it is quite surprising that despite impairment of Th1 responses by treatment with SEA in vitro, removal of SEA in culture conditions can reverse this impairment. This is further supported by our data that show that treatment of *S. mansoni*

infection with an anti-helminthic such as praziquantel, can reverse the accumulation of arginase-1-expressing lung macrophages and decrease disease severity during TB. These findings are notable and underscore the potential for the broad application of antihelminthics as a cost-effective strategy to overcome the effects of helminth driven arginase-1-mediated disease severity during TB, and to decrease the risk for TB reactivation in susceptible, co-infected individuals.

Our data demonstrate that while the effects of *Schistosoma* co-infection on *Mtb* control are small, its influence on *Mtb*-induced lung inflammation and pathology are dramatic. Considering that the *Mtb* burden was not profoundly different in co-infected mice when compared *Mtb*-infected mice, the exacerbated inflammation observed in co-infected hosts is likely not due to differences in the mycobacterial antigenic load. Instead, we demonstrate that helminth infection results in induction of high arginase-1-expressing macrophages within the lung, which are organized as type 2 granulomas, and are morphologically and functionally different from the type 1 granulomas containing high iNOS-expressing macrophages induced in response to *Mtb* infection. The induction of high arginase-1-expressing macrophages results in increased lung pathology in the *S. mansoni* *Mtb*-co-infected hosts, projecting an inflammatory role for arginase-1 in *Mtb* infection. These data are further supported by the increased expression of *Arg1* mRNA expression in CD11c⁺ lung cells and increased inflammation observed in SEA treated *Mtb*-infected mice, suggesting that presence of *Schistosoma* antigens is sufficient to induce inflammation and lung pathology during *Mtb* infection. Our recent studies showed that the presence of B cell follicles harboring T cells interacting with macrophages within granulomas are associated with *Mtb* control during TB latency [102], while presence of granulocytes within the tubercle granulomas causes increased inflammation and exacerbates

disease severity in clinical disease [126]. Accordingly, the increased inflammation associated with *Schistosoma* co-infection and SEA immunization results in reduced formation of protective lymphoid follicles, with the concomitant formation of inflammatory granulomas containing both neutrophils and eosinophils. These data suggest that accumulation of helminth infection induced arginase-1-expressing macrophages in the lungs initiates the formation of “inflammatory” rather than “protective” granulomas during TB. That *S. mansoni*, *Mtb* co-infected BMC mice that lack arginase-1-expressing myeloid cells exhibit decreased lung inflammation and increased formation of protective B cell follicles provides direct evidence that helminth induced arginase-1 expression in myeloid cells mediates disease exacerbation in co-infected hosts. Interestingly, in a dermal *Mtb* infection model resulting in hypoxic lung granulomas, absence of arginase-1 in macrophages resulted in exacerbated inflammation in iNOS deficient mice [189]. It is possible that arginase-1 expression in macrophages can function to either limit or exacerbate inflammation depending upon the availability or absence of iNOS, and this needs to be carefully examined in the future. In the context of pulmonary *Mtb* infection, macrophages were found to express either iNOS, arginase-1, or co-express both iNOS and arginase-1, with the arginase-1-expressing macrophages localized to lymphocytic cuffs of granulomas in *Mtb*-infected macaques [190]. Accordingly, *Mtb* infection can induce arginase-1 expression in macrophages [174], and high levels of both arginase-1 and iNOS activity was detected in *Mtb*-infected macaque granulomas [190]. Consistent with these studies, the correlation between increased arginase-1 expression and increased inflammation in genetically diverse outbred mice and humans with ATB in our study, further suggests that genetic factors that drive increased arginase-1 production may contribute to increased pathology and disease severity during TB. Importantly, similar to the mouse model of co-infection, we detected increased arginase-1 activity in the serum of ATB

patients co-infected with helminths when compared to ATB patients without helminth co-infections. This is consistent with the presence of arginase-1-expressing macrophages within granulomas found within lungs of TB patients [190, 191], where arginase-1 is expressed both in granuloma associated macrophages [190, 191] and in type II pneumocytes [191]. Arginine is a crucial amino acid that modulates immune responses to *Mtb*, as it is a common substrate for both iNOS and arginase-1. Loss of arginase-1 in macrophages enhances protection against *Mtb* control, possibly due to increased availability of arginine for iNOS activity [174]. Interestingly, *Mtb* infection in mice deficient in arginase-1 expression within macrophages, also exhibit smaller, more lymphocytic granulomas [174], further supporting our hypothesis that arginase-1 regulates inflammation within TB granulomas. Based on these data, we propose that arginase-1 induced due to helminth co-infections, helminthic products, and host genetics, mediates the formation of more inflammatory TB granulomas. Finally, increased reactivation of *Mtb* infection after SEA treatment, suggests that helminth co-infection likely facilitates increased TB reactivation rates.

Arginase-1 has been implicated in models of lung injury, where increased expression of arginase-1 coincides with collagen deposition and fibrosis in pulmonary diseases such as asthma, cystic fibrosis, idiopathic pulmonary fibrosis (IPF), and chronic obstructive pulmonary disease (COPD) [192]. In animal models of silicosis, another inflammatory lung disease characterized by fibrosis, arginase activity and arginase-1 expression are enhanced in alveolar macrophages [192]. In contrast, in *S. mansoni* induced Th2 driven inflammation, macrophage-specific arginase-1 was demonstrated to function as a suppressor of fibrosis [193]. Our studies demonstrate that in the lungs of mice co-infected with *Schistosoma* and *Mtb*, increased accumulation of arginase-1 expressing macrophages organized as type 2 granulomas results in increased collagen

expression, increased *Mmp13* and *Ccl3* expression (data not shown), molecules implicated in lung fibrosis [192]. That accumulation of arginase-1-expressing macrophages coincide with exacerbated inflammation in a Th1 dominated disease such as TB is unexpected, as other models of acute and chronic Th2-mediated lung inflammation showed neither a pathogenic nor a protective role for myeloid-expressed arginase-1 [194]. In addition, our data show that praziquantel treatment in co-infected mice is able to control *S. mansoni* infection to fully reverse the increased inflammation and higher *Mtb* bacterial burden seen in co-infected mice, to levels seen in *Mtb*-infected mice. This is in contrast to the co-infection in BMC mice specifically lacking arginase-1 expression in myeloid cells, where increased inflammation is reversed but increased *Mtb* burden is unaffected. These data together suggest that while the increased inflammation seen in co-infected mice is helminth-driven and arginase-1-dependent, the increase in *Mtb* burden although helminth driven, is not directly dependent on arginase-1-expression in macrophages. Future studies delineating the specific mechanisms by which helminth induced responses drive the fibrosis and increased inflammation in a Th1 disease such as TB, will shed further light on the mechanisms of *Mtb* control, disease and TB reactivation in helminth-TB co-infected populations.

In conclusion, our data suggest that contrary to the well-known anti-inflammatory role for arginase-1 and its inhibitory effects on Th1 responses, arginase-1 has a prominent role in driving inflammation and mediating lung damage during TB. These novel data provide new insights into the mechanisms by which helminth co-infections drive increased susceptibility and disease progression in TB. In addition, our data show that the effects of helminth products on impairment of Th1 responses are reversible and support the use of antihelminthics as a cost-effective strategy to

improve *M. bovis* BCG vaccination, boost efficient immune responses against *Mtb* and to decrease the risk for TB reactivation in susceptible, co-infected individuals.

5.5 ACKNOWLEDGEMENTS

The author would like to thank Javier Rangel-Moreno, PhD (University of Rochester, NY) for immunofluorescence processing and analysis. Kristin Griffiths performed the praziquantel treatment experiment, carried out the mouse treatments with BSA and PPD and set up the bone marrow chimera experiment. Radha Gopal performed the DO infection, published in [195], from which the RNA for RNAseq done in this study was extracted. RNAseq and analysis of the DO mice was carried out by Dr. Makedonka Mitreva and Bruce Rosa (The Genome Institute, Washington University in St. Louis, MO). The lab of Dr. Subash Babu ran the Arginase-1 activity assay on serum samples from helminth-infected and control TB patients. An additional thanks is offered to Samantha Slight, Radha Gopal and Kristin Griffiths for their assistance with experiments, and Wing Lam for performing the *S.mansoni* infections. Finally, we also thank Keke Fairfax and Amber Smith for SEA preparation and Dr. Markus Mohrs for kindly providing us IFN- γ -YFP reporter mice, and Nathella Pavan Kumar, R. Sridhar and V.V. Banurekha for assistance with recruitment of patients. This work was supported by Children's Hospital of Pittsburgh of UPMC, Washington University in St. Louis, NIH grant HL105427 to S.A. Khader, Children's Hospital of Pittsburgh Research Advisory Committee Grant from Children's Hospital of Pittsburgh of the UPMC Health System to L. Monin, Department of Molecular Microbiology, Washington University in St. Louis, and Alexander and Gertrude Berg Fellowship to K.L. Griffiths. J. Rangel-Moreno was supported by funds of the Department of Medicine, University

of Rochester, and U19 AI91036. We thank Servier Medical Art (www.servier.com) for authorizing the reproduction of their images for generation of the *Schistosoma* egg cycle figure.

6.0 NTM DISEASE, AN EMERGING OPPORTUNISTIC INFECTION

6.1.1 Non-tuberculous mycobacteria

In previous chapters, we have focused on the effect of the cytokine milieu and helminth co-infections in shaping immune responses against primary infection and recall responses to *Mtb*. The genus *Mycobacterium*, however, encompasses numerous organisms, some of which are emerging opportunistic pathogens. In particular, non-tuberculous mycobacteria (NTM) are a diverse group of environmentally ubiquitous organisms with the potential of causing a wide spectrum of disease in humans. Exposure to NTMs is thought to occur through different sources, and biofilm formation in household and public water sources, such as showerheads and plumbing systems, is thought to be one of the possible exposure mechanisms [196-198]. NTMs most commonly cause disease in people with structural lung abnormalities, including cystic fibrosis (CF) patients and patients with primary ciliary dyskinesia, where average prevalence rates of 20% and 10%, respectively, have been reported [199]. In addition, female patients with a specific morphotype consisting of a thin body habitus, scoliosis, pectus excavatum and mitral valve prolapse, have been shown to have a higher rate of NTM infection. Similar to TB, immune suppression, and in particular treatment with TNF- α blockers [200], HIV infection and defects in IL-12 and IFN- γ are associated with serious cases of disseminated NTM disease [201].

Recently, concerns have been raised about the increasing rates of NTM infections in CF patients. The prevalence of chronic lung disease due to NTM is increasing and, in many areas of the US, exceeds that of *Mtb*. Indeed, it has been postulated that the true prevalence of NTM disease is higher than that of TB due to relative inefficacy of NTM treatments [202]. The most common NTM is the *Mycobacterium avium* complex (MAC), but other species, including *Mycobacterium abscessus*, are becoming particularly relevant in CF patients. *M. abscessus* infection accounts for 16% of NTM infections in CF patients and can cause a serious, life-threatening disease. In addition, it constitutes one of the most clinically virulent and antibiotic-resistant NTM species [203], and treatment can be rendered difficult by the discordance that often occurs between in vitro antibiotic susceptibility tests and clinical effectiveness [199]. In fact, *M. abscessus* treatment options are limited, with a treatment failure rate outcome of 50% for antibiotic treatment, and lung resection often being the sole option to treat disease [204]. The finding of NTM infection, and in particular *M. abscessus*, in CF patients is considered a contraindication for lung transplantation [205].

6.1.2 Host responses to NTM infection

Despite the demonstration that NTM can cause disease over 60 years ago, host immunity to NTM has been understudied in comparison to other related mycobacteria, including *Mtb* and *Mycobacterium leprae*. NTM disease in humans can present in different manifestations. Hypersensitivity pneumonitis can occur via inhalation of NTM in aerosolized droplets from sources such as showerheads or baths, and is thought to be the main source of MAC infections in HIV patients in the USA. In addition, people with lung disease, smokers or previously *Mtb*-infected individuals, can develop cavitary disease, with symptoms comparable to those seen in

TB. Finally, patients can develop nodular bronchiectasis, which is mostly observed in female patients with a thin body habitus.

M.abscessus infection has been described in immunocompromised individuals and in patients deficient in IL-12 and IFN- γ [206], pointing toward a role of adaptive immunity and, in particular, the Th1 subset, in host control of infection. This resonates with findings in a mouse model of intratracheal *M.abscessus* infection, in which SCID mice exposed to 10^4 cfu of *M.abscessus* were more susceptible than wild type hosts, and presented with small areas of perivascular inflammation [207]. More recently, two studies demonstrated a role for IFN- γ in protection against *M.abscessus* intravenous or aerosol infection of mice [208, 209]. In the aerosol model of infection, which better reproduces the natural route of infection, wild type mice spontaneously clear the infection. In contrast, *Ifng*^{-/-} mice were unable to control bacterial burden 60 days after infection, and developed large pulmonary lesions with foamy cell formation [208]. Given that IFN- γ negatively regulates IL-17, *Ifng*^{-/-} mice produce an intensified IL-17 response that mediates neutrophil recruitment and lung damage during other mycobacterial infections [210].

Interestingly, a recent study showed that patients infected with *M.abscessus* exhibit decreased serum levels of Th1 markers and increased Th17 responses, and that low levels of the chemokines IP-10 and MIG are associated with successful sputum conversion after antibiotic treatment [211]. In addition, large numbers of neutrophils, one of the main cell types recruited in response to IL-17 signaling, accumulate in CF patients infected with *M. abscessus*. This points toward a potential role of the Th1/Th17 balance in *M.abscessus* infection outcome. However, the exact mechanisms leading to *M.abscessus* infection containment and the relative contributions of different Th subsets to *M.abscessus* pathology versus control remain poorly understood.

6.1.3 Co-infections during NTM infections in CF

Mucus accumulation and inhibition of lung antimicrobial peptides through high ion concentration are thought to underlie the increased predisposition of CF patients to infection. Indeed, numerous pathogens can persist in the lungs of these individuals and contribute to the decline in respiratory function [212]. Importantly, this increased susceptibility to lung infections makes co-infections between NTM and other characteristic CF pathogens common. Indeed, a recent study has revealed the presence of *Pseudomonas*-derived genes in the genome of *M. abscessus*, and epidemiological data show that *P. aeruginosa* and *M. abscessus* frequently coexist in the lung environment [213]. Similarly, *A. fumigatus* can colonize the lungs in CF patients and induce allergic bronchopulmonary aspergillosis [212], and is associated with aggravation of NTM pathology [5].

In this context, common CF co-infections may alter the course of NTM disease, and the nature and mechanisms behind such changes in NTM containment have not been studied in depth. *A.fumigatus* has been shown to induce Th17 signature cytokine production and neutrophilia [214], which have been associated with the development of pathology in a number of inflammatory conditions. These Th17 responses are beneficial for *Aspergillus* given that they inhibit the Th1 responses required to control infection and promote biofilm formation [214, 215]. Given the importance of Th1 immunity in mycobacterial control, a concomitant *A.fumigatus* infection may also be detrimental for mycobacterial containment. In addition, neutrophils have been shown to promote *M.abscessus* biofilm formation, thereby promoting bacterial persistence [216]. *A. fumigatus* has also evolved a number of strategies to evade the immune response, among which is TLR-2-dependent stimulation of IL-10 secretion [217]. In addition, PBMCs from CF patients secreted increased amounts of IL-10 when exposed to recombinant *A.fumigatus*

antigens, in comparison to PBMCs from healthy individuals [218]. Upon blockade of IL-10, Th1 responses were enhanced, suggesting that IL-10 may play a role in inhibiting *A.fumigatus* T cell responses in CF [218]. This raises the question of whether such inhibition of the immune response by *A.fumigatus* may affect concomitant immunity to NTM infections and their associated pathology.

In this work, we have characterized the immune mechanisms required for *M.abscessus* control in a mouse model, and explored the participation of Th17 cells in *M.abscessus* infection containment. In addition, we have studied the effect of previous *A.fumigatus* infection, which induces a potent Th17 immune response, on a subsequent challenge with *M.abscessus*. Together, our data provide novel insights into how CF prevalent fungal diseases affect the pathology and control of emerging opportunistic NTM infections, such as *M.abscessus*.

7.0 THE EFFECT OF TH17-SKEWING INFECTIONS ON IMMUNITY TO NON-TUBERCULOUS MYCOBACTERIA

7.1 SUMMARY

Cystic fibrosis (CF) is an autosomal recessive disease caused by mutations in the CF transmembrane conductance regulator (CFTR) gene. Mutations in this chloride channel lead to mucus accumulation, subsequent recurrent pulmonary infections and inflammation, which is responsible for lung deterioration and failure. Recently, concerns have been raised about the increasing rates of nontuberculous mycobacterial (NTM) infections in CF patients. Of particular relevance is infection with *Mycobacterium abscessus*, which causes a serious, life-threatening disease and constitutes one of the most antibiotic-resistant NTM species. Interestingly, an increased prevalence of NTM infections associated with severe lung deterioration has been reported in CF patients that are also infected with *P. aeruginosa* or *A. fumigatus*. The latter infections are common in CF patients and induce Th17 signature cytokine production and neutrophilia. We studied the immune requirements for *M.abscessus* containment using a mouse model of infection, and found that adaptive immunity and IFN- γ , but not IL-17 receptor signaling, were required for containment of infection. In a model of co-infection with *A.fumigatus*, co-infected mice exhibited decreased bacterial burden when infected with an intermediate dose of *M.abscessus*. This increased control was mucus-independent, but dependent

on the presence of both Tbx21 and Rorc. In turn, co-infection using a high dose of *M. abscessus* did not significantly alter bacterial control, but reduced *M. abscessus*-driven lung pathology with a concomitant increase in IL-10 production and Treg lung infiltration. Together, our results demonstrate that CF-prevalent fungal infections can ameliorate *M. abscessus* control and pulmonary damage in a mouse model.

7.2 METHODS

Animals

C57BL/6 (B6) animals were purchased from Taconic. *Ifng*^{-/-} mice on the B6 background were purchased from The Jackson Laboratory (Bar Harbor, ME). *IL17rc*^{-/-}, *IL17ra*^{-/-}, *Rag1*^{-/-}, *Rag2*^{-/-}*Il2rg*^{-/-}, *Stat1*^{-/-} and *Stat6*^{-/-} mice were maintained in the animal facility at the University of Pittsburgh. Experimental mice were age- and sex-matched and used between the ages of 6-8 weeks. All mice were maintained and used in accordance with the approved University of Pittsburgh IACUC guidelines.

Experimental infections

Mycobacterium abscessus strain L948 was grown in Middlebrook 7H9 broth containing 0.05% Tween-80 to mid-log phase and frozen in 1mL aliquots at -80°C. For *M. abscessus* infections, animals were oropharyngeally infected with 1000-1x10⁶ (CFU) of bacteria using the tongue-pull method. Briefly, mice were anesthetized with 3% isoflurane, suspended by their front incisors, and the tongue was extended using forceps. The bacterial suspension was pipetted into the trachea, and the tongue was held until normal breathing resumed. In some cases, a second challenge was performed 1 week after the initial infection. Lung bacterial burden was

established by plating out organ homogenates on 7H10 agar plates. For co-infection with *A.fumigatus*, mice were oropharyngeally infected with 2.5×10^7 *A.fumigatus* conidia 3 days prior to *M.abscessus* challenge.

Lung single-cell preparation and detection of cytokine-producing cells by ELISpot assay

Lung suspensions from *M.abscessus*-infected mice were prepared as described previously [84] and were used in ELISpot assays as described below. Antigen-specific IFN- γ -producing and IL-17-producing cells were analyzed by ELISpot assay. Multi-screen HA filter plates (Millipore, Billerica, MA) were coated with anti-IFN- γ (BD Biosciences) or anti-IL-17 (R&D Systems) antibodies. Single cell suspensions were added to the plate at a starting concentration of 1×10^5 cells/well and doubling dilutions made. Cells were cultured overnight in the presence of 1×10^6 irradiated splenocytes and 10 μ g/mL heat killed *M.abscessus* and 10 U/mL recombinant mouse IL-2. The following day, biotinylated anti-IFN- γ or anti-IL-17 antibody (both from eBioscience, San Diego, CA) was added and incubated overnight. Plates were developed by incubation with streptavidin-alkaline phosphatase (Vector Labs, Burlingame, CA) for two hours, followed by incubation with NBT/BCIP (Sigma Aldrich). Spots were enumerated using a CTL-ImmunoSpot analyzer (CTL, Shaker Heights, OH) and the frequency and total number of responding cells calculated as described before [84].

Detection of cytokine-producing cells by flow cytometry

The presence of cells producing IFN- γ and IL-17, as well as additional immune populations, was determined by flow cytometry. Single cell suspensions were stimulated for five hours in the presence of 50 ng/mL phorbol-myristate acetate and 750 ng/mL ionomycin, as well as 5 μ L/mL GolgiStop (BD Biosciences). Cells were treated with Fc Block (anti-CD16/CD32,

BD Biosciences) before surface staining for CD3, CD4 CD44, CD25, MHC class II, CD11c or CD11b. Cells were then fixed and permeabilized using the Cytotfix/Cytoperm fixation permeabilization kit (BD Biosciences) before staining for IL-17 and IFN- γ , or according to the instructions for the Foxp3 Transcription Factor Staining Buffer Set (eBioscience) prior to Foxp3 staining. Cell staining was analyzed on an LSRII (BD Biosciences), and results were processed using FlowJo (Treestar, Ashland, OR).

Determination of protein concentration

ELISA antibody pairs (DuoSet; R&D Biosystems) or Milliplex kits (Millipore) were used to detect cytokine levels in cell culture supernatants.

Real-time PCR.

RNA was extracted using the RNeasy kit (Qiagen) and cDNA was then amplified with FAM-tagged probes and PCR primers on a Vii7 thermocycler. Specific gene expression was calculated relative to *Gapdh* expression. Primer and probe sequences targeting specific genes were commercially purchased (ABI Biosystems).

Morphometric analysis.

Lungs from infected mice were inflated with 10% neutral buffered formalin and paraffin embedded. Lung sections were stained with H&E stain (Colorado Histo-Prep) and processed for light microscopy. Images were obtained with a Zeiss Axioplan 2 microscope and were recorded with a Zeiss AxioCam digital camera. Caudal lobes underwent morphometric analysis in a blinded manner using the morphometric tool of Zeiss Axioplan microscope, which determines the area defined by the squared pixel value for each inflammatory focus [102]. PAS staining was performed by the pathology core at Children's Hospital of Pittsburgh of UPMC.

Generation of BMDMs (Bone Marrow-derived Macrophages)

BMDMs were generated from the bone marrow of C57BL/6 mice. Cells were extracted from femurs and 1×10^7 cells were plated with 10 mL of cDMEM supplemented with 20 ng/mL mouse recombinant GM-CSF (PeproTech). Cells were cultured for 3 days at 37°C in 5% CO₂, after which an additional 10 mL of cDMEM containing 20 ng/mL rmGM-CSF was added. On day 7, the adherent cells were collected by centrifugation and counted.

In vitro *Mtb*-killing assay.

For killing assays, BMDMs were pre-treated with medium or 100 µg/mL zymosan or curdlan for 24 h. BMDMs were then infected with *M. abscessus* at an MOI of 1 for 48 h. At the end of the culture period, macrophages were washed twice with PBS, lysed by a 5 min incubation with 0.05% SDS. Following SDS neutralization with 10% BSA, intracellular *M. abscessus* burden was determined by plating of serial dilutions on 7H10 plates.

Detection of nitrites by the Griess reaction.

Culture supernatants were assessed for nitrite production by using the Griess Reagent System Kit (Promega, Madison, WI), according to the manufacturer's instructions.

Sputum processing

Fresh sputum samples were collected from CF patients, weighed and incubated with a volume (mL) of 10% Sputolysin in PBS equivalent to the mass (g) of the sputum sample, for 15 min at 37°C with shaking. Following the incubation, cells were separated from the supernatant after centrifugation at 805 xg for 10 min.

Statistical analysis

Differences between the means of multiple experimental groups were analyzed using one-way ANOVA with Tukey's post-hoc test. For all other analyses, we used the two-tailed

Student's t-test. Differences were considered significant when $p \leq 0.05$. For all figures, data represent mean \pm SD. All analyses were performed using GraphPad Prism Software.

Study approval.

All individuals were examined as part of a clinical research protocol approved by the Institutional Review Board of the University of Pittsburgh and informed written consent was obtained from all participants. All mice were used following the National Institutes of Health guidelines for housing and care of laboratory animals and in accordance with University of Pittsburgh and Washington University in St. Louis Institutional Animal Care and Use Committee guidelines. All efforts were made to minimize suffering and pain as described in these approved protocols.

7.3 RESULTS

The immune mechanisms required for containment of *M. abscessus* in a mouse model have not been extensively studied. In order to analyze the immune response induced by *M. abscessus* infection, we optimized an in vitro *M. abscessus* infection system. For that purpose, mouse bone marrow-derived macrophages (BMDMs) were infected with varying MOI of *M. abscessus* and cytokine production 48 and 120 hours post-infection was analyzed. Interestingly, IL-1 β , an important cytokine that mediates production of IL-17 by $\gamma\delta^-$ and CD4 $^+$ T cells, was upregulated at high MOI 120 hours (Fig 22A) post infection.

To delineate the immunological requirements for *Mycobacterium abscessus* control, we optimized a *M. abscessus* mouse infection model, adapted from a previous publication [208]. Briefly, 6-8 week-old C57BL/6 mice were oropharyngeally infected with *M. abscessus* L948 strain. We studied the kinetics of infection in C57BL/6 mice with varying doses of *M. abscessus* and found that mice infected with *M. abscessus* rapidly control the infection, with complete bacterial clearance occurring at the 21 and 28 day time points for the 10^3 and 2×10^4 inoculums, respectively (Fig 22B). When mice received two weekly doses of 1×10^6 cfu of *M. abscessus*, bacterial burden was low, but not completely cleared by day 28 post-infection (Fig 22B). In immune competent mice, bacteria did not disseminate to the spleen, indicating that immune mechanisms elicited by the bacterium in immune competent wild type mice were sufficient to maintain the infection localized in the primary organ of infection (data not shown). This is also highlighted by the low degree of lung pathology observed in mice infected at the low *M. abscessus* doses, which consisted of small perivascular inflammatory foci, mostly composed of lymphocytic aggregates (Fig 22C). In contrast, mice that received two doses of 1×10^6 cfu of

M. abscessus presented with mixed lympho-histiocytic infiltrates surrounding the blood vessels and bronchi, which also extended into the lung parenchyma (Fig 22C). In order to determine *M. abscessus* antigen-specific T cell responses, we standardized an antigen-driven ELISpot assay, using heat-killed *M. abscessus* to stimulate lung cell suspensions from infected animals. Interestingly, at the peak of the response (14 dpi), mice harbored no detectable *M. abscessus*-specific IFN- γ -producing cells, but rather developed a Th17 response (Fig 22D). Given the undetectable lung pathology and fast clearance of infection in mice challenged with the 10^3 cfu dose, we excluded that inoculum size from subsequent experiments.

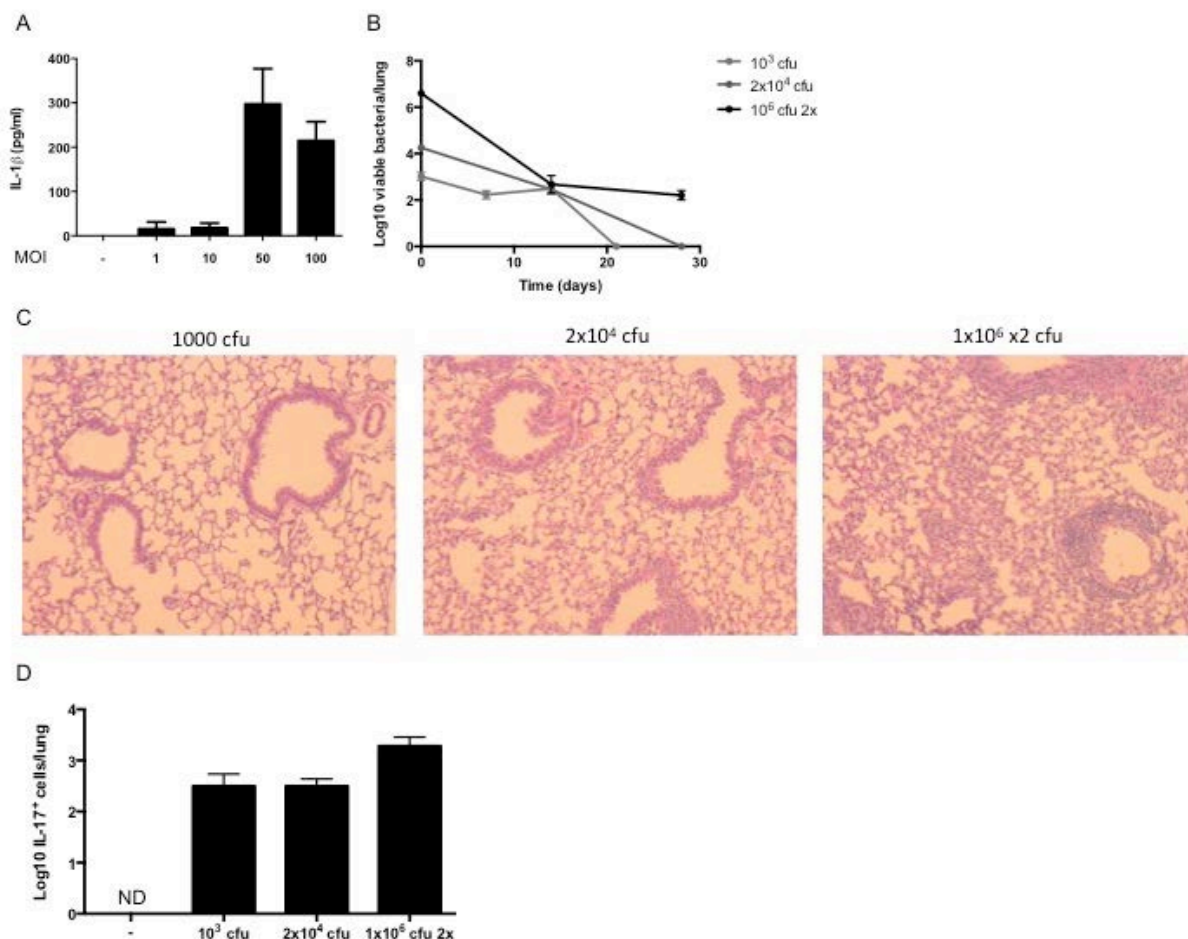


Figure 22. *M. abscessus* infection is rapidly controlled by C57BL/6 mice and induces potent Th17 responses.

(A) BMDMs were left untreated (-) or infected with varying MOI of *M. abscessus* for 120 hours and IL-1 β levels in the culture supernatants determined by ELISA. (B) C57BL/6 mice were oropharyngeally infected with *M. abscessus* and lung bacterial burden was determined between days 0 and 28 post-infection by plating on 7H10 agar. (C) Pulmonary inflammation was assessed on day 14 post-infection on FFPE lung sections stained with H&E. 100X magnification. (D) The number of IL-17-producing, *M. abscessus*-specific T cells was determined in the lungs of infected mice 14 days post-infection by antigen-driven ELISpot.

We initially assessed the broader requirement for NK cells and adaptive immunity in the control of *M. abscessus* challenge. For that purpose, *Rag2^{-/-}Il2rg^{-/-}* mice, which lack NK, B and T cells were challenged with 2×10^4 cfu of *M. abscessus* and bacterial burden assessed 2 weeks post-infection. Lung bacterial burden at this time was slightly elevated in *Rag2^{-/-}Il2rg^{-/-}* mice (Fig 23A), indicating that adaptive immunity and NK cells play a role in limiting bacterial control. However, the only slight increase in bacterial burden may indicate a more prominent role of innate immunity in the control of low infectious doses this pathogen. In contrast, *Rag1^{-/-}* mice infected with 2 weekly doses of 1×10^6 cfu *M. abscessus* presented a 1 log increase in bacterial burden in comparison to wild type mice (Fig 23D). Given that Th1 and Th17 responses have been involved in primary defense against mycobacteria, we next determined the effect of IL-17RA and IFN- γ deficiency on *M. abscessus* infection. For that purpose, *Il17ra^{-/-}* or *Ifng^{-/-}* mice were infected with 2×10^4 or two weekly challenges of 1×10^6 cfu of *M. abscessus*. Bacterial burden assessment 2 weeks after challenge showed comparable levels of *M. abscessus* in the lungs of C57BL/6, *Il17ra^{-/-}* and *Ifng^{-/-}* mice infected with 2×10^4 cfu *M. abscessus* (Fig 23B,C). Similarly, C57BL/6 and *Il17rc^{-/-}* mice were able to control *M. abscessus* infection at the 1×10^6 cfu dose to a similar extent (Fig 23E). Surprisingly, and like C57BL/6 infected controls, *Ifng^{□□□}* mice infected with 2×10^4 cfu *M. abscessus* were able to clear infection by day 30 post-

infection. However, when exposed to two challenges with 1×10^6 cfu *M. abscessus*, *Ifng*^{-/-} mice exhibited a significant increase in bacterial burden (Fig 23F). These *Ifng*^{-/-} mice harbored increased Th17 cells in the lung (Fig 23H) and a significant reduction in macrophage MHC class II expression, suggesting that Th17 cells alone were not sufficient to mediate protective responses (Fig 23I). These data indicate that IL-17RA signaling is dispensable for *M. abscessus* control in an oropharyngeal model of infection, while IFN- γ was required for protection against repeated exposure but not single low dose exposure to *M. abscessus*. Taken together, these data indicate that control of higher infectious doses of the pathogen is more dependent on a functional adaptive immune system.

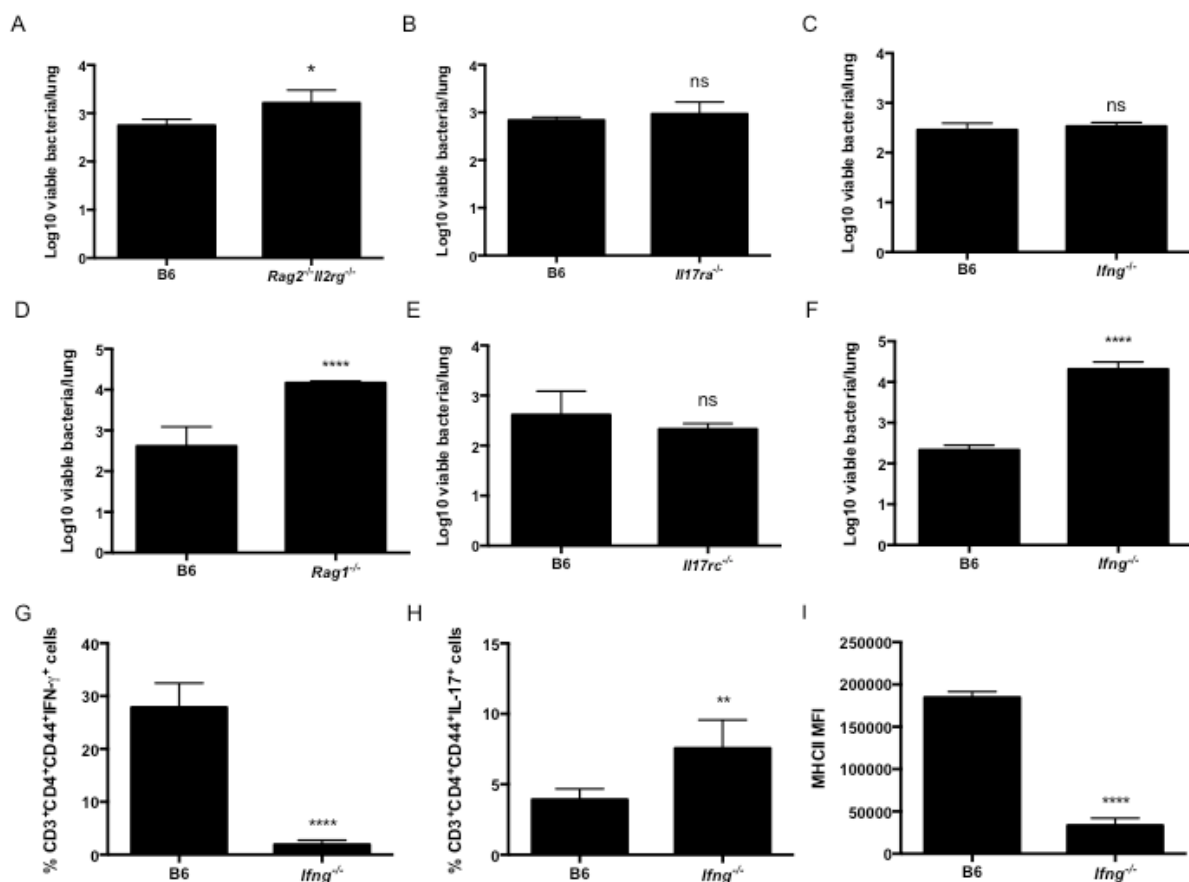


Figure 23. Adaptive immunity, and IFN- γ , but not IL-17R signaling, are required for *M. abscessus* control.

(A,D) C57BL/6 (B6) and *Ifng*^{-/-}, (B) *Il17ra*^{-/-}, (C) *Rag2*^{-/-}*Il2rg*^{-/-} (E) *Il17rc*^{-/-} and (F) *Rag1*^{-/-} mice were oropharyngeally infected with 2x10⁴ cfu (A-C) or 2 doses of 1x10⁶ cfu (D-F) of *M.abscessus* and lung bacterial burden was determined on D14 post-infection. Lung (G) Th1 (CD3⁺CD4⁺CD44⁺IFN-γ⁺), (H) Th17 (CD3⁺CD4⁺CD44⁺IL-17⁺) and (I) MHC II mean fluorescence intensity (MFI) in macrophages were determined by flow cytometry in C57BL/6 or *Ifng*^{-/-} mice infected with 2 doses of 1x10⁶ cfu *M.abscessus*. *p≤0.05, **p≤0.01, ***p≤0.0001, ns- not significant.

We subsequently addressed the effect of *A.fumigatus* co-infection on *M.abscessus* control and associated lung pathology. For that purpose, we infected C57BL/6 mice with 2.5x10⁷ *A.fumigatus* conidia and challenged the mice with *M.abscessus* 3 days later, coinciding with the peak of *A.fumigatus*-induced IL-17 responses. Interestingly, we observed a differential effect of *A.fumigatus* co-infection on *M.abscessus* control and pathology, depending on the infectious dose of *M.abscessus*.

Surprisingly, at a low dose of *M.abscessus* infection (2x10⁴ cfu), co-infected mice had slightly improved *M.abscessus* control (Fig 24A). Similarly to *A.fumigatus*-only infected mice, *A.fumigatus*, *M.abscessus* co-infected mice cleared *A.fumigatus* infection, as evidenced by failure to amplify *A.fumigatus* 18S rRNA and absence of GMS staining (data not shown). Co-infected mice, however, harbored more lung inflammation, as evidenced by more numerous inflammatory foci in comparison to *M.abscessus*-infected mice (Fig 24B). This was associated with increased mucus accumulation evidenced by PAS staining (Fig 24C). Since *A.fumigatus* infection can cause mucus accumulation, we studied whether deficient *M.abscessus* attachment to lung cells upon infection could underlie the decreased bacterial burden in co-infected mice. We thus challenged previously *A.fumigatus*-infected mice for 1 hour and assessed lung bacterial burden. *M.abscessus* burden did not significantly differ between control and *A.fumigatus*-

infected mice, suggesting that the effects of *A.fumigatus* on *M.abscessus* control occur at a later point during infection (Fig 24D). We further tested the importance of mucus on *A.fumigatus*-induced *M.abscessus* control by infecting *Stat6*^{-/-} mice, which are unable to produce mucus. Co-infected *Stat6*^{-/-} mice were able to control *M.abscessus* to an extent similar to C57BL/6 mice (Fig 24E), indicating that mucus production directly does not play a role in *M.abscessus* control.

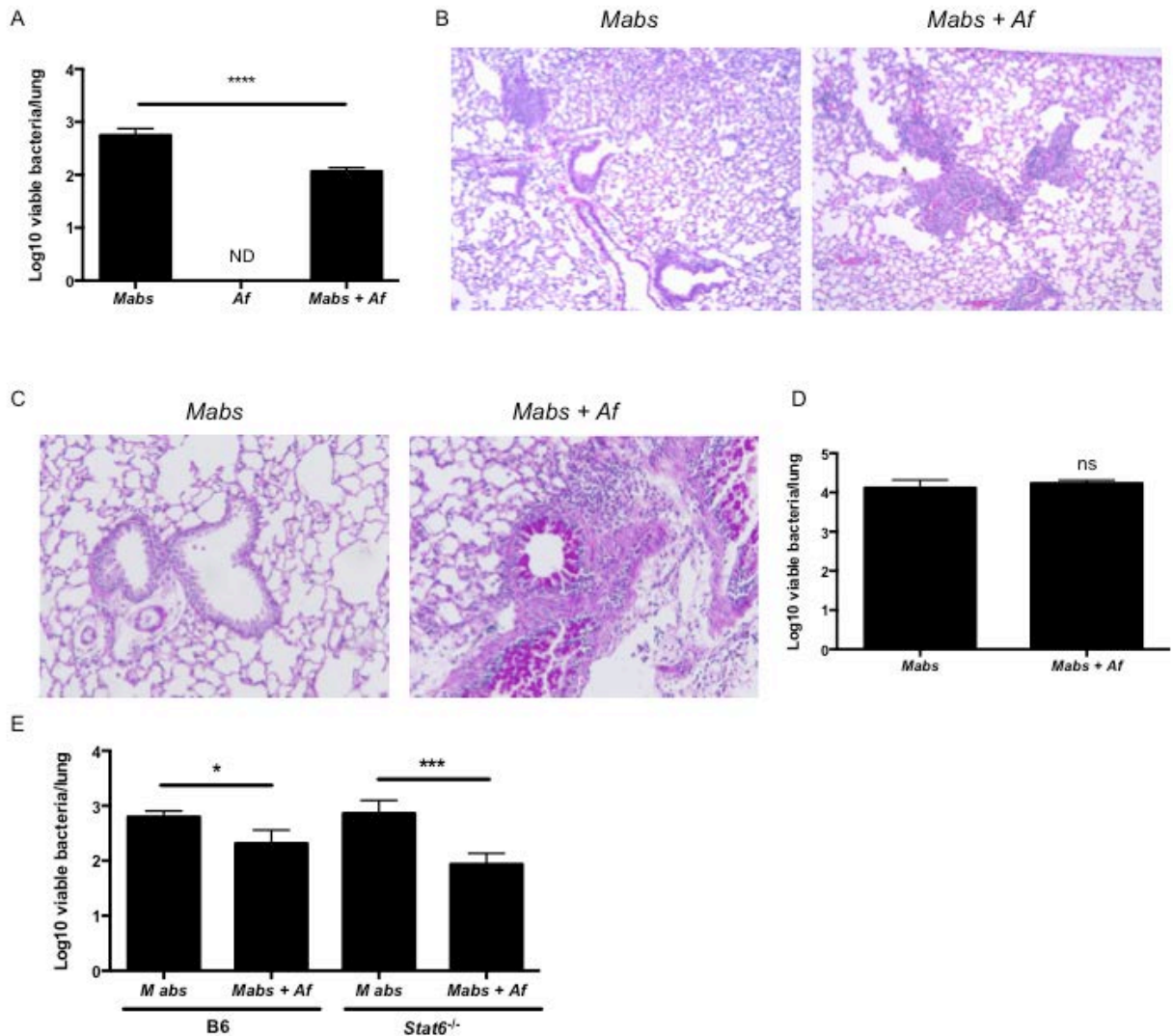


Figure 24. *A. fumigatus* infection enhances *M.abscessus* control via a mucus-independent mechanism.

C57BL/6 (B6) *A.fumigatus*-infected (*Mabs*+*Af*) or control (*Mabs*) mice were challenged with 2×10^4 cfu of *M.abscessus* 3 days later. A group of mice only received *A.fumigatus*-infection (*Af*). (A) Lung bacterial burden was determined 14 dpi. (B) Pulmonary inflammation was assessed on D14 FFPE lung sections stained with H&E. 100X

magnification. (C) FFPE lung sections were analyzed for mucus and glycogen production by the PAS stain. 200X magnification. (D) Lung bacterial burden was determined 1 hour following *M.abscessus* challenge. (E) B6 or *Stat6*^{-/-} *A.fumigatus*-infected or control mice were challenged with 2x10⁴ cfu of *M.abscessus* 3 days later. Lung bacterial burden was determined 14 dpi. *p≤0.05, ***p≤0.001, ****p≤0.0001, ns- not significant.

We subsequently sought to determine which immune mechanisms are responsible for improved *M.abscessus* control in co-infected mice. We found that co-infected mice harbored higher numbers of *M.abscessus*-specific Th17 cells in their lungs 2 weeks after challenge, as evaluated by antigen-driven ELISpot (Fig 25A). We therefore infected *Il17ra*^{-/-} mice with *M.abscessus* alone or *A.fumigatus* and *M.abscessus*, and found that *Il17ra*^{-/-} co-infected mice harbored slightly higher numbers of bacteria in their lungs when compared to co-infected C57BL/6 mice (Fig 25B). This indicates that IL-17RA signaling is partially involved in *A.fumigatus*-induced *M.abscessus* control. Because interferon signaling has been associated with improved anti-mycobacterial responses, we next determined the effect of STAT-1 deficiency on *A.fumigatus*-induced *M.abscessus* control. Interestingly, we found that *Stat1*^{-/-} co-infected mice retained protection (Fig 25C), indicating that interferon signaling may not be required for the protection observed in co-infected mice. Because multiple mechanisms may simultaneously contribute to *M.abscessus* control in co-infected mice, we next co-infected *Tbx21*^{-/-}, *Rorc*^{-/-} or *Tbx21*^{-/-}*Rorc*^{-/-} mice, which lack Th1, Th17 or both Th1 and Th17 responses, respectively. Interestingly, we found that, individually, each transcription factor was dispensable for *A.fumigatus*-induced *M.abscessus* protection (Fig 25D). However, co-infected mice lacking both transcription factors failed to improve protection against *M.abscessus* challenge (Fig 25D). Together, these results pointed toward a role for Th1 and Th17 responses in control of *M.abscessus* in *A.fumigatus* co-infected mice.

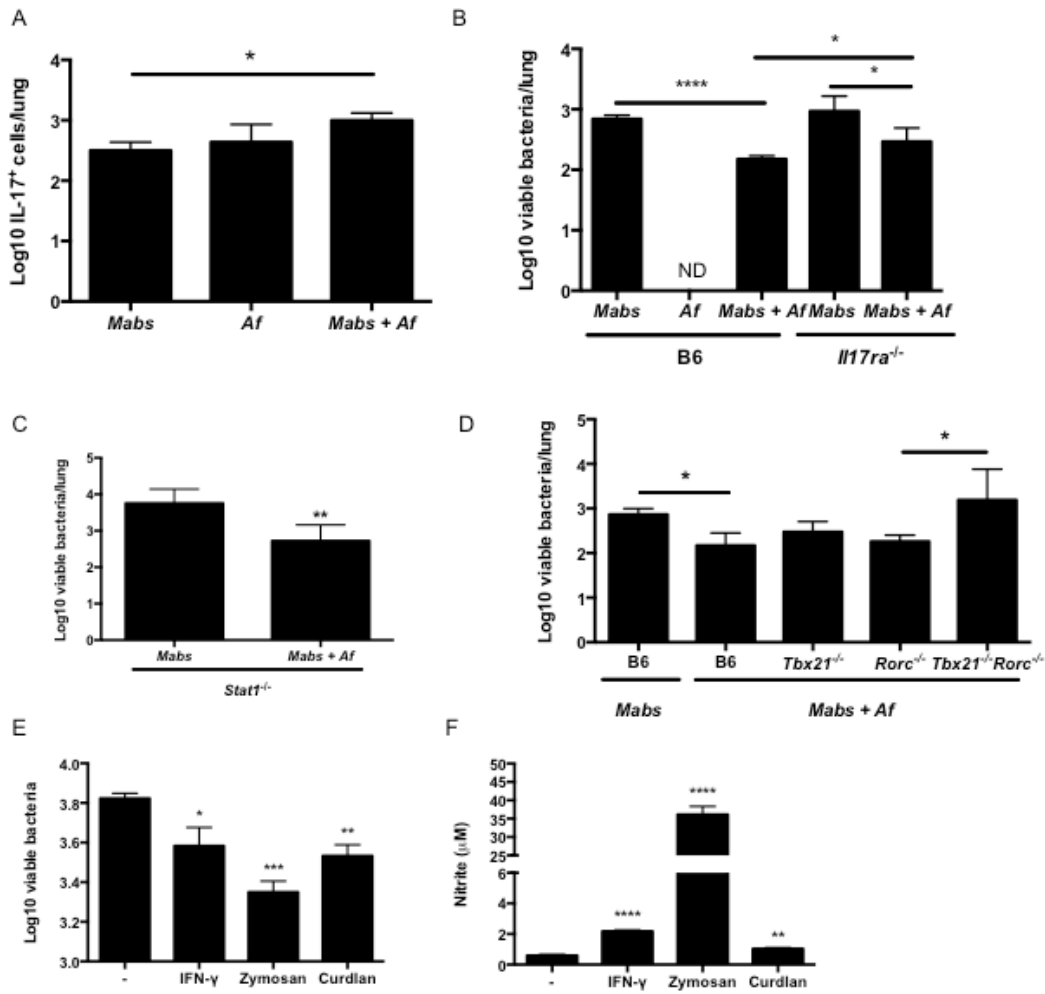


Figure 25. *A. fumigatus*-induced *M. abscessus* control is STAT-1 independent but IL-17RA, Tbx21 and Rorc-dependent.

C57BL/6 (B6) *A.fumigatus*-infected (*Mabs*+*Af*) or control (*Mabs*) mice were challenged with 2×10^4 cfu of *M.abscessus* 3 days later. A group of mice only received *A.fumigatus*-infection (*Af*). (A) The number of IL-17-producing, *M.abscessus*-specific T cells was determined in the lungs of infected mice 14 dpi. B6 and (B) *Il17ra*^{-/-} (C) *Stat1*^{-/-} (D) *Tbx21*^{-/-}, *Rorc*^{-/-} and *Tbx21*^{-/-}*Rorc*^{-/-} *A.fumigatus*-infected or control mice were challenged with 2×10^4 cfu of *M.abscessus* 3 days later. Lung bacterial burden was determined 14 dpi. IFN-γ, zymosan and curdlan-treated or control BMDMs were infected with *M.abscessus* (MOI 1) for 48 hours. (E) The number of viable bacteria within macrophages and (F) nitrite levels in the supernatants were determined. *p≤0.05, **p≤0.01, ***p≤0.001, ****p≤0.0001, ND- not detectable.

A potential mechanism leading to improved control of *M.abscessus* in *A.fumigatus* infected mice could be activation of macrophages to induce *M.abscessus* killing. We therefore set up an in vitro system to address this hypothesis. Bone marrow-derived macrophages (BMDMs) were generated in vitro in the presence of GM-CSF and upon differentiation into DCs were treated for 24h with fungal products, including zymosan and curdlan. Interestingly, both fungal products were able to induce better bacterial killing (Fig 25E). This was associated with improved iNOS activation, as measured by nitrite quantification using the Griess method (Fig 25F).

Together, our results show that at a low infectious dose of *M.abscessus*, *A.fumigatus* infection confers improved protection that is mediated by *Tbx21* and *Rorc*-expressing cells. In addition, *A. fumigatus* antigens could potentiate macrophage activation, which could, in turn, improve *M. abscessus* control in co-infected mice.

In contrast, in mice receiving high doses of *M.abscessus* (1×10^6 cfu given twice), previous *A. fumigatus* infection is associated with a significant reduction in lung inflammation (Fig 26A). Interestingly, this reduction was not accompanied by a change in *M.abscessus* control, as lung bacterial burden did not differ between single-infected and co-infected mice (Fig 26B). Histological findings were confirmed by flow cytometric analysis of lung populations, which revealed decreased macrophage (Fig 26C) and activated CD4⁺ T cell numbers (Fig 26D). Within the remaining infiltrating CD4⁺ T cells, co-infection led to an increased percentage of Th17 cells (Fig 26E), with no changes in the percentage of Th1 cells (Fig 26F).

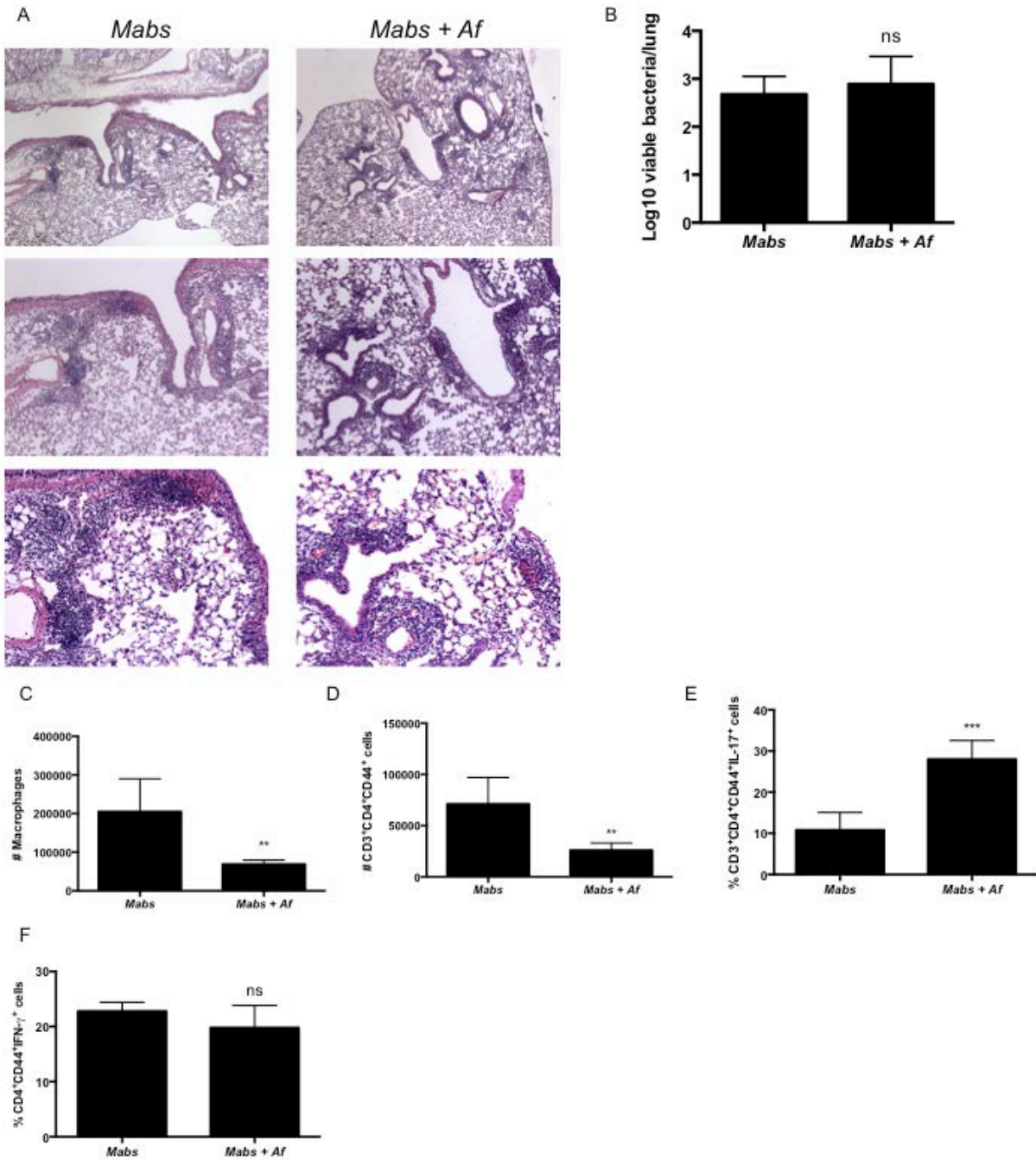


Figure 26. *A.fumigatus* infection reduces *M.abscessus*-driven lung inflammation.

C57BL/6 *A.fumigatus*-infected (*Mabs+Af*) or control mice (*Mabs*) were challenged with 1×10^6 cfu of *M.abscessus* 3 days later. Mice were rechallenged with an equivalent dose of *M.abscessus* 1 week later. (A) Pulmonary inflammation was assessed on D14 FFPE lung sections stained with H&E. Top panel-50X magnification, middle panel-100X magnification, bottom panel-200X magnification. (B) Lung bacterial burden was determined on D14 post-infection. The number of lung (C) macrophages, (D) activated CD4⁺ T cells (CD3⁺CD4⁺CD44⁺), as well as the

percentage of (E) Th17 (CD3⁺CD4⁺CD44⁺IL-17⁺) and (F) Th1 (CD3⁺CD4⁺CD44⁺IFN- γ ⁺) cells was determined on D14 by flow cytometry. **p \leq 0.01, ***p \leq 0.001, ns- not significant.

In order to evaluate the mechanisms leading to improved lung pathology in co-infected mice, we assessed cytokine and chemokine levels in lung homogenates. In line with decreased lung inflammation and infiltrating immune cells, there was a concomitant reduction in chemokines mediating T cell chemotaxis, including IP-10/CXCL-10 (Fig 27A), RANTES/CCL-5 (Fig 27B) and MIG/CXCL-9 (Fig 27C). In order to define the mechanism driving decreased inflammation during *A.fumigatus* infection, we analyzed induction of cytokines and chemokines by lung cell suspensions following treatment with *A.fumigatus* swollen, heat-inactivated conidia and *M.abscessus* infection in vitro. We found decreased IP-10 levels in supernatants of lung cell suspensions pre-treated with *A.fumigatus* conidia, which reproduced our in vivo findings (Fig 27D). Interestingly, this reduction in chemokine production was accompanied by increased levels of the anti-inflammatory cytokine IL-10 (Fig 27E). In vivo, co-infected mice harbored increased levels of IL-10-producing CD4⁺ T cells 14 days post-infection (Fig 27F). However, when lung cell suspensions were incubated with *A.fumigatus* conidia in the presence of an IL-10-blocking antibody, chemokine expression was unaltered (data not shown), demonstrating that chemokine inhibition by *A.fumigatus* is IL-10 pathway independent. In addition, co-infected mice harbored a higher percentage (Fig 27G) and total number of Tregs (Fig 27H) in their lungs, underscoring a potential role for Treg induction in control of *M.abscessus*-driven lung pathology during co-infection with *A.fumigatus*. Together, these data demonstrate that *A.fumigatus*-driven suppression of chemokine production is associated with increases in immune regulatory mechanisms, and is independent of IL-10 in vitro.

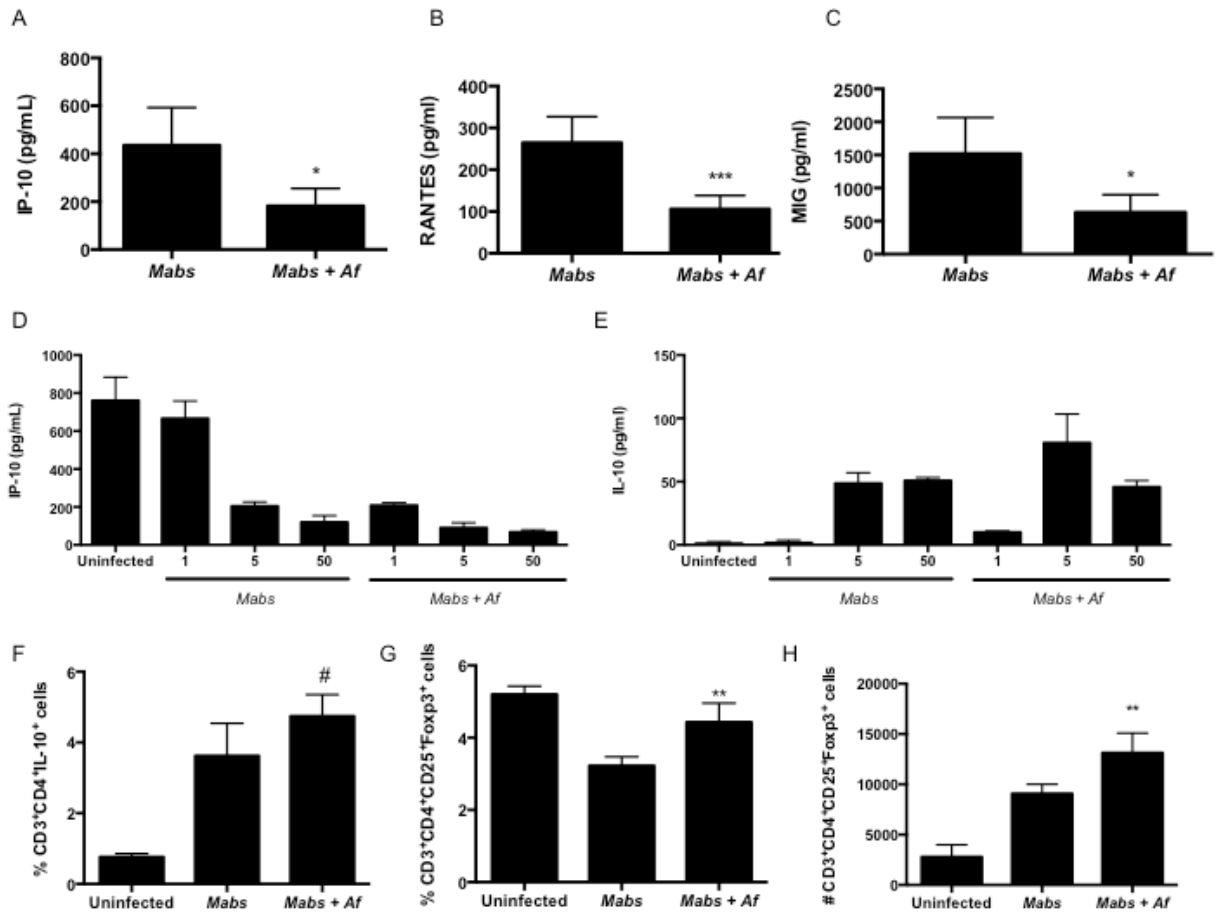


Figure 27. *A.fumigatus* reduced *M.abscessus*-driven lung inflammation is associated with increased IL-10 and Treg accumulation in infected lungs.

C57BL/6 *A.fumigatus*-infected (*Mabs+Af*) or control mice (*Mabs*) were challenged with 1×10^6 cfu of *M.abscessus* 3 days later. Mice were rechallenged with an equivalent dose of *M.abscessus* 1 week later. (A) IP-10, (B) RANTES and (C) MIG protein levels in lung homogenates were determined on D14 post-infection. Lung cell suspensions from C57BL/6 mice were treated with swollen, heat-killed *A.fumigatus* conidia for 24h. Cells were subsequently infected with varying MOIs of *M.abscessus* for 4 days and (D) IP-10 and (E) IL-10 protein levels were determined in culture supernatants. C57BL/6 uninfected, *A.fumigatus*-infected (*Mabs+Af*) or control mice (*Mabs*) were challenged with 1×10^6 cfu of *M.abscessus* 3 days later. Mice were rechallenged with an equivalent dose of *M.abscessus* 1 week later. (F) the percentage of lung Th cells producing IL-10 (CD3⁺CD4⁺IL-10⁺) and the (G) percentage and (H) number of Tregs (CD3⁺CD4⁺CD25⁺Foxp3⁺) were determined on D14 post-infection by flow cytometry. # $p=0.0886$, * $p \leq 0.05$, ** $p \leq 0.01$, *** $p \leq 0.001$.

Given the potential clinical relevance of our findings in CF patients, we then compared cytokine and chemokine lung levels in the sputum of CF patients infected with NTM-alone, *A.fumigatus*-alone or co-infected with NTM and *A.fumigatus*. Interestingly, the co-infected patient expressed higher sputum protein levels for IL-17A (Fig 28A), IL-6 (Fig 28B), IP-10 (Fig 28C) and RANTES (Fig 28D), and did not exhibit higher levels of IL-10 (data not shown) indicating that co-infected patients may exhibit an increased inflammatory response,. However, our limited sample size of samples from CF patients precludes any major conclusions to be drawn from these data.

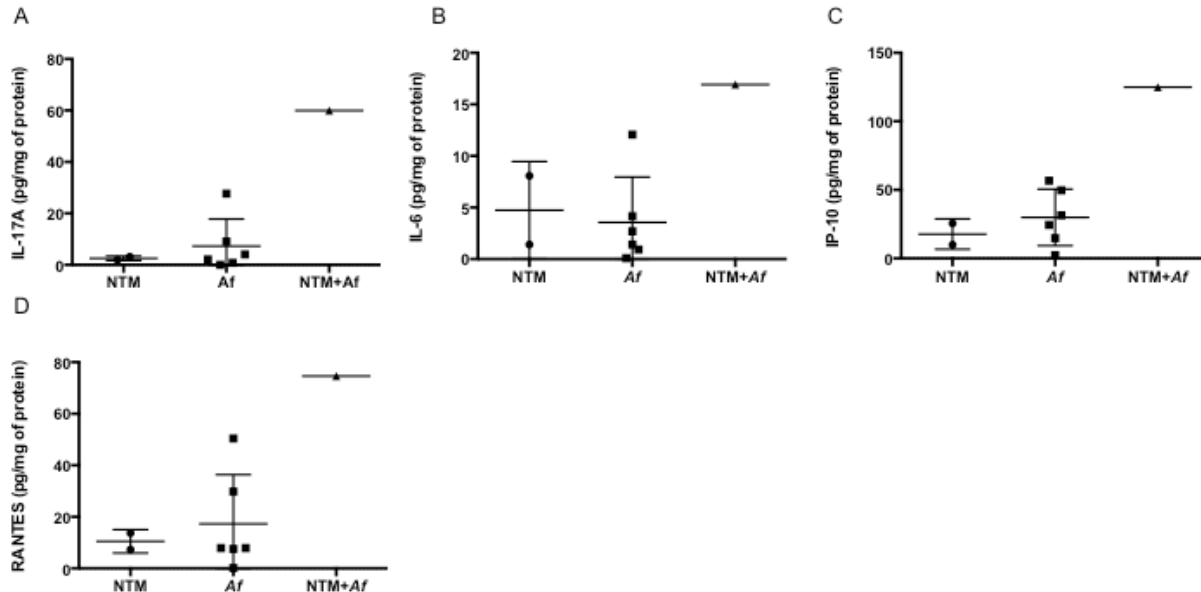


Figure 28. CF patients co-infected with NTM and *A.fumigatus* exhibit increased sputum IL-17A, IL-6, IP-10 and RANTES levels.

Sputum was collected from CF patients infected with NTM (NTM), *A.fumigatus* (*Af*) or NTM and *A.fumigatus* (NTM+*Af*) and protein levels of (A) IL-17A, (B) IL-6, (C) IP-10 and (D) RANTES were determined. The pg of each individual cytokine or chemokine relative to the total mg of protein used in the assay are reported.

7.4 DISCUSSION

Despite the demonstration that NTM can cause disease over 60 years ago, host immunity to NTM has been understudied in comparison to other related mycobacteria, including *Mtb* and *Mycobacterium leprae*. In particular, adaptive immunity and IFN- γ -secreting Th1 cells have been implicated in *M. abscessus* control [206-209], but no studies have focused on Th17 cells in *M. abscessus* infection. Our results are in line with previously published reports demonstrating the higher susceptibility of B and T cell deficient mice to *M. abscessus* infection [207, 209]. In contrast with previous publications that used low dose aerosol delivery [208], oropharyngeal infection of *Ifng*^{-/-} mice with *M. abscessus* L948 at an intermediate dose (2×10^4 cfu) did not significantly increase bacterial burden or lung pathology. However, using a larger inoculum size (1×10^6 cfu given twice), we were able to demonstrate the higher susceptibility of *Ifng*^{-/-} mice to *M. abscessus* infection. Interestingly, the difference between our data and published reports may be due to the infection route used in this study. In a study that compared in vivo mucociliary clearance of an insoluble particulate radiotracer following aerosol delivery, oropharyngeal aspiration or intratracheal delivery, aerosol delivery led to a higher retention of the particles [219]. The immune response elicited by the particles also differed between delivery routes, with higher KC expression after aerosol instillation and higher TNF- α levels and immune cell recruitment after oropharyngeal delivery [219]. In addition, differential distribution of mycobacteria and their antigens along the respiratory tract as a product of the delivery route may activate different innate immune cells, or alter the magnitude of immune activation. For instance, dendritic cells, which detect foreign antigens along the respiratory mucosa, are unevenly distributed along the respiratory tract, with dendritic cell density diminishing when we descend

from the upper respiratory tract down the bronchial tree [220]. Thus, in our model, oropharyngeal delivery, together with a differential distribution of mycobacteria along the respiratory tract, may stimulate immune control mechanisms, allowing improved containment of infection at intermediate infection doses.

In previous chapters, we have shown that Th cell responses during mycobacterial infections are plastic, and can acquire different cytokine secretion profiles in response to microenvironmental cues. In order to understand the effect of co-infections on *M. abscessus*-specific Th responses, we first need to characterize the Th responses arising naturally during infection. The contribution of the IL-17 pathway and Th17 cells to control of *M. abscessus* infection has not been explored. Consistent with a previous study using human PBMCs [221], we showed that in vitro infection of macrophages with *M. abscessus* induces IL-1 β , a cytokine involved in Th17 differentiation. In addition, using a model of oropharyngeal *M. abscessus* infection, we demonstrated the dose-dependent induction of *M. abscessus*-specific Th17 cells. Despite the induction of Th17 responses, however, IL-17 receptor signaling was dispensable for *M. abscessus* control. Taken together, our data indicate that IL-17 receptor signaling is not critical for *M. abscessus* control. These results, together with the comparable control of an intermediate dose of *M. abscessus* in *Ifng*^{-/-} and C57BL/6 mice bring forth the interesting notion that *M. abscessus* infection can be easily controlled, even by immune compromised mice. This is particularly relevant given that *M. abscessus* is ubiquitous in the environment and is an opportunistic pathogen that normally only affects individuals with structural lung abnormalities. The exact mechanisms responsible for mycobacterial persistence in these susceptible individuals, which may involve mucus thickening, promotion of biofilm formation [222], failure of mucociliary clearance [223] and abnormal immune responses, remain to be defined. Recently,

our lab and others have found that IL-17 plays a role in driving pathology, without altering mycobacterial control, in *Mtb* H37Rv [195] and *M.avium* [224] infections. In addition, IL-17 expression during infection with the *Mtb* clinical isolate from the Beijing lineage, HN878, was required for control of infection [210], highlighting a dual role for IL-17 in driving both containment of primary mycobacterial infection and pathology. *Ifng*^{-/-} mice infected with a high dose of *M.abscessus* exhibited increased lung Th17 cell accumulation. Future studies will enable us to further elucidate the involvement of the IL-17 pathway in *M.abscessus*-driven pathology.

One of the hallmarks of CF is the presence of recurring infective pulmonary exacerbations, which are associated with a decline in lung function [225, 226]. Importantly, CF patients tend to harbor a variety of pathogens in their lungs, and how such infections interact with each other to affect lung function is still unknown. Using CF patient samples, several recent studies showed that *A.fumigatus* colonization is frequently associated with *M.abscessus* infection [227-229]. This association may be due to the more advanced disease and lung damage that predisposes patients to *M.abscessus* infection, and potentially to other opportunistic pathogens such as *A.fumigatus* [227]. *M.abscessus*-infected CF patients tend to receive lengthy treatments of intravenous antimicrobials, and antibiotic-resistant *Aspergillus* prevalence is higher in these patients [227]. Thus, sustained antibiotic treatment could lead to the generation of an ecologic niche that enables survival of antibiotic-resistant *Aspergillus* in *M.abscessus*-infected patients. Alternatively, one disease may directly affect the other through host-intrinsic mechanisms, such as competition between immune responses. Using a mouse model of co-infection between *A.fumigatus* and *M.abscessus*, we sought to determine the effect of *A.fumigatus* on protection and lung pathology in *M.abscessus* infection. Interestingly, we found an *M.abscessus* dose-dependent effect of *A.fumigatus*.

At intermediate doses of *M.abscensus*, previous *A.fumigatus* infection enhanced immune control of *M.abscensus*. Using several gene-deficient mouse strains, we showed that this effect was partly IL-17RA-dependent. In addition, when both T-bet and ROR γ t, the master transcription factors for the Th1 and Th17 subsets, respectively, were absent, *A.fumigatus*-induced protection was lost. These data suggest that the Th1 and Th17 pathways, or innate immune cells expressing T-bet and ROR γ t, can act redundantly to limit *M.abscensus* infection in co-infected mice. This is in line with previous findings in TB, where IL-23 was shown to compensate for IL-12p70 deficiency and to stimulate the induction of *Mtb*-specific Th1 and Th17 cells [104]. In addition, innate immune cell activation may contribute to enhanced *M.abscensus* control in co-infected mice, as in vitro stimulation of macrophages with fungal β -glucan products such as zymosan and curdlan promoted enhanced macrophage activation and *M.abscensus* killing. β -glucans can signal through a variety of immune receptors, including CR3, TLR2/6 and dectin-1, which is thought to be the main β -glucan receptor on leukocytes [230]. Previous studies have found that macrophages can become activated in response to β -glucans, increasing TNF- α and iNOS expression in a MyD88 and NF- κ B-dependent manner [231-233]. Thus, both innate and adaptive immunity may contribute to *M.abscensus* containment in co-infected mice. The relative contribution of each will be explored in future studies through the use of knockout mouse strains.

In contrast, at higher infectious doses of *M.abscensus*, previous *A.fumigatus* infection did not affect *M.abscensus* clearance. Instead, *M.abscensus*-driven lung pathology was reduced in co-infected mice, and was accompanied by a reduction in lung infiltrating immune cells. In addition, *A.fumigatus* reduced expression of T cell recruiting chemokines to the lungs during mycobacterial infection in vivo. This was associated with a trend towards increased IL-10

production in vivo. Furthermore, our in vitro studies showed that downregulation of chemokine responses was associated with increased production of the anti-inflammatory cytokine IL-10. IL-10 has been shown to inhibit production of proinflammatory cytokines, by acting directly on cells of the innate immune system. In turn, it can enhance differentiation of Tregs and their own secretion of IL-10, while inhibiting effector Th responses [234]. IL-10 may have different effects depending on the infectious organism, either promoting infection through the blockade of effector mechanisms responsible for pathogen clearance or alleviating pathology and tissue damage [235]. IL-10 expression can be induced by β -glucans in a dectin-1-dependent mechanism, leading to the adoption of a regulatory-like phenotype in mouse macrophages [236]. However, in vitro blocking experiments did not reveal a reversal of diminished cytokine and chemokine production. This may be due to the increased cell death observed in *M.abscessus*-infected cells in vitro (data not shown). Further studies will allow us to elucidate the nature of the IL-10-producing cells in vivo, and the involvement of this mediator in controlling *M.abscessus*-driven pathology in vivo in co-infected mice. Treg accumulation was also significantly enhanced in vivo in co-infected mice, which may underscore an important role for this regulatory cell subset in limiting lung pathology during *A.fumigatus* and *M.abscessus* co-infection. Future studies will allow us to determine whether these cells play a functional role in this phenomenon.

A.fumigatus can thwart the host immune response via additional mechanisms, including evasion of the complement system and inhibition of phagolysosome acidification in macrophages and lung epithelial cells [237]. More recently, *A.fumigatus* has been shown to induce indoleamine 2,3-dioxygenase (IDO), an enzyme that catabolizes tryptophan into kynurenines [238]. IDO plays a dual role in limiting infection through tryptophan depletion and regulating inflammation via inhibition of effector T cells and promotion of Treg differentiation

[238, 239]. In addition, IDO activity can limit the growth of *M.avium*, and its activation via TLR adjuvants enhanced the effectiveness of anti-mycobacterial drugs in vitro and in vivo [240]. We will explore the involvement of this pathway in Treg accumulation and regulation of *M.abscessus* pathology in future experiments.

An important consideration in these results is the timing of *A.fumigatus* infection. *A.fumigatus* is highly ubiquitous in the environment [241], with average levels of conidia in the air ranging between 1 and 100 conidia/m³, but agitation activities such as turning of compost can bring conidia concentrations up to 10⁴-10⁷ conidia/m³ of air [242]. Thus, given the high probability of an individual to be exposed to or colonized with *A.fumigatus*, in all of our studies, *A.fumigatus* infection was performed prior to *M.abscessus* challenge. Our finding that *A.fumigatus* affects *M.abscessus* containment and pathology begs the question of whether inverting the order of delivery would alter the nature of the effects. It is possible that *A.fumigatus*-driven dampening of *M.abscessus* pathology is due to the fact that *M.abscessus* was given during the resolution phase of fungal infection, where *A.fumigatus* burden is undetectable. Therefore, studying whether these effects are equivalent whether *M.abscessus* is given before *A.fumigatus* will be important to better understand the dynamics of interactions between co-infected pathogens in CF.

We also studied sputum cytokine and chemokine levels in CF patients infected with NTM alone, *A.fumigatus* alone, or co-infected with NTM and *A.fumigatus*. Interestingly, IL-17A, IL-6 and the chemokines IP-10 and RANTES were upregulated in the sputum of a patient harboring a *M.abscesuss* and *A.fumigatus* co-infection in comparison to NTM-infected or *A.fumigatus*-infected patients. However, this patient did not exhibit increased levels of IL-10. These data are in discordance with our findings in the mouse model, but are not definitive given

the low number of patient samples analyzed. However, they suggest that overall, co-infected patients harbor higher levels of inflammatory mediators. There is also a disparity between the elevated levels of proinflammatory mediators in the sputum of CF patients and the relatively low level of inflammatory mediators and pathology in *M.abscessus*-infected mice. Indeed, comparably to TB, NTM infection in humans can develop into a cavitary disease [201], with a symptomatology comparable to that of pulmonary TB. The persistence observed in CF patients may be due to the characteristic inflammation seen in the CF lung, which is characterized by accumulation of neutrophils. Previous studies have shown that neutrophils can directly promote *M.abscessus* biofilm formation [216], a phenomenon that may be insufficient in *M.abscessus*-infected immune competent mice. In addition, the presence of additional co-infecting pathogens, in CF, such as *P.aeruginosa*, deficient TLR signaling or structural lung abnormalities that predispose these patients to worsened pathogen clearance may all explain the enhanced inflammation and persistence of *M.abscessus* in patients when compared to mice. In this regard, gut-corrected CFTR-deficient mice, or elastase-treated mice, which will present increased lung damage, may prove better models to study the full impact of fungal co-infections on subsequent NTM infections.

Taken together, our results demonstrate that CF-prevalent fungal infections can ameliorate *M.abscessus* control and pulmonary damage early during *M.abscessus* infection, using a mouse model. The long term effects of *A.fumigatus* co-infection on *M.abscessus* control and pathology, as well as the clinical significance of these findings, will be elucidated in future studies.

7.5 ACKNOWLEDGEMENTS

The author would like to thank Javier Rangel-Moreno, PhD (University of Rochester, NY) and Tim Oury, MD, PhD for analysis and scoring of lung pathology sections, Waleed Elsegeiny and Taylor Eddens for technical assistance during mouse experiments, and Kelly Flentie, PhD and Christina Stallings, PhD for instructions on growing *M.abscessus* biofilms. An additional thanks is offered to Elizabeth Hartigan, Kathy Iurlano and Erinn Kasubinski for assistance with recruitment of patients and collection of CF patient sputum specimens. This work was supported by a CF Foundation Pilot Grant to S.A. Khader and J. Kolls. Children's Hospital of Pittsburgh of UPMC, Washington University in St. Louis, NIH grant HL105427 to S.A. Khader and Children's Hospital of Pittsburgh Research Advisory Committee Grant from Children's Hospital of Pittsburgh of the UPMC Health System to L. Monin. J. Rangel-Moreno was supported by funds of the Department of Medicine, University of Rochester, and U19 AI91036.

8.0 CONCLUSIONS, SIGNIFICANCE AND FUTURE DIRECTIONS

Several mycobacterial pathogens can establish infections that pose a serious challenge to global health. The World Health Organization reported 8.7 million new cases of TB and 1.4 million TB related deaths in 2011. Furthermore, about one third of the world's population is latently infected with *Mtb*, and at risk of progressing to active disease. In fact, of the two billion infected individuals, 10%, that is, 200 million people, will likely progress to active disease throughout their lifetime. Current efforts to control this disease are aimed at the development of novel, effective vaccines, the generation of new drug regimes and an improvement in diagnostic and prognostic markers. The availability of such prognostic markers will allow the identification of populations at risk of TB reactivation and in need of closer medical surveillance. Therefore, a better understanding of the factors that influence TB reactivation in seemingly healthy, immune competent individuals, is paramount. Recently, several studies have shown that Th cell responses are plastic, and can acquire different effector characteristics in response to changes in the microenvironment. Our data show that Th responses in a chronic infection setting such as TB, are plastic, and can be modulated by changes in the cytokine milieu and co-infection. Future studies will allow us to determine the full impact of Th modulation and plasticity on TB reactivation.

In countries with poorly developed infrastructure, *Mtb* is often co-endemic with helminth infections. It is currently estimated that 1 billion people in developing countries are infected with

one or more helminths. Schistosomiasis, caused by platyhelminth flukes of the genus *Schistosoma* affects about 207 million individuals. Helminth infections are usually chronic and induce strong Th2 and Treg responses, which are able to regulate the development and/or effector functions of Th1 and Th17 cells. Consistent with this, several human studies suggest that infections with helminths hinder the capacity to mount effective immune responses against BCG, and may be associated with TB reactivation in HIV-infected patients.

Thus, while the full impact of co-infections on the severity of mycobacterial disease and the development of immunity to mycobacteria remains an open question, there is persuasive published evidence, supported by our data, to warrant investigation of co-infections as a relevant and important factor for the control of mycobacterial disease. An important secondary consideration is that it will be important to understand whether treatments for mycobacteria affect disease manifestations associated with co-infections. In this work, we have demonstrated for the first time that Th responses in the context of TB are plastic. In particular Th1 cells can acquire the cytokine secretion profiles of Th2 and Tfh, but not Th17 cells. In addition, Th17 cells, which are important for mucosal vaccine recall responses in TB, are highly plastic, with the ability to acquire cytokine secretion profiles of Th1, Th2 and Tfh cells. Given the association of Th1 responses with primary containment of *Mtb*, we expected improved bacterial containment in mice that received IFN- γ -sufficient Th17 cells. However, unexpectedly, Th17 cells lacking IFN- γ -secretion capacity led to more efficacious control of *Mtb* infection. IL-23 expression in host mice and CXCR5 expression on Th17 cells was required for bacterial containment. Together, these data indicate that developing vaccination strategies and adjuvants that boost IL-23 and CXCR5 expression, while limiting IFN- γ production, may enhance mycobacterial containment.

In addition, we have described a novel role for arginase-1 in driving lung inflammation during *S.mansoni-Mtb* co-infection. Importantly, this increased inflammation was associated with increased bacterial burden on day 30 post-*Mtb* infection and a reduction in protective immune responses. These effects could be reproduced by administration of SEA, a helminth antigen preparation, indicating that the mere presence of helminth antigens in the absence of a productive parasite life cycle can hinder *Mtb* control. Importantly, deworming strategies reversed the effect of co-infection, providing evidence for the utilization of anti-helminthics as a cost-effective strategy to limit TB reactivation in populations where TB and helminths are co-endemic. A recent study in free-ranging African buffalos showed that treatment with anti-helminthics at a population level could lead to an enhancement of *M.bovis* transmission due to increased survival of the treated animals [243]. Thus, the potential outcomes of deworming at a population-level scale are not obvious and should carefully be studied prior to the implementation of therapeutic interventions. In addition, arginase-1-mediated increased inflammation and breakage of *Mtb* containment in co-infected hosts may lead to an unexpectedly higher susceptibility of *Mtb* to antibiotic treatment. Whether this occurs in vivo remains to be explored. Finally, the exact mechanisms mediating enhanced inflammation via arginase-1, as well as its potential effect on vaccine recall responses will be elucidated in future studies.

In turn, NTM infections are currently emerging as a serious health concern in patients with previous lung conditions and transplant patients, including CF patients. Of particular relevance is *M. abscessus* infection, which constitutes the most drug-resistant NTM and is associated with poor treatment outcome. Indeed, sputum conversion occurs in 50-60% of treated patients, highlighting the low efficacy of treatment. Further, transition of *M. abscessus* from an environmentally-adapted form to the human-adapted morphotype has been associated with

development of a highly invasive and pathogenic disease. Defining the mechanisms that potentiate or limit bacterial persistence and tissue damage in patients at high risk of NTM infections will enable us to envision novel therapeutic avenues for treatment of NTM disease. In this work, we have verified the importance of adaptive immunity and Th1 cells for *M.abscessus* control. In addition, we have shown that other CF-prevalent infectious diseases such as *A.fumigatus* infection can impact *M.abscessus* containment and lung inflammation depending on the infectious dose of *M.abscessus*. Control of intermediate doses of *M.abscessus* in a co-infection setting is mediated by Th1 and Th17 cells, while reduced pathology upon repeated exposure to high doses of *M.abscessus* may be caused by enhanced regulatory mechanisms, such as Treg activation and IL-10 production. Future studies will allow us to identify the mechanisms mediating this reduction in lung pathology and the full impact of common CF co-infections on NTM infections in humans.

Together, our results provide novel information on the dynamic interplay between host genetics, competing host responses to parasitic and fungal antigens and *Mtb* co-infection.

9.0 RELEVANT PUBLICATIONS

1. **Monin L**, Griffiths KL, Slight S, Lin Y, Rangel-Moreno, J, Khader SA. Immune requirements for protective Th17 recall responses to *Mycobacterium tuberculosis* challenge. *Mucosal Immunology*. 2015; doi: 10.1038/mi.2014.136

2. **Monin L**, Khader SA. Chemokines in tuberculosis: the good, the bad and the ugly. *Seminars in Immunology*. 2014;26(6):552-8.

3. Gopal R, **Monin L**, Slight S, Uche U, Blanchard E, Fallert Junecko BA, Ramos-Payan R, Stallings CL, Reinhart TA, Kolls JK, Kaushal D, Nagarajan U, Rangel-Moreno J, Khader SA. Unexpected role for IL-17 in protective immunity against hypervirulent *Mycobacterium tuberculosis* HN878 infection. *PLoS Pathogens*. 2014; 10(5):e1004099

4. Madan-Lala R, Sia JK, King R, Adekambi T, **Monin L**, Khader SA, Pulendran B, Rengarajan J. *Mycobacterium tuberculosis* impairs dendritic cell functions through the serine hydrolase Hip1. *Journal of Immunology*. 2014;192(9):4263-72.

5. Gopal R, **Monin L**, Torres D, Slight S, Mehra S, McKenna KC, Fallert Junecko BA, Reinhart TA, Kolls J, Báez-Saldaña R, Cruz-Lagunas A, Rodríguez-Reyna TS, Kumar NP, Tessier P, Roth J, Selman M, Becerril-Villanueva E, Baquera-Heredia J, Cumming B, Kasprowicz VO, Steyn AJ, Babu S, Kaushal D, Zúñiga J, Vogl T, Rangel-Moreno J, Khader SA. S100A8/A9 proteins mediate neutrophilic inflammation and lung pathology during tuberculosis. *American Journal of Respiratory and Critical Care Medicine*. 2013;188(9):1137-46.

6. Slight SR, **Monin L**, Gopal R, Avery L, Davis M, Cleveland H, Oury TD, Rangel-Moreno J, Khader SA. IL-10 restrains IL-17 to limit lung pathology characteristics following pulmonary infection with *Francisella tularensis* live vaccine strain. *American Journal of Pathology*. 2013;183(5):1397-404.

7. **Monin L**, Khader SA. B cells produce CXCL13 in lymphoid neogenesis during chronic obstructive pulmonary disease. The new kid on the block? *American Journal of Respiratory and Critical Care Medicine*. 2013;187(11):1162-4.

Under revision:

8. **Monin L**, Griffiths L, Lam WY, Gopal R, Kang DD, Rajamanickam A, Cruz-Lagunas A, Zúñiga J, Babu S, Kolls JK, Mitreva M, Rosa BA, Ramos-Payan R, Murray PJ, Rangel-Moreno J, Pearce EJ, Khader SA. Helminth-induced arginase-1 exacerbates lung inflammation and disease severity in tuberculosis. *Journal of Clinical Investigation*, under revision.

BIBLIOGRAPHY

- [1] World Health O. Global tuberculosis control: WHO report 2014. 2014.
- [2] Kaufmann SHE. Envisioning future strategies for vaccination against tuberculosis. *Nat Rev Immunol.* 2006;6:699-704.
- [3] Lienhardt C, Glaziou P, Uplekar M, Lönnroth K, Getahun H, Raviglione M. Global tuberculosis control: lessons learnt and future prospects. *Nat Rev Microbiol.* 2012;10:407-416.
- [4] Scanga BCA, Mohan VP, Yu K, Joseph H, Tanaka K, Chan J, et al. Depletion of CD4+ T Cells Causes Reactivation of Murine Persistent Tuberculosis Despite Continued Expression of Interferon- γ and Nitric Oxide Synthase 2. *J Exp Med.* 2000;192.
- [5] Esther CR, Esserman Da, Gilligan P, Kerr A, Noone PG. Chronic Mycobacterium abscessus infection and lung function decline in cystic fibrosis. *Journal of cystic fibrosis : official journal of the European Cystic Fibrosis Society.* 2010;9:117-123.
- [6] Greendyke R, Byrd TF. Differential antibiotic susceptibility of Mycobacterium abscessus variants in biofilms and macrophages compared to that of planktonic bacteria. *Antimicrobial agents and chemotherapy.* 2008;52:2019-2026.
- [7] Jereb J, Etkind SC, Joglar OT, Moore M, Taylor Z. Tuberculosis contact investigations: outcomes in selected areas of the United States, 1999. *Int J Tuberc Lung Dis.* 2003;7:S384-390.
- [8] Poulsen A. Some clinical features of tuberculosis. 1. Incubation period. *Acta tuberculosea Scandinavica.* 1950;24:311-346.
- [9] Wallgren A. The time-table of tuberculosis. *Tubercle.* 1948;29:245-251.
- [10] Zumla A, Raviglione M, Hafner R, von Reyn CF. Tuberculosis. *N Engl J Med.* 2013;368:745-755.
- [11] Caws M, Thwaites G, Dunstan S, Hawn TR, Lan NT, Thuong NT, et al. The influence of host and bacterial genotype on the development of disseminated disease with Mycobacterium tuberculosis. *PLoS pathogens.* 2008;4:e1000034.
- [12] Ramakrishnan L. Revisiting the role of the granuloma in tuberculosis. *Nat Rev Immunol.* 2012;12:352-366.

- [13] Orme IM, Basaraba RJ. The formation of the granuloma in tuberculosis infection. *Seminars in immunology*. 2014;26:601-609.
- [14] Pawlowski A, Jansson M, Skold M, Rottenberg ME, Kallenius G. Tuberculosis and HIV co-infection. *PLoS pathogens*. 2012;8:e1002464.
- [15] Koul A, Arnoult E, Lounis N, Guillemont J, Andries K. The challenge of new drug discovery for tuberculosis. *Nature*. 2011;469:483-490.
- [16] Gunther G. Multidrug-resistant and extensively drug-resistant tuberculosis: a review of current concepts and future challenges. *Clinical medicine*. 2014;14:279-285.
- [17] Goonetilleke NP, McShane H, Hannan CM, Anderson RJ, Brookes RH, Hill AV. Enhanced immunogenicity and protective efficacy against *Mycobacterium tuberculosis* of bacille Calmette-Guerin vaccine using mucosal administration and boosting with a recombinant modified vaccinia virus Ankara. *J Immunol*. 2003;171:1602-1609.
- [18] Verreck FA, Vervenne RA, Kondova I, van Kralingen KW, Remarque EJ, Braskamp G, et al. MVA.85A boosting of BCG and an attenuated, *phoP* deficient *M. tuberculosis* vaccine both show protective efficacy against tuberculosis in rhesus macaques. *PLoS One*. 2009;4:e5264.
- [19] Vordermeier HM, Villarreal-Ramos B, Cockle PJ, McAulay M, Rhodes SG, Thacker T, et al. Viral booster vaccines improve *Mycobacterium bovis* BCG-induced protection against bovine tuberculosis. *Infect Immun*. 2009;77:3364-3373.
- [20] Williams A, Goonetilleke NP, McShane H, Clark SO, Hatch G, Gilbert SC, et al. Boosting with poxviruses enhances *Mycobacterium bovis* BCG efficacy against tuberculosis in guinea pigs. *Infect Immun*. 2005;73:3814-3816.
- [21] Hunter RL. Pathology of post primary tuberculosis of the lung: an illustrated critical review. *Tuberculosis (Edinb)*. 2011;91:497-509.
- [22] Gupta UD, Katoch VM. Animal models of tuberculosis. *Tuberculosis (Edinb)*. 2005;85:277-293.
- [23] Balasubramanian V, Wiegshaus EH, Smith DW. Mycobacterial infection in guinea pigs. *Immunobiology*. 1994;191:395-401.
- [24] Dannenberg AM, Jr. Pathogenesis of pulmonary *Mycobacterium bovis* infection: basic principles established by the rabbit model. *Tuberculosis (Edinb)*. 2001;81:87-96.
- [25] Gupta UD, Katoch VM. Animal models of tuberculosis for vaccine development. *The Indian journal of medical research*. 2009;129:11-18.
- [26] Ordway DJ, Orme IM. Animal models of mycobacteria infection 2011.
- [27] Middlebrook G. An apparatus for airborne infection of mice. *Proceedings of the Society for Experimental Biology and Medicine Society for Experimental Biology and Medicine*.

1952;80:105-110.

[28] Cooper AM, Khader SA. The role of cytokines in the initiation, expansion, and control of cellular immunity to tuberculosis. *Immunol Rev.* 2008;226:191-204.

[29] Flynn JL. Lessons from experimental *Mycobacterium tuberculosis* infections. *Microbes Infect.* 2006;8:1179-1188.

[30] Scanga CA, Mohan VP, Joseph H, Chan J, Flynn JL, Yu K. Reactivation of Latent Tuberculosis : Variations on the Cornell Murine Model Reactivation of Latent Tuberculosis : Variations on the Cornell Murine Model. 1999;67.

[31] Kaushal D, Mehra S, Didier PJ, Lackner AA. The non-human primate model of tuberculosis. *Journal of medical primatology.* 2012;41:191-201.

[32] Capuano SV, 3rd, Croix DA, Pawar S, Zinovik A, Myers A, Lin PL, et al. Experimental *Mycobacterium tuberculosis* infection of cynomolgus macaques closely resembles the various manifestations of human *M. tuberculosis* infection. *Infect Immun.* 2003;71:5831-5844.

[33] Cosma CL, Klein K, Kim R, Beery D, Ramakrishnan L. *Mycobacterium marinum* Erp is a virulence determinant required for cell wall integrity and intracellular survival. *Infect Immun.* 2006;74:3125-3133.

[34] Volkman HE, Clay H, Beery D, Chang JC, Sherman DR, Ramakrishnan L. Tuberculous granuloma formation is enhanced by a mycobacterium virulence determinant. *PLoS biology.* 2004;2:e367.

[35] Tonjum T, Welty DB, Jantzen E, Small PL. Differentiation of *Mycobacterium ulcerans*, *M. marinum*, and *M. haemophilum*: mapping of their relationships to *M. tuberculosis* by fatty acid profile analysis, DNA-DNA hybridization, and 16S rRNA gene sequence analysis. *Journal of clinical microbiology.* 1998;36:918-925.

[36] Swaim LE, Connolly LE, Volkman HE, Humbert O, Born DE, Ramakrishnan L. *Mycobacterium marinum* infection of adult zebrafish causes caseating granulomatous tuberculosis and is moderated by adaptive immunity. *Infect Immun.* 2006;74:6108-6117.

[37] Corbett EL, Watt CJ, Walker N, Maher D, Williams BG, Raviglione MC, et al. The Growing Burden of Tuberculosis- Global trends and interactions with the HIV epidemic. *Arch Intern Med.* 2003;163:1009-1021.

[38] Cegielski JP, McMurray DN. The relationship between malnutrition and tuberculosis: evidence from studies in humans and experimental animals. *Int J Tuberc Lung Dis.* 2004;8:286-298.

[39] Keane J, Gershon S, Wise RP, Mirabile-Levens E, Kasznica J, Schwieterman WD, et al. Tuberculosis associated with infliximab, a tumor necrosis factor alpha-neutralizing agent. *The New England Journal of Medicine.* 2001;345:1098-1104.

- [40] Guirado E, Schlesinger LS, Kaplan G. Macrophages in tuberculosis: friend or foe. *Seminars in immunopathology*. 2013;35:563-583.
- [41] Kleinnijenhuis J, Oosting M, Joosten LA, Netea MG, Van Crevel R. Innate immune recognition of *Mycobacterium tuberculosis*. *Clin Dev Immunol*. 2011;2011:405310.
- [42] Kang DD, Lin Y, Rangel-Moreno J, Randall TD, Khader SA. Profiling early lung immune responses in the mouse model of tuberculosis. *PLoS One*. 2011;6:e16161-e16161.
- [43] Cooper AM, Khader SA. The role of cytokines in the initiation, expansion, and control of cellular immunity to tuberculosis. *Immunological reviews*. 2008;226:191-204.
- [44] Tian T, Woodworth J, Sköld M, Behar M. In vivo depletion of CD11c+ cells delays the CD4+ T cell response to *Mycobacterium tuberculosis* and exacerbates the outcome of infection. *The Journal of Immunology*. 2005;175:3268-3272.
- [45] Wolf AJ, Linas B, Trevejo-Nuñez GJ, Kincaid E, Tamura T, Takatsu K, et al. *Mycobacterium tuberculosis* Infects Dendritic Cells with High Frequency and Impairs Their Function In Vivo. *J Exp Med*. 2007;179.
- [46] Bhatt K, Hickman SP, Salgame P. Cutting Edge : A New Approach to Modeling Early Lung Immunity in Murine Tuberculosis. *The Journal of Immunology*. 2004;172:2748-2751.
- [47] Srivastava S, Ernst JD. Cell-to-cell transfer of *M. tuberculosis* antigens optimizes CD4 T cell priming. *Cell Host Microbe*. 2014;15:741-752.
- [48] Samstein M, Schreiber HA, Leiner IM, Susac B, Glickman MS, Pamer EG. Essential yet limited role for CCR2+ inflammatory monocytes during *Mycobacterium tuberculosis*-specific T cell priming. *eLife*. 2013;2:e01086.
- [49] Reiley WW, Calayag MD, Wittmer ST, Huntington JL, Pearl JE, Fountain JJ, et al. ESAT-6-specific CD4 T cell responses to aerosol *Mycobacterium tuberculosis* infection are initiated in the mediastinal lymph nodes. *Proc Natl Acad Sci U S A*. 2008;105:10961-10966.
- [50] Urdahl KB, Shafiani S, Ernst JD. Initiation and regulation of T-cell responses in tuberculosis. *Mucosal Immunol*. 2011;4:288-293.
- [51] Diedrich CR, Mattila JT, Klein E, Janssen C, Phuah J, Sturgeon TJ, et al. Reactivation of latent tuberculosis in cynomolgus macaques infected with SIV is associated with early peripheral T cell depletion and not virus load. *PLoS One*. 2010;5:e9611-e9611.
- [52] Nakayamada S, Takahashi H, Kanno Y, O'Shea JJ. Helper T cell diversity and plasticity. *Curr Opin Immunol*. 2012.
- [53] Cooper AM, Dalton DK, Stewart TA, Griffin JP, Russell DG, Orme IM. Disseminated Tuberculosis in Interferon-gamma Gene-disrupted Mice. *J Exp Med*. 1993;178:2243-2247.
- [54] Flynn BJJ, Chan J, Triebold KJ, Dalton DK, Stewart TA, Bloom BR. An Essential Role for

Interferon-gamma in Resistance to Mycobacterium tuberculosis Infection. *J Exp Med*. 1993;178:2249-2254.

[55] Kaufmann SH. How can immunology contribute to the control of tuberculosis? *Nat Rev Immunol*. 2001;1:20-30.

[56] Slight SR, Rangel-Moreno J, Gopal R, Lin Y, Fallert Junecko BA, Mehra S, et al. CXCR5 + T helper cells mediate protective immunity against tuberculosis. *J Clin Invest*. 2013;123:712-726.

[57] Gopal R, Lin Y, Obermajer N, Slight S, Nuthalapati N, Ahmed M, et al. IL-23-dependent IL-17 drives Th1-cell responses following Mycobacterium bovis BCG vaccination. *Eur J Immunol*. 2012;42:364-373.

[58] Groom JR, Luster AD. CXCR3 ligands: redundant, collaborative and antagonistic functions. *Immunol Cell Biol*. 2011;89:207-215.

[59] Campbell JD, HayGlass KT. T cell chemokine receptor expression in human Th1- and Th2-associated diseases. *Archivum immunologiae et therapiae experimentalis*. 2000;48:451-456.

[60] Mehra S, Pahar B, Dutta NK, Conerly CN, Philippi-Falkenstein K, Alvarez X, et al. Transcriptional reprogramming in nonhuman primate (rhesus macaque) tuberculosis granulomas. *PLoS One*. 2010;5:e12266.

[61] Khader SA, Rangel-moreno J, Jeffrey J, Martino CA, Reiley WW, John E, et al. In a Murine Tuberculosis Model, the Absence of Homeostatic Chemokines Delays Granuloma Formation and Protective Immunity. *The Journal of Immunology*. 2009;183.

[62] Pitzalis C, Jones GW, Bombardieri M, Jones SA. Ectopic lymphoid-like structures in infection, cancer and autoimmunity. *Nat Rev Immunol*. 2014;14:447-462.

[63] Khader SA, Bell GK, Pearl JE, Fountain JJ, Rangel-moreno J, Cilley GE, et al. IL-23 and IL-17 in the establishment of protective pulmonary CD4 + T cell responses after vaccination and during Mycobacterium tuberculosis challenge. *Nat Immunol*. 2007;8:369-377.

[64] Gopal R, Rangel-Moreno J, Slight S, Lin Y, Nawar HF, Fallert Junecko BA, et al. Interleukin-17-dependent CXCL13 mediates mucosal vaccine-induced immunity against tuberculosis. *Mucosal Immunol*. 2013;6:972-984.

[65] Netea MG, van Crevel R. BCG-induced protection: effects on innate immune memory. *Seminars in immunology*. 2014;26:512-517.

[66] Calmette A. Preventive Vaccination Against Tuberculosis with BCG. *Proceedings of the Royal Society of Medicine*. 1931;24:1481-1490.

[67] Lienhardt C, Fruth U, Greco M. The blueprint for vaccine research & development: walking the path for better TB vaccines. *Tuberculosis (Edinb)*. 2012;92 Suppl 1:S33-35.

- [68] Rook GA, Dheda K, Zumla A. Immune responses to tuberculosis in developing countries: implications for new vaccines. *Nature reviews Immunology*. 2005;5:661-667.
- [69] Elias D, Akuffo H, Britton S. PPD induced in vitro interferon gamma production is not a reliable correlate of protection against *Mycobacterium tuberculosis*. *Transactions of the Royal Society of Tropical Medicine and Hygiene*. 2005;99:363-368.
- [70] Mittrucker HW, Steinhoff U, Kohler A, Krause M, Lazar D, Mex P, et al. Poor correlation between BCG vaccination-induced T cell responses and protection against tuberculosis. *Proc Natl Acad Sci U S A*. 2007;104:12434-12439.
- [71] Tameris MD, Hatherill M, Landry BS, Scriba TJ, Snowden MA, Lockhart S, et al. Safety and efficacy of MVA85A, a new tuberculosis vaccine, in infants previously vaccinated with BCG: a randomised, placebo-controlled phase 2b trial. *Lancet*. 2013;381:1021-1028.
- [72] Tameris M, Geldenhuys H, Luabeya AK, Smit E, Hughes JE, Vermaak S, et al. The candidate TB vaccine, MVA85A, induces highly durable Th1 responses. *PLoS One*. 2014;9:e87340.
- [73] Kaufmann SH. Tuberculosis vaccine development: strength lies in tenacity. *Trends Immunol*. 2012;33:373-379.
- [74] Bettelli E, Carrier Y, Gao W, Korn T, Strom TB, Oukka M, et al. Reciprocal developmental pathways for the generation of pathogenic effector TH17 and regulatory T cells. *Nature*. 2006;441:235-238.
- [75] Mangan PR, Harrington LE, O'Quinn DB, Helms WS, Bullard DC, Elson CO, et al. Transforming growth factor-beta induces development of the T(H)17 lineage. *Nature*. 2006;441:231-234.
- [76] Veldhoen M, Hocking RJ, Atkins CJ, Locksley RM, Stockinger B. TGFbeta in the context of an inflammatory cytokine milieu supports de novo differentiation of IL-17-producing T cells. *Immunity*. 2006;24:179-189.
- [77] Wei L, Laurence A, Elias KM, O'Shea JJ. IL-21 is produced by Th17 cells and drives IL-17 production in a STAT3-dependent manner. *J Biol Chem*. 2007;282:34605-34610.
- [78] Korn T, Bettelli E, Oukka M, Kuchroo VK. IL-17 and Th17 Cells. *Annu Rev Immunol*. 2009;27:485-517.
- [79] McGeachy MJ, Cua DJ. Th17 cell differentiation: the long and winding road. *Immunity*. 2008;28:445-453.
- [80] Zepp J, Wu L, Li X. IL-17 receptor signaling and T helper 17-mediated autoimmune demyelinating disease. *Trends in immunology*. 2011;32:232-239.
- [81] Hu Y, Shen F, Crellin NK, Ouyang W. The IL-17 pathway as a major therapeutic target in autoimmune diseases. *Annals of the New York Academy of Sciences*. 2011;1217:60-76.

- [82] Kolls JK, Khader SA. The role of Th17 cytokines in primary mucosal immunity. *Cytokine Growth Factor Rev.* 2010;21:443-448.
- [83] Lin Y, Slight SR, Khader SA. Th17 cytokines and vaccine-induced immunity. *Semin Immunopathol.* 2010;32:79-90.
- [84] Khader SA, Bell GK, Pearl JE, Fountain JJ, Rangel-Moreno J, Cilley GE, et al. IL-23 and IL-17 in the establishment of protective pulmonary CD4⁺ T cell responses after vaccination and during *Mycobacterium tuberculosis* challenge. *Nature immunology.* 2007;8:369-377.
- [85] Lindenstrom T, Woodworth J, Dietrich J, Aagaard C, Andersen P, Agger EM. Vaccine-induced th17 cells are maintained long-term postvaccination as a distinct and phenotypically stable memory subset. *Infect Immun.* 2012;80:3533-3544.
- [86] Desel C, Dorhoi A, Bandermann S, Grode L, Eisele B, Kaufmann SH. Recombinant BCG DeltaureC hly⁺ induces superior protection over parental BCG by stimulating a balanced combination of type 1 and type 17 cytokine responses. *J Infect Dis.* 2011;204:1573-1584.
- [87] Coomes SM, Pelly VS, Wilson MS. Plasticity within the alphabeta(+)CD4(+) T-cell lineage: when, how and what for? *Open biology.* 2013;3:120157.
- [88] Cooney LA, Towery K, Endres J, Fox DA. Sensitivity and resistance to regulation by IL-4 during Th17 maturation. *J Immunol.* 2011;187:4440-4450.
- [89] Harrington LE, Hatton RD, Mangan PR, Turner H, Murphy TL, Murphy KM, et al. Interleukin 17-producing CD4⁺ effector T cells develop via a lineage distinct from the T helper type 1 and 2 lineages. *Nat Immunol.* 2005;6:1123-1132.
- [90] Park H, Li Z, Yang XO, Chang SH, Nurieva R, Wang YH, et al. A distinct lineage of CD4 T cells regulates tissue inflammation by producing interleukin 17. *Nat Immunol.* 2005;6:1133-1141.
- [91] Laurence A, Tato CM, Davidson TS, Kanno Y, Chen Z, Yao Z, et al. Interleukin-2 signaling via STAT5 constrains T helper 17 cell generation. *Immunity.* 2007;26:371-381.
- [92] Luger D, Silver PB, Tang J, Cua D, Chen Z, Iwakura Y, et al. Either a Th17 or a Th1 effector response can drive autoimmunity: conditions of disease induction affect dominant effector category. *J Exp Med.* 2008;205:799-810.
- [93] Hirota K, Duarte JH, Veldhoen M, Hornsby E, Li Y, Cua DJ, et al. Fate mapping of IL-17-producing T cells in inflammatory responses. *Nat Immunol.* 2011;12:255-263.
- [94] Panzer M, Sitte S, Wirth S, Drexler I, Sparwasser T, Voehringer D. Rapid in vivo conversion of effector T cells into Th2 cells during helminth infection. *J Immunol.* 2012;188:615-623.
- [95] Raymond M, Van VQ, Wakahara K, Rubio M, Sarfati M. Lung dendritic cells induce T(H)17 cells that produce T(H)2 cytokines, express GATA-3, and promote airway inflammation.

J Allergy Clin Immunol. 2011;128:192-201 e196.

[96] Cosmi L, Maggi E, Santarlasci V, Capone M, Cardilicchia E, Frosali F, et al. Identification of a novel subset of human circulating memory CD4(+) T cells that produce both IL-17A and IL-4. J Allergy Clin Immunol. 2010;125:222-230 e221-224.

[97] Lee YK, Turner H, Maynard CL, Oliver JR, Chen D, Elson CO, et al. Late developmental plasticity in the T helper 17 lineage. Immunity. 2009;30:92-107.

[98] Jones GW, McLoughlin RM, Hammond VJ, Parker CR, Williams JD, Malhotra R, et al. Loss of CD4+ T cell IL-6R expression during inflammation underlines a role for IL-6 trans signaling in the local maintenance of Th17 cells. J Immunol. 2010;184:2130-2139.

[99] Lohning M, Hegazy AN, Pinschewer DD, Busse D, Lang KS, Hofer T, et al. Long-lived virus-reactive memory T cells generated from purified cytokine-secreting T helper type 1 and type 2 effectors. J Exp Med. 2008;205:53-61.

[100] Grogan JL, Mohrs M, Harmon B, Lacy DA, Sedat JW, Locksley RM. Early transcription and silencing of cytokine genes underlie polarization of T helper cell subsets. Immunity. 2001;14:205-215.

[101] Reiley WW, Calayag MD, Wittmer ST, Huntington JL, Pearl JE, Fountain JJ, et al. ESAT-6-specific CD4 T cell responses to aerosol Mycobacterium tuberculosis infection are initiated in the mediastinal lymph nodes. Proc Natl Acad Sci U S A. 2008;105:10961-10966.

[102] Slight SR, Rangel-Moreno J, Gopal R, Lin Y, Fallert Junecko BA, Mehra S, et al. CXCR5+ T helper cells mediate protective immunity against tuberculosis. The Journal of clinical investigation. 2013.

[103] Ghilardi N, Kljavin N, Chen Q, Lucas S, Gurney AL, De Sauvage FJ. Compromised humoral and delayed-type hypersensitivity responses in IL-23-deficient mice. J Immunol. 2004;172:2827-2833.

[104] Khader SA, Pearl JE, Sakamoto K, Gilmartin L, Bell GK, Jelley-Gibbs DM, et al. IL-23 compensates for the absence of IL-12p70 and is essential for the IL-17 response during tuberculosis but is dispensable for protection and antigen-specific IFN-gamma responses if IL-12p70 is available. J Immunol. 2005;175:788-795.

[105] Gopal R, Lin Y, Obermajer N, Slight S, Nuthalapati N, Ahmed M, et al. IL-23-dependent IL-17 drives Th1-cell responses following Mycobacterium bovis BCG vaccination. European journal of immunology. 2012;42:364-373.

[106] Griffiths KL, Stylianou E, Poyntz HC, Betts GJ, Fletcher HA, McShane H. Cholera toxin enhances vaccine-induced protection against Mycobacterium tuberculosis challenge in mice. PLoS One. 2013;8:e78312.

[107] Monin L, Griffiths KL, Slight S, Lin Y, Rangel-Moreno J, Khader SA. Immune requirements for protective Th17 recall responses to Mycobacterium tuberculosis challenge.

Mucosal Immunol. 2015.

[108] McGeachy MJ, Chen Y, Tato CM, Laurence A, Joyce-Shaikh B, Blumenschein WM, et al. The interleukin 23 receptor is essential for the terminal differentiation of interleukin 17-producing effector T helper cells in vivo. *Nature immunology*. 2009;10:314-324.

[109] Zhou L, Ivanov, II, Spolski R, Min R, Shenderov K, Egawa T, et al. IL-6 programs T(H)-17 cell differentiation by promoting sequential engagement of the IL-21 and IL-23 pathways. *Nat Immunol*. 2007;8:967-974.

[110] Macatonia S, Doherty T, Knight S, O'Garra A. Differential effect of IL-10 on dendritic cell-induced T cell proliferation and IFN-g production. *Journal of Immunology*. 1993;150:3755-3765.

[111] Macatonia SE, Hosken NA, Litton M, Vieira P, Hsieh CS, Culpepper JA, et al. Dendritic cells produce IL-12 and direct the development of Th1 cells from naive CD4+ T cells. *Journal of Immunology*. 1995;154:5071-5079.

[112] Cooper AM, Magram J, Ferrante J, Orme IM. Interleukin 12 (IL-12) is crucial to the development of protective immunity in mice intravenously infected with mycobacterium tuberculosis. *J Exp Med*. 1997;186:39-45.

[113] Wolf AJ, Desvignes L, Linas B, Banaiee N, Tamura T, Takatsu K, et al. Initiation of the adaptive immune response to Mycobacterium tuberculosis depends on antigen production in the local lymph node, not the lungs. *The Journal of experimental medicine*. 2008;205:105-115.

[114] Kang DD, Lin Y, Moreno JR, Randall TD, Khader SA. Profiling early lung immune responses in the mouse model of tuberculosis. *PLoS One*. 2011;6:e16161.

[115] Khader SA, Rangel-Moreno J, Fountain JJ, Martino CA, Reiley WW, Pearl JE, et al. In a murine tuberculosis model, the absence of homeostatic chemokines delays granuloma formation and protective immunity. *J Immunol*. 2009;183:8004-8014.

[116] Cooper AM, Dalton DK, Stewart TA, Griffin JP, Russell DG, Orme IM. Disseminated tuberculosis in interferon gamma gene-disrupted mice. *Journal of Experimental Medicine*. 1993;178:2243-2247.

[117] Griffiths KL, Khader SA. Novel vaccine approaches for protection against intracellular pathogens. *Current opinion in immunology*. 2014;28:58-63.

[118] Haines CJ, Chen Y, Blumenschein WM, Jain R, Chang C, Joyce-Shaikh B, et al. Autoimmune memory T helper 17 cell function and expansion are dependent on interleukin-23. *Cell reports*. 2013;3:1378-1388.

[119] Martin-Orozco N, Chung Y, Chang SH, Wang YH, Dong C. Th17 cells promote pancreatic inflammation but only induce diabetes efficiently in lymphopenic hosts after conversion into Th1 cells. *European journal of immunology*. 2009;39:216-224.

- [120] Nandi B, Behar SM. Regulation of neutrophils by interferon- γ limits lung inflammation during tuberculosis infection. *The Journal of experimental medicine*. 2011;208:2251-2262.
- [121] Vilaplana C, Prats C, Marzo E, Barril C, Vegue M, Diaz J, et al. To achieve an earlier IFN- γ response is not sufficient to control *Mycobacterium tuberculosis* infection in mice. *PLoS One*. 2014;9:e100830.
- [122] Rangel-Moreno J, Carragher DM, de la Luz Garcia-Hernandez M, Hwang JY, Kusser K, Hartson L, et al. The development of inducible bronchus-associated lymphoid tissue depends on IL-17. *Nat Immunol*. 2011;12:639-646.
- [123] Khader SA, Guglani L, Rangel-Moreno J, Gopal R, Fallert Junecko BA, Fountain JJ, et al. IL-23 Is Required for Long-Term Control of *Mycobacterium tuberculosis* and B Cell Follicle Formation in the Infected Lung. *J Immunol*. 2011;187:5402-5407.
- [124] Gopal R, Monin L, Slight S, Uche U, Blanchard E, B AFJ, et al. Unexpected Role for IL-17 in Protective Immunity against Hypervirulent *Mycobacterium tuberculosis* HN878 Infection. *PLoS pathogens*. 2014;10:e1004099.
- [125] Cruz A, Fraga AG, Fountain JJ, Rangel-Moreno J, Torrado E, Saraiva M, et al. Pathological role of interleukin 17 in mice subjected to repeated BCG vaccination after infection with *Mycobacterium tuberculosis*. *The Journal of experimental medicine*. 2010;207:1609-1616.
- [126] Gopal R, Monin L, Torres D, Slight S, Mehra S, McKenna KC, et al. S100A8/A9 proteins mediate neutrophilic inflammation and lung pathology during tuberculosis. *American journal of respiratory and critical care medicine*. 2013;188:1137-1146.
- [127] Salgame P, Yap GS, Gause WC. Effect of helminth-induced immunity on infections with microbial pathogens. 2013;14.
- [128] Kwan CK, Ernst JD. HIV and tuberculosis: a deadly human syndemic. *Clinical microbiology reviews*. 2011;24:351-376.
- [129] Collins KR, Quinones-Mateu ME, Toossi Z, Arts EJ. Impact of tuberculosis on HIV-1 replication, diversity, and disease progression. *AIDS reviews*. 2002;4:165-176.
- [130] Getahun H, Gunneberg C, Granich R, Nunn P. HIV infection-associated tuberculosis: the epidemiology and the response. *Clin Infect Dis*. 2010;50 Suppl 3:S201-207.
- [131] Geldmacher C, Schuetz A, Ngwenyama N, Casazza JP, Sanga E, Saathoff E, et al. Early depletion of *Mycobacterium tuberculosis*-specific T helper 1 cell responses after HIV-1 infection. *J Infect Dis*. 2008;198:1590-1598.
- [132] Diedrich CR, Mattila JT, Klein E, Janssen C, Phuah J, Sturgeon TJ, et al. Reactivation of latent tuberculosis in cynomolgus macaques infected with SIV is associated with early peripheral T cell depletion and not virus load. *PLoS One*. 2010;5:e9611.

- [133] Rosas-Taraco AG, Arce-Mendoza AY, Caballero-Olin G, Salinas-Carmona MC. Mycobacterium tuberculosis upregulates coreceptors CCR5 and CXCR4 while HIV modulates CD14 favoring concurrent infection. *AIDS research and human retroviruses*. 2006;22:45-51.
- [134] Spear GT, Kessler HA, Rothberg L, Phair J, Landay AL. Decreased oxidative burst activity of monocytes from asymptomatic HIV-infected individuals. *Clinical immunology and immunopathology*. 1990;54:184-191.
- [135] Wahl SM, Allen JB, Gartner S, Orenstein JM, Popovic M, Chenoweth DE, et al. HIV-1 and its envelope glycoprotein down-regulate chemotactic ligand receptors and chemotactic function of peripheral blood monocytes. *J Immunol*. 1989;142:3553-3559.
- [136] World Health O. *World Malaria Report*. 2014.
- [137] Scott CP, Kumar N, Bishai WR, Manabe YC. Short report: modulation of Mycobacterium tuberculosis infection by Plasmodium in the murine model. *Am J Trop Med Hyg*. 2004;70:144-148.
- [138] Mueller AK, Behrends J, Hagens K, Mahlo J, Schaible UE, Schneider BE. Natural transmission of Plasmodium berghei exacerbates chronic tuberculosis in an experimental co-infection model. *PLoS One*. 2012;7:e48110.
- [139] Colombatti R, Penazzato M, Bassani F, Vieira CS, Lourenco AA, Vieira F, et al. Malaria prevention reduces in-hospital mortality among severely ill tuberculosis patients: a three-step intervention in Bissau, Guinea-Bissau. *BMC infectious diseases*. 2011;11:57.
- [140] Perry S, Hussain R, Parsonnet J. The impact of mucosal infections on acquisition and progression of tuberculosis. *Mucosal Immunol*. 2011;4:246-251.
- [141] van Amsterdam K, van Vliet AH, Kusters JG, van der Ende A. Of microbe and man: determinants of Helicobacter pylori-related diseases. *FEMS microbiology reviews*. 2006;30:131-156.
- [142] D'Elia MM, Amedei A, Benagiano M, Azzurri A, Del Prete G. Helicobacter pylori, T cells and cytokines: the "dangerous liaisons". *FEMS immunology and medical microbiology*. 2005;44:113-119.
- [143] Perry S, de Jong BC, Solnick JV, de la Luz Sanchez M, Yang S, Lin PL, et al. Infection with Helicobacter pylori is associated with protection against tuberculosis. *PLoS One*. 2010;5:e8804.
- [144] Hotez PJ, Brindley PJ, Bethony JM, King CH, Pearce EJ, Jacobson J. Helminth infections: the great neglected tropical diseases. *J Clin Invest*. 2008;118:1311-1321.
- [145] Crompton DW, Nesheim MC. Nutritional impact of intestinal helminthiasis during the human life cycle. *Annual review of nutrition*. 2002;22:35-59.
- [146] Jackson JA, Friberg IM, Little S, Bradley JE. Review series on helminths, immune

modulation and the hygiene hypothesis: immunity against helminths and immunological phenomena in modern human populations: coevolutionary legacies? *Immunology*. 2009;126:18-27.

[147] Maizels RM, Balic A, Gomez-Escobar N, Nair M, Taylor MD, Allen JE. Helminth parasites--masters of regulation. *Immunological reviews*. 2004;201:89-116.

[148] Diaz A, Allen JE. Mapping immune response profiles: the emerging scenario from helminth immunology. *Eur J Immunol*. 2007;37:3319-3326.

[149] Terrazas CA, Terrazas LI, Gomez-Garcia L. Modulation of dendritic cell responses by parasites: a common strategy to survive. *J Biomed Biotechnol*. 2010;2010:357106.

[150] Colley DG, García AA, Lambertucci JR, Parra JC, Katz N, Rocha RS, et al. Immune responses during human schistosomiasis. XII. Differential responsiveness in patients with hepatosplenic disease. *The American Journal of Tropical Medicine and Hygiene*. 1986;35:793-802.

[151] Baumgart M, Tompkins F, Leng J, Hesse M. Naturally occurring CD4⁺Foxp3⁺ regulatory T cells are an essential, IL-10-independent part of the immunoregulatory network in *Schistosoma mansoni* Egg-induced inflammation. *The Journal of Immunology*. 2006;176:5374-5387.

[152] van der Kleij D, Latz E, Brouwers JFHM, Kruize YCM, Schmitz M, Kurt-Jones Ea, et al. A novel host-parasite lipid cross-talk. Schistosomal lyso-phosphatidylserine activates toll-like receptor 2 and affects immune polarization. *J Biol Chem*. 2002;277:48122-48129.

[153] Smits HH, Hammad H, van Nimwegen M, Soullie T, Willart Ma, Lievers E, et al. Protective effect of *Schistosoma mansoni* infection on allergic airway inflammation depends on the intensity and chronicity of infection. *J Allergy Clin Immunol*. 2007;120:932-940.

[154] Sabin EA, Araujo MI, Carvalho EM, Pearce EJ. Impairment of tetanus toxoid-specific Th1-like immune responses in humans infected with *Schistosoma mansoni*. *The Journal of infectious diseases*. 1996;173:269-272.

[155] Hartgers FC, Obeng BB, Kruize YCM, Dijkhuis A, McCall M, Sauerwein RW, et al. Responses to malarial antigens are altered in helminth-infected children. *The Journal of infectious diseases*. 2009;199:1528-1535.

[156] Cooke A, Tonks P, Jones FM, O'Shea H, Hutchings P, Fulford AJC, et al. Infection with *Schistosoma mansoni* prevents insulin dependent diabetes mellitus in non-obese diabetic mice. *Parasite Immunology*. 1999;21:169-176.

[157] Osada Y, Shimizu S, Kumagai T, Yamada S, Kanazawa T. *Schistosoma mansoni* infection reduces severity of collagen-induced arthritis via down-regulation of pro-inflammatory mediators. *International Journal for Parasitology*. 2009;39:457-464.

[158] Elias D, Wolday D, Akuffo H, Petros B, Bronner U, Britton S. Effect of deworming on human T cell responses to mycobacterial antigens in helminth-exposed individuals before and

after bacille Calmette-Guerin (BCG) vaccination. *Clin Exp Immunol.* 2001;123:219-225.

[159] Elias D, Akuffo H, Britton S. Helminthes could influence the outcome of vaccines against TB in the tropics. *Parasite Immunol.* 2006;28:507-513.

[160] Elias D, Britton S, Aseffa A, Engers H, Akuffo H. Poor immunogenicity of BCG in helminth infected population is associated with increased in vitro TGF-beta production. *Vaccine.* 2008;26:3897-3902.

[161] Brown M, Miiro G, Nkurunziza P, Watera C, Quigley MA, Dunne DW, et al. Schistosoma mansoni, nematode infections, and progression to active tuberculosis among HIV-1-infected Ugandans. *Am J Trop Med Hyg.* 2006;74:819-825.

[162] Elias D, Wolday D, Akuffo H, Petros B, Bronner U, Britton S. Effect of deworming on human T cell responses to mycobacterial antigens in helminth-exposed individuals before and after bacille Calmette-Guérin (BCG) vaccination. *Clinical and experimental immunology.* 2001;123:219-225.

[163] Elias D, Akuffo H, Thors C, Pawlowski A, Britton S. Low dose chronic Schistosoma mansoni infection increases susceptibility to Mycobacterium bovis BCG infection in mice. *Clin Exp Immunol.* 2005;139:398-404.

[164] Elias D, Akuffo H, Pawlowski A, Haile M, Schon T, Britton S. Schistosoma mansoni infection reduces the protective efficacy of BCG vaccination against virulent Mycobacterium tuberculosis. *Vaccine.* 2005;23:1326-1334.

[165] Potian JA, Rafi W, Bhatt K, McBride A, Gause WC, Salgame P. Preexisting helminth infection induces inhibition of innate pulmonary anti-tuberculosis defense by engaging the IL-4 receptor pathway. *J Exp Med.* 2011;208:1863-1874.

[166] Hotez PJ, Brindley PJ, Bethony JM, King CH, Pearce EJ, Jacobson J. Helminth infections: the great neglected tropical diseases. *The Journal of clinical investigation.* 2008;118:1311-1321.

[167] van der Werf MJ, de Vlas SJ, Brooker S, Looman CW, Nagelkerke NJ, Habbema JD, et al. Quantification of clinical morbidity associated with schistosome infection in sub-Saharan Africa. *Acta tropica.* 2003;86:125-139.

[168] Pearce EJ, MacDonald AS. The immunobiology of schistosomiasis. *Nat Rev Immunol.* 2002;2:499-511.

[169] Colley DG, Bustinduy AL, Secor WE, King CH. Human schistosomiasis. *Lancet.* 2014;383:2253-2264.

[170] Dunne DW, Pearce EJ. Immunology of hepatosplenic schistosomiasis mansoni: a human perspective. *Microbes Infect.* 1999;1:553-560.

[171] Doenhoff MJ, Cioli D, Utzinger J. Praziquantel: mechanisms of action, resistance and new derivatives for schistosomiasis. *Current opinion in infectious diseases.* 2008;21:659-667.

- [172] Bisoffi Z, Buonfrate D, Sequi M, Mejia R, Cimino RO, Krolewiecki AJ, et al. Diagnostic accuracy of five serologic tests for *Strongyloides stercoralis* infection. *PLoS neglected tropical diseases*. 2014;8:e2640.
- [173] Mayer K, Mohrs K, Crowe S, Johnson L, Rhyne P, Woodland D, et al. The functional heterogeneity of type I effector T cells in response to infection is related to the potential for IFN- γ production. *Journal of Immunology*. 2005;174:7732-7739.
- [174] El Kasmi KC, Qualls JE, Pesce JT, Smith AM, Thompson RW, Henao-Tamayo M, et al. Toll-like receptor-induced arginase 1 in macrophages thwarts effective immunity against intracellular pathogens. *Nature immunology*. 2008;9:1399-1406.
- [175] Zaretsky AG, Taylor JJ, King IL, Marshall FA, Mohrs M, Pearce EJ. T follicular helper cells differentiate from Th2 cells in response to helminth antigens. *The Journal of experimental medicine*. 2009;206:991-999.
- [176] Crosby A, Jones FM, Kolosionek E, Southwood M, Purvis I, Soon E, et al. Praziquantel reverses pulmonary hypertension and vascular remodeling in murine schistosomiasis. *American journal of respiratory and critical care medicine*. 2011;184:467-473.
- [177] Pearce EJ, MacDonald AS. The immunobiology of schistosomiasis. *Nature reviews Immunology*. 2002;2:499-511.
- [178] Liu R, Dong HF, Guo Y, Zhao QP, Jiang MS. Efficacy of praziquantel and artemisinin derivatives for the treatment and prevention of human schistosomiasis: a systematic review and meta-analysis. *Parasites & vectors*. 2011;4:201.
- [179] Scanga C, Mohan V, Joseph H, Yu K, Chan J, Flynn J. Reactivation of latent tuberculosis: variations on the Cornell murine model. *Infection and Immunity*. 1999;67:4531-4538.
- [180] Nouailles G, Dorhoi A, Koch M, Zerrahn J, Weiner J, 3rd, Fae KC, et al. CXCL5-secreting pulmonary epithelial cells drive destructive neutrophilic inflammation in tuberculosis. *J Clin Invest*. 2014;124:1268-1282.
- [181] Murray PJ, Wynn TA. Protective and pathogenic functions of macrophage subsets. *Nature reviews Immunology*. 2011;11:723-737.
- [182] Potian JA, Rafi W, Bhatt K, McBride A, Gause WC, Salgame P. Preexisting helminth infection induces inhibition of innate pulmonary anti-tuberculosis defense by engaging the IL-4 receptor pathway. *The Journal of experimental medicine*. 2011;208:1863-1874.
- [183] Erb KJ, Trujillo C, Fugate M, Moll H. Infection with the helminth *Nippostrongylus brasiliensis* does not interfere with efficient elimination of *Mycobacterium bovis* BCG from the lungs of mice. *Clin Diagn Lab Immunol*. 2002;9:727-730.
- [184] Rafi W, Bhatt K, Gause WC, Salgame P. "Primary and memory immunity to *Mycobacterium tuberculosis* infection is not compromised in mice with chronic enteric helminth infection". *Infect Immun*. 2015.

- [185] Babu S, Bhat SQ, Kumar NP, Jayantasri S, Rukmani S, Kumaran P, et al. Human type 1 and 17 responses in latent tuberculosis are modulated by coincident filarial infection through cytotoxic T lymphocyte antigen-4 and programmed death-1. *J Infect Dis.* 2009;200:288-298.
- [186] Liu Z, Liu Q, Hamed H, Anthony RM, Foster A, Finkelman FD, et al. IL-2 and autocrine IL-4 drive the in vivo development of antigen-specific Th2 T cells elicited by nematode parasites. *J Immunol.* 2005;174:2242-2249.
- [187] Panzer M, Sitte S, Wirth S, Drexler I, Sparwasser T, Voehringer D. Rapid in vivo conversion of effector T cells into Th2 cells during helminth infection. *The Journal of immunology.* 2012;188:615-623.
- [188] Everts B, Hussaarts L, Driessen NN, Meevissen MH, Schramm G, van der Ham AJ, et al. Schistosome-derived omega-1 drives Th2 polarization by suppressing protein synthesis following internalization by the mannose receptor. *J Exp Med.* 2012;209:1753-1767, S1751.
- [189] Duque-Correa MA, Kuhl AA, Rodriguez PC, Zedler U, Schommer-Leitner S, Rao M, et al. Macrophage arginase-1 controls bacterial growth and pathology in hypoxic tuberculosis granulomas. *Proc Natl Acad Sci U S A.* 2014;111:E4024-4032.
- [190] Mattila JT, Ojo OO, Kepka-Lenhart D, Marino S, Kim JH, Eum SY, et al. Microenvironments in tuberculous granulomas are delineated by distinct populations of macrophage subsets and expression of nitric oxide synthase and arginase isoforms. *J Immunol.* 2013;191:773-784.
- [191] Pessanha AP, Martins RA, Mattos-Guaraldi AL, Vianna A, Moreira LO. Arginase-1 expression in granulomas of tuberculosis patients. *FEMS Immunol Med Microbiol.* 2012;66:265-268.
- [192] Maarsingh H, Pera T, Meurs H. Arginase and pulmonary diseases. *Naunyn Schmiedebergs Arch Pharmacol.* 2008;378:171-184.
- [193] Pesce JT, Ramalingam TR, Mentink-Kane MM, Wilson MS, El Kasmi KC, Smith AM, et al. Arginase-1-expressing macrophages suppress Th2 cytokine-driven inflammation and fibrosis. *PLoS pathogens.* 2009;5:e1000371.
- [194] Barron L, Smith AM, El Kasmi KC, Qualls JE, Huang X, Cheever A, et al. Role of arginase 1 from myeloid cells in th2-dominated lung inflammation. *PLoS One.* 2013;8:e61961.
- [195] Gopal R, Monin L, Torres D, Slight SR, Mehra S, McKenna K, et al. S100A8/A9 proteins mediate neutrophilic inflammation and lung pathology during tuberculosis. *American Journal of Respiratory and Critical Care Medicine.* 2013;188:1137-1146.
- [196] Feazel LM, Baumgartner LK, Peterson KL, Frank DN, Harris JK, Pace NR. Opportunistic pathogens enriched in showerhead biofilms. *Proc Natl Acad Sci U S A.* 2009;106:16393-16399.
- [197] Nishiuchi Y, Maekura R, Kitada S, Tamaru A, Taguri T, Kira Y, et al. The recovery of *Mycobacterium avium-intracellulare* complex (MAC) from the residential bathrooms of patients

with pulmonary MAC. *Clin Infect Dis*. 2007;45:347-351.

[198] Falkinham JO, 3rd. Nontuberculous mycobacteria from household plumbing of patients with nontuberculous mycobacteria disease. *Emerg Infect Dis*. 2011;17:419-424.

[199] Griffith DE, Aksamit T, Brown-Elliott BA, Catanzaro A, Daley C, Gordin F, et al. An official ATS/IDSA statement: diagnosis, treatment, and prevention of nontuberculous mycobacterial diseases. *Am J Respir Crit Care Med*. 2007;175:367-416.

[200] Winthrop KL, Chang E, Yamashita S, Iademarco MF, LoBue PA. Nontuberculous mycobacteria infections and anti-tumor necrosis factor-alpha therapy. *Emerg Infect Dis*. 2009;15:1556-1561.

[201] Orme IM, Ordway DJ. Host response to nontuberculous mycobacterial infections of current clinical importance. *Infect Immun*. 2014;82:3516-3522.

[202] Iseman MD, Marras TK. The importance of nontuberculous mycobacterial lung disease. *Am J Respir Crit Care Med*. 2008;178:999-1000.

[203] Nessar R, Cambau E, Reytrat JM, Murray A, Gicquel B. Mycobacterium abscessus: a new antibiotic nightmare. *J Antimicrob Chemother*. 2012;67:810-818.

[204] Jeon K, Kwon OJ, Lee NY, Kim BJ, Kook YH, Lee SH, et al. Antibiotic treatment of Mycobacterium abscessus lung disease: a retrospective analysis of 65 patients. *Am J Respir Crit Care Med*. 2009;180:896-902.

[205] Lobo LJ, Noone PG. Respiratory infections in patients with cystic fibrosis undergoing lung transplantation. *The Lancet Respiratory medicine*. 2014;2:73-82.

[206] Sexton P, Harrison AC. Susceptibility to nontuberculous mycobacterial lung disease. *Eur Respir J*. 2008;31:1322-1333.

[207] Byrd TF, Lyons CR. Preliminary characterization of a Mycobacterium abscessus mutant in human and murine models of infection. *Infect Immun*. 1999;67:4700-4707.

[208] Ordway D, Henao-Tamayo M, Smith E, Shanley C, Harton M, Trout J, et al. Animal model of Mycobacterium abscessus lung infection. *J Leukoc Biol*. 2008;83:1502-1511.

[209] Rottman M, Catherinot E, Hochedez P, Emile JF, Casanova JL, Gaillard JL, et al. Importance of T cells, gamma interferon, and tumor necrosis factor in immune control of the rapid grower Mycobacterium abscessus in C57BL/6 mice. *Infect Immun*. 2007;75:5898-5907.

[210] Gopal R, Monin L, Slight S, Uche U, Blanchard E, Fallert Junecko BA, et al. Unexpected role for IL-17 in protective immunity against hypervirulent Mycobacterium tuberculosis HN878 infection. *PLoS pathogens*. 2014;10:e1004099.

[211] Kim SY, Koh WJ, Kim YH, Jeong BH, Park HY, Jeon K, et al. Importance of reciprocal balance of T cell immunity in Mycobacterium abscessus complex lung disease. *PLoS One*.

2014;9:e109941.

[212] Saiman L, Siegel J. *Infection Control in Cystic Fibrosis* 2004;17.

[213] De Groote Ma, Huitt G. Infections due to rapidly growing mycobacteria. *Clinical infectious diseases : an official publication of the Infectious Diseases Society of America*. 2006;42:1756-1763.

[214] Zelante T, Bozza S, De Luca A, D'Angelo C, Bonifazi P, Moretti S, et al. Th17 cells in the setting of *Aspergillus* infection and pathology. *Medical mycology*. 2009;47 Suppl 1:S162-169.

[215] Zelante T, Iannitti RG, De Luca A, Arroyo J, Blanco N, Servillo G, et al. Sensing of mammalian IL-17A regulates fungal adaptation and virulence. *Nat Commun*. 2012;3:683-683.

[216] Malcolm KC, Nichols EM, Caceres SM, Kret JE, Martiniano SL, Sagel SD, et al. *Mycobacterium abscessus* induces a limited pattern of neutrophil activation that promotes pathogen survival. *PLoS One*. 2013;8:e57402-e57402.

[217] Netea MG, Warris A, Van der Meer JW, Fenton MJ, Verver-Janssen TJ, Jacobs LE, et al. *Aspergillus fumigatus* evades immune recognition during germination through loss of toll-like receptor-4-mediated signal transduction. *J Infect Dis*. 2003;188:320-326.

[218] Casaulta C, Schoni MH, Weichel M, Cramer R, Jutel M, Daigle I, et al. IL-10 controls *Aspergillus fumigatus*- and *Pseudomonas aeruginosa*-specific T-cell response in cystic fibrosis. *Pediatric research*. 2003;53:313-319.

[219] Foster WM, Walters DM, Longphre M, Macri K, Miller LM. Methodology for the measurement of mucociliary function in the mouse by scintigraphy. *Journal of applied physiology*. 2001;90:1111-1117.

[220] Condon TV, Sawyer RT, Fenton MJ, Riches DW. Lung dendritic cells at the innate-adaptive immune interface. *J Leukoc Biol*. 2011;90:883-895.

[221] Jonsson B, Ridell M, Wold AE. Non-tuberculous mycobacteria and their surface lipids efficiently induced IL-17 production in human T cells. *Microbes Infect*. 2012;14:1186-1195.

[222] Malcolm KC, Nichols EM, Caceres SM, Kret JE, Martiniano SL, Sagel SD, et al. *Mycobacterium abscessus* induces a limited pattern of neutrophil activation that promotes pathogen survival. *PLoS One*. 2013;8:e57402.

[223] Rowe SM, Miller S, Sorscher EJ. Cystic fibrosis. *The New England journal of medicine*. 2005;352:1992-2001.

[224] Matsuyama M, Ishii Y, Yageta Y, Ohtsuka S, Ano S, Matsuno Y, et al. Role of Th1/Th17 balance regulated by T-bet in a mouse model of *Mycobacterium avium* complex disease. *J Immunol*. 2014;192:1707-1717.

[225] Marshall BC. Pulmonary exacerbations in cystic fibrosis: it's time to be explicit! *Am J*

Respir Crit Care Med. 2004;169:781-782.

[226] Britto MT, Kotagal UR, Hornung RW, Atherton HD, Tsevat J, Wilmott RW. Impact of recent pulmonary exacerbations on quality of life in patients with cystic fibrosis. *Chest*. 2002;121:64-72.

[227] Catherinot E, Roux AL, Vibet MA, Bellis G, Ravilly S, Lemonnier L, et al. *Mycobacterium avium* and *Mycobacterium abscessus* complex target distinct cystic fibrosis patient subpopulations. *J Cyst Fibros*. 2013;12:74-80.

[228] Verregghen M, Heijerman HG, Reijers M, van Ingen J, van der Ent CK. Risk factors for *Mycobacterium abscessus* infection in cystic fibrosis patients; a case-control study. *J Cyst Fibros*. 2012;11:340-343.

[229] Esther CR, Jr., Esserman DA, Gilligan P, Kerr A, Noone PG. Chronic *Mycobacterium abscessus* infection and lung function decline in cystic fibrosis. *J Cyst Fibros*. 2010;9:117-123.

[230] Martin KR. Editorial: beta-glucans: going through GM-CSF to get to dectin. *J Leukoc Biol*. 2012;91:521-524.

[231] Kataoka K, Muta T, Yamazaki S, Takeshige K. Activation of macrophages by linear (1 \rightarrow 3)-beta-D-glucans. Implications for the recognition of fungi by innate immunity. *J Biol Chem*. 2002;277:36825-36831.

[232] Vassallo R, Standing JE, Limper AH. Isolated *Pneumocystis carinii* cell wall glucan provokes lower respiratory tract inflammatory responses. *J Immunol*. 2000;164:3755-3763.

[233] Hashimoto T, Ohno N, Adachi Y, Yadomae T. Nitric oxide synthesis in murine peritoneal macrophages by fungal beta-glucans. *Biological & pharmaceutical bulletin*. 1997;20:1006-1009.

[234] Redford PS, Murray PJ, O'Garra A. The role of IL-10 in immune regulation during *M. tuberculosis* infection. *Mucosal Immunol*. 2011;4:261-270.

[235] Couper KN, Blount DG, Riley EM. IL-10: the master regulator of immunity to infection. *J Immunol*. 2008;180:5771-5777.

[236] Elcombe SE, Naqvi S, Van Den Bosch MW, MacKenzie KF, Cianfanelli F, Brown GD, et al. Dectin-1 regulates IL-10 production via a MSK1/2 and CREB dependent pathway and promotes the induction of regulatory macrophage markers. *PLoS One*. 2013;8:e60086.

[237] Heinekamp T, Schmidt H, Lapp K, Pahtz V, Shopova I, Koster-Eiserfunke N, et al. Interference of *Aspergillus fumigatus* with the immune response. *Seminars in immunopathology*. 2015;37:141-152.

[238] Zelante T, Fallarino F, Bistoni F, Puccetti P, Romani L. Indoleamine 2,3-dioxygenase in infection: the paradox of an evasive strategy that benefits the host. *Microbes Infect*. 2009;11:133-141.

- [239] Romani L, Zelante T, De Luca A, Bozza S, Bonifazi P, Moretti S, et al. Indoleamine 2,3-dioxygenase (IDO) in inflammation and allergy to *Aspergillus*. *Medical mycology*. 2009;47 Suppl 1:S154-161.
- [240] Hayashi T, Rao SP, Takabayashi K, Van Uden JH, Kornbluth RS, Baird SM, et al. Enhancement of innate immunity against *Mycobacterium avium* infection by immunostimulatory DNA is mediated by indoleamine 2,3-dioxygenase. *Infect Immun*. 2001;69:6156-6164.
- [241] Latge JP. *Aspergillus fumigatus* and aspergillosis. *Clinical microbiology reviews*. 1999;12:310-350.
- [242] O'Gorman C. Airborne *Aspergillus fumigatus* conidia: a risk factor for aspergillosis. *Fungal Biology Reviews*. 2011:151-157.
- [243] Ezenwa VO, Jolles AE. *Epidemiology*. Opposite effects of anthelmintic treatment on microbial infection at individual versus population scales. *Science*. 2015;347:175-177.